Physical and kinetic studies on cetyltrimethylammonium bromide-phenyl acetate systems.

Shetewi, B. B.

Award date:
1975

Awarding institution:
University of Bath

PHYSICAL AND KINETIC STUDIES ON CETYLTRIMETHYLAMMONIUM BROMIDE - PHENYL ACETATE SYSTEMS

T H E S I S

submitted by B.B. SHETEWI, B.Pharm., M.P.S.

Life Honorary Member of The Pharmaceutical Society of Egypt

for the degree of Doctor of Philosophy

of the

University of Bath

1975

This research has been carried out in the School of Pharmacy of the University of Bath under the supervision of D.J.G. Davies, M.Sc., Ph.D., M.P.S. and B.J. Meakin B.Pharm., M.P.S.

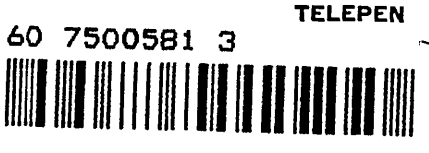

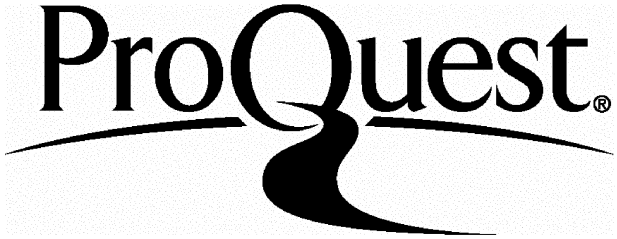

ProQuest LLC
789 East Eisenhower Parkway
P.O. Box 1346
Ann Arbor, MI 48106-1346

ACKNOWLEDGEMENTS

The author wishes to extend his most heartfelt gratitude for the guidance, advice and encouragement received from Mr. B.J. Meakin and Dr. D.J.G. Davies throughout the span of this work. He wishes to express his most sincere thanks to Professor D.A. Norton for providing the facilities for the research and to all the academic and non-academic members of the School for their sustained interest and assistance whenever they were needed.

Appreciation is extended to the Government of the Libyan Arab Republic for providing the moral and financial support and to the members of the Libyan Embassy in London for their help and encouragement.

The author's thanks are also due to Dr. D. Attwood of the School of Pharmacy, University of Manchester, for his help and useful discussions on light scattering and to Dr. A.A. Woolf, of the School of Chemistry, Bath University, for the use of the Wayne Kerr Conductivity Bridge.

Special thanks are due to Mrs. S.J. Carter for her diligence in the typing of the manuscript.

Last, but by no means least, the author thanks his wife and his family for their patience, their understanding and for providing the incentive. Without them the whole exercise would have been meaningless.

TO

THE MEMORY OF MY FATHER

SUMMARY

The introduction is in three sections, the first of these dealing with the mechanisms and factors affecting the rate of ester hydrolysis. The second part deals with the classification and general characteristics of surface active agents such as micellization and solubilization. The final part discusses micellar catalysis with special emphasis on reactions involving cationic surfactants, particularly CETYLTRIMETHYLAMMONIUM BROMIDE (CTAB).

The experimental section describes the kinetic investigations of the effect of CTAB on the base catalysed hydrolysis of PHENYL ACETATE under standard conditions at various pHs. It was found that the surfactant, above its critical micelle concentration (CMC) decreased the rate of hydrolysis. This action was tentatively attributed to the difference in the partition of the ester between the micellar phase and the bulk aqueous phase. Comparison of the partition coefficients determined from the kinetic data with those obtained from solubility and gel filtration techniques support this hypothesis and suggest a change in the physical characteristics of the micelle at a concentration in the region of 1×10^{-2}M. Further evidence for such a change was obtained by viscometry and light scattering studies.

In the final section the results of these studies are discussed and the importance of pH in micellar catalysis and partitioning behaviour is established.

▼ ▼ ▼ ▼ ▼

CONTENTS

INTRODUCTION

SECTION 1

MECHANISMS OF ESTER HYDROLYSIS AND REACTION KINETICS

A. ESTER HYDROLYSIS

The mechanisms of ester hydrolysis and reaction kinetics in simple solutions are well documented (1 - 5). Only a brief description of the relevant factors which influence these processes is therefore given here.

There are a number of pathways by which the hydrolysis of carboxylic acid esters can take place. This may involve bond breakage at one or two possible sites involving either an acyl-oxygen bond breakage or, less frequently, the fission of an alkyl-oxygen bond, Fig. (1.1). The hydrolysis, in the first place, is a nucleophilic

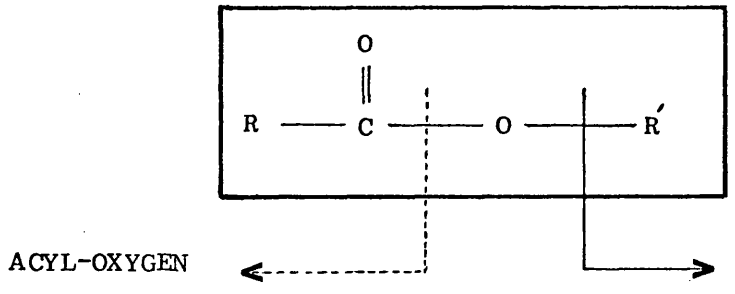

FIGURE (1.1)

substitution at the acyl carbon where an (-OH) group is substituted for an (-OR) moiety. The hydrolysis in the second case is a nucleophilic substitution at the alkyl carbon and the (-OH) group in this case is substituted for the (- O - $\overset{\overset{O}{\|}}{C}$ - R) entity. These two substitution reactions can proceed either by a unimolecular or a bimolecular mechanism and the hydrolysis can take place through an attack on the ester itself, in basic or neutral solutions, or through an attack on its conjugate acid: $\left(R - \overset{\overset{O}{\|}}{C} - \overset{+}{O}\begin{matrix} R' \\ H \end{matrix} \right)$ in acid media.

Various possible combinations of the above pathways allow eight conceivable mechanisms for ester hydrolysis. An accepted notation for these reactions is due to Ingold (4). The letters B and A represent the substrate itself or its conjugate acid, the symbols AC and AL denote whether acyl-oxygen or alkyl-oxygen bond breakage takes place and the numbers 1 and 2 refer to the molecularity of the reaction. Using this notation a BAC_2 process indicates a bimolecular reaction involving an acyl-oxygen fission carried out in a basic or neutral medium, i.e. the species under attack is the ester molecule itself. This mechanism accounts for almost all base-catalysed ester hydrolyses and can be represented by the following scheme:

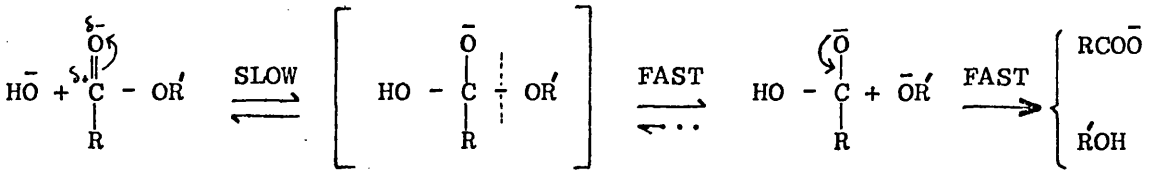

The first step is reversible, the final is irreversible. The existence of the intermediate anion resulting from the first forward step has been established using O^{18} labelled materials.

The second very common mechanism of hydrolysis is the acid-catalysed hydrolysis of ester, the AAC_2 mechanism. It differs from the BAC_2 in that it is experimentally reversible, resulting in the acid catalysed esterification reaction. This mechanism proceeds through the following scheme.

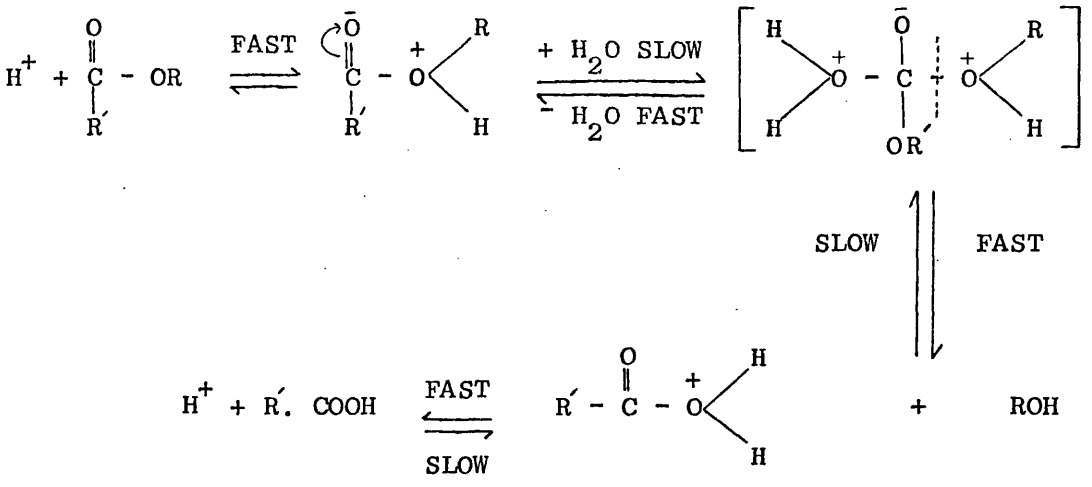

The nucleophilic attack to form the transition complex, which then reacts with water may also be carried out by a variety of other anionic nucleophiles, often buffer ions, and water itself, although these species are usually much less efficient hydrolytic agents than hydrogen and hydroxyl ions.

B. REACTION KINETICS

(i) Rate of reaction. The law of mass action states that the rate of a reaction, at a constant temperature, is proportional to the product of the molar concentration of each reactant raised to a power equal to the number of molecules of the substance undergoing the reaction, thus in a general reaction:

$$xA + yB \longrightarrow \text{Products}$$

the rate of the reaction can be expressed as equation (1.1).

$$\text{Rate} = -\frac{1}{x}\frac{d[A]}{dt} = -\frac{1}{y}\frac{d[B]}{dt} = k[A]^x [B]^y \quad \ldots\ldots (1.1)$$

where $d[A]/dt$ and $d[B]/dt$ represent the change in concentration of components A and B with time, respectively, and "k" is the rate constant. The negative sign indicates

a decrease in the concentration of the components A and B. The rate constant for the products would be $\frac{+ d [\text{Products}]}{dt}$ indicating that they increase with time.

(ii) Order of reaction. The overall order of a reaction is the sum of the exponents of the concentration terms that occur in the rate expression. In the general reaction given above, the overall order of the reaction is (x + y) while the order with respect to B is (y) and with respect to A is (x). For a drug with a concentration C and an order of reaction (n), undergoing degradation, such as an ester hydrolysis, the rate with respect to the drug would be given by equation (1.2)

$$\text{Rate} = - \frac{d[C]}{dt} = k [C]^n \quad \ldots\ldots\ldots\ldots\ldots\ldots (1.2)$$

(n) would be zero for a zero order reaction, 1 for a first order reaction, 2 for a second order reaction, etc. Integration of equation (1.2) between the concentration C corresponding to the original concentration of the substance at t = o and C_t, the concentration after a time interval t, leads to the following equations (1.3, 1.4 and 1.5)

ZERO ORDER $\quad C_t - C_o = - kt \quad \ldots\ldots\ldots (1.3)$

FIRST ORDER $\quad \log_e C_t - \log_e C_o = - kt \quad \ldots\ldots\ldots (1.4)$

SECOND ORDER $\quad \frac{1}{C_t} - \frac{1}{C_o} = - kt \quad \ldots\ldots\ldots (1.5)$

Ester hydrolysis is generally a bimolecular process involving an attacking species such as hydrogen or hydroxyl ions. If the concentration of the attacking species is kept constant throughout the process, as, for instance, by

buffering the system, then the rate equation apparently reduces to a first order process, equation (1.6):

$$\frac{dc}{dt} = - k \left[\text{ESTER}\right] \left[\text{ATTACKING SPECIES}\right] = - k_{obs} \left[\text{ESTER}\right] \quad ....(1.6)$$

where the observed rate constant, k_{obs}, is the product of the true second order rate constant k_1 and the concentration of the attacking species.

(iii) Influence of pH. Most hydrolytic reactions are carried out in buffer solutions at a constant pH. Under these conditions the observed rate constant obtained under acidic conditions is given by equation (1.7):

$$k_{obs} = k_1 \left[H_3O^+\right] \quad .....(1.7)$$

$$\text{or} \qquad \log k_{obs} = \log k_1 - \text{pH} \quad .....(1.7)$$

Similarly, under basic conditions, the relationship can be expressed by equation (1.8):

$$\log k_{obs} = \log k_2 - pK_w + \text{pH} \quad .....(1.8)$$

where k_1 and k_2 are the specific rate constants for the hydroxonium ion and the hydroxyl ion respectively.

From equations (1.7 and 1.8) straight lines of unit slope should be obtained when log k_{obs} is plotted against pH showing that the rate of the hydroxyl ion catalysed reaction should increase with increase in pH whereas that for hydrogen ion catalysis decreases. Fig. (1.2) shows the general profiles for pH - k_{obs} for the various pH - rate relationships. "I" shows a reaction which is subject to hydrogen and hydroxyl ion catalysis with an intermediate region where both OH^- and H_3O^+ contribute to k_{obs}, "II" and "III" show reactions where

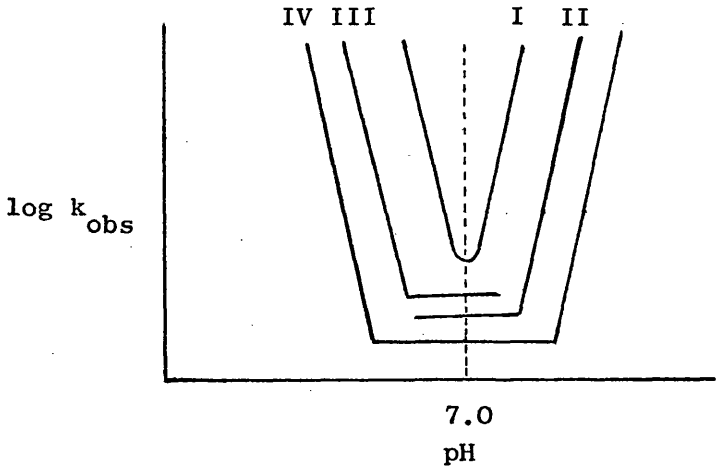

Fig.(1.2) A schematic representation of how k_{obs} varies with pH.

hydrogen and hydroxyl ion catalysis respectively are absent and "IV" illustrates the case where there is both specific hydroxyl and hydroxonium ion catalysis with an intermediate position independent of pH, and solvent catalysis is the primary mode of reaction in this region. For a system such as "IV", the observed rate constant is given by equation (1.9) where k_o is the term representing the solvent catalysed process,

$$k_{obs} = k_1\left[H_3O^+\right] + k_2\left[OH^-\right] + k_o \quad \ldots\ldots\ldots\ldots \quad (1.9)$$

(iv) Effect of substrate species. Where an ester is capable of existing in more than one form e.g. a neutral (E) and a protonated form (EH^+), both forms are susceptible to nucleophilic attack which will proceed at different rates. Under these circumstances the rate expression becomes

equation (1.10):

$$k_{obs} = k_1^{E}\left[H_3O^+\right]\frac{\left[E\right]}{\left[E_T\right]} + k_2^{E}\left[OH^-\right]\frac{\left[E\right]}{\left[E_T\right]} + k_o^{E}\frac{\left[E\right]}{\left[E_T\right]}$$

$$+ k_1^{EH^+}\left[H_3O^+\right]\frac{\left[EH^+\right]}{\left[E_T\right]} + k_2^{EH^+}\left[OH^-\right]\frac{\left[EH^+\right]}{\left[E_T\right]} + k_o^{EH^+}\frac{\left[EH^+\right]}{\left[E_T\right]} \quad \ldots (1.10)$$

where $\left[E_T\right]$ = Total ester concentration i.e. $= \left[E\right] + \left[EH^+\right]$

This can lead to discontinuities in the pH profiles in the region of the pK_a values of the substrate.

(v) General Acid-Base Catalysis. When buffer salts accelerate hydrolytic reactions, it is said that the reaction is subject to general acid-base catalysis. The equation for such a reaction involving a single ester species becomes (1.11):

$$k_{obs} = k_o + k_1\left[H_3O^+\right] + k_2\left[OH^-\right] + k_3\left[HA\right]$$

$$+ k_4\left[A^-\right] + k_5\left[B\right] + k_6\left[BH^+\right] \quad \ldots\ldots\ldots\ldots\ldots\ldots (1.11)$$

where $k_3 - k_6$ are the specific rate constants due to general acid $\left[HA\right]$ and conjugate base $\left[A^-\right]$, general base $\left[B\right]$ and conjugate acid $\left[BH^+\right]$ respectively arising from the buffer constituent (s).

(vi) Influence of ionic strength. The ionic strength of the system may directly influence the rate of the reaction in that system by modifying the activities of the reacting species and the transition complex. This is known as the PRIMARY SALT EFFECT. Application of the Debye-Hückel theory leads to equation (1.12):

$$\log k_\mu = \log k_o + \sqrt{\frac{\mu}{D^3T^3\rho}}\left(2 Z_A Z_B\right) \times 1.83 \times 10^6 \quad \ldots (1.12)$$

where k_μ is the rate constant of the reaction,

k_o is the rate constant at zero ionic strength,

μ is the ionic strength,

D is the dielectric constant of the medium,

T is the absolute temperature,

ρ is the density of the solution,

and Z_A , Z_B are the charge on the ion A and B respectively. From equation (1.12) it can be deduced that a reaction between two positive or two negative ions will be accelerated by increases in ionic strength while a reaction between a negative and a positive ion will be retarded. Deviations from equation (1.12) are observed as the ionic strength of the medium is increased. This is to be expected, for in the deduction of the equation the solutions have been assumed to be very dilute. Plots of k_μ against $\sqrt{\mu}$ are usually linear up to an ionic strength of 0.3.

A SECONDARY SALT EFFECT also exists. It is due to the influence of ionic strength on dissociation constants which modifies rate equation (1.11) when the substrate exists in more than one form.

(vii) Effect of temperature. In accordance with all chemical reactions, the rate at which a hydrolysis proceeds is increased by raising the temperature. A quantitative relationship, derived empirically, between temperature and reaction rate is given by the Arrhenius equation (1.13):

$$k_T = A \cdot e^{-E/RT} \qquad \ldots\ldots\ldots\ldots\ldots\ldots \quad (1.13)$$

where k_T is the reaction rate constant,

A is the frequency factor which involves the frequency of molecular collisions,

E is the activation energy for formation of the transition complex,

R is the gas constant,

and T is the absolute temperature.

Eyring and Wynne-Jones (6), using the transition state theory, developed an absolute rate equation. Their equation (1.14) relates the Arrhenius factor, A, to the entropy of activation and the Arrhenius energy of activation, E, to the enthalpy of activation:

$$k_T = \frac{RT}{Nh} \cdot e^{\frac{\Delta S^*}{R}} e^{\frac{-\Delta H^*}{RT}} \qquad \ldots\ldots\ldots\ldots\ldots\ldots \quad (1.14)$$

where ΔS^* and ΔH^* represent the entropy and enthalpy of activation respectively, N is Avogadro's number and h is Planck's constant. A plot of $\log_e k_T/T$ versus $\frac{1}{T}$ results in a linear relationship from which the entropy and enthalpy of activation can be evaluated.

SECTION 2

SURFACE ACTIVE AGENTS

A. DEFINITION AND CLASSIFICATION

Surface active agents, as the name implies, are substances capable of affecting the state of surfaces and boundaries of the systems in which they exist. The marked lowering of surface tension when surface active agents are added to water is a familiar phenomenon. The practical application of these materials has been known for a long time as evidenced by the use of soaps in cleansing, greases as lubricants and naturally occurring proteinaceous materials as glues and emulsifyers. The preparation of synthetic compounds, generally known as SURFACTANTS, has widened the field of application and increased our knowledge of the physical and chemical properties of these materials.

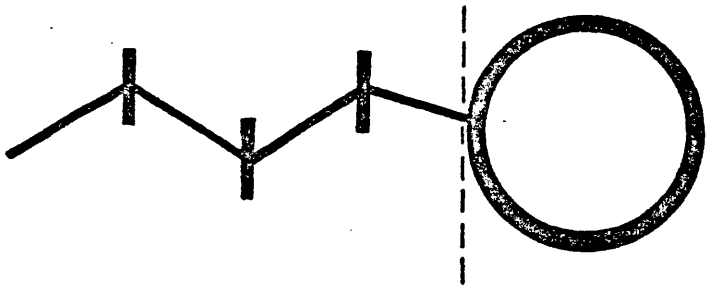

FIGURE (1.3). SCHEMATIC REPRESENTATION OF THE TWO REGIONS OF A SURFACTANT MOLECULE.

An early study by Hartley (7) recognised that the surfactant molecule could be arbitarily divided into a hydrophobic portion and a hydrophilic head group as shown in figure (1.3). The hydrophobic portion may consist of a straight or branched alkyl hydrocarbon chain or an alkaryl group. The hydrophilic part has polar groups, which may be neutral such as polyoxyethylene groups, sugar residues and glycerides or charged such as sulphate, carboxylate and quaternary ammonium ions. It is the delicate balance of contributions from these opposing parts of the molecule that give rise to all the characteristic properties of the surfactant systems.

The nature of the hydrophilic group determines the subdivision of surfactants into four groups indicated below, which have been extensively described by Schwartz, Perry and Berch (8) and by Moilliet, Collie and Black (9).

Basic Classification of Surfactants

(i) Anionic Surfactants have a negatively charged head group, e.g. Sodium dodecyl sulphate (SDS)

$$C_{12}H_{25} - SO_4^- \; Na^+$$

(ii) Cationic Surfactants where the head group carries a positive charge, e.g. cetyltrimethylammonium bromide (CTAB):

$$\left[CH_3 - (CH_3)_{15} - \underset{\displaystyle CH_3}{\overset{\displaystyle CH_3}{\overset{|}{\underset{|}{N^+}}}} - CH_3 \right] \; Br^-$$

(iii) Non-ionic Surfactants where the hydrophilic head group is not ionised. This group can be exemplified by polyoxyethylene glycols of the general formula:

$$CH_3(CH_2)_y.COO\,(CH_2CH_2O)_x-CH_2-CH_2-OH$$

(iv) Ampholytic Surfactants can exist as zwitterionic, anionic or cationic depending on the pH of the medium, e.g.

3-dimethyl dodecyl amino-propane-1-sulphonate:

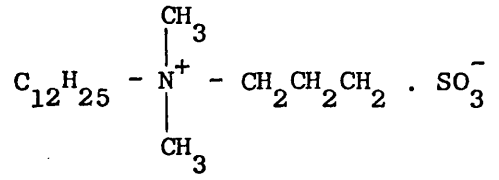

Generally, only materials with a chain length of between 8 and 18 carbon atoms are effective as surfactants. Usually materials with a chain length greater than C_{18} are insoluble or slightly soluble in water at room temperature.

B. MICELLE FORMATION

Ionic surfactants can be completely ionised and can thus behave as simple ionic substances. They do, however possess certain properties that differentiate them from the simple electrolytes which have become apparent from a variety of physical determinations on their solutions. It is found that once a certain concentration is reached aggregation of the organic ions, or monomers, takes place. This process of aggregation was termed MICELLIZATION by McBain (10) and the concentration at which it takes place is known as the CRITICAL MICELLE CONCENTRATION (CMC). The evidence for the existence of micelles is based on the fact that the physical properties of surfactant solutions exhibit an abrupt discontinuity which takes place over a narrow concentration range, the CMC. The magnitude of this range is dependent on many factors such as the nature and structure of the surface active agent, the nature of the solvent, temperature and the presence of impurities. Ionic surfactants show a marked dependence on the presence of added salts with respect to these properties. In this study we shall be dealing

mainly with cationic surfactants and with CTAB in particular. Occasional reference to other classes of surfactants is, however, necessary for comparison purposes.

(i) Critical Micelle Concentration. The abrupt and dramatic changes in many physical properties that accompany the attainment of the CMC within a surfactant solution have been utilised to determine its value experimentally (11, 12). Methods routinely used include measurement of surface tension, conductivity, solubilization, viscosity, refractive index and turbidity. The CMC is obtained from the intersection of the extrapolated linear branches of the experimental curve when the physical property is plotted against the concentration of the surfactant. Experiments designed to support the mass action theory of micelle formation have shown, however, that dimers do form in dilute solutions of sodium dodecyl sulphate below the CMC indicating that the change takes place over a narrow range of concentration (13).

(ii) Effect of temperature on the CMC. With ionic surfactants, such as n-dodecyltrimethylammonium bromide or sodium dodecyl sulphate, a curve with a minimum value in the range of 25 - 30^{o} is obtained when the CMC is plotted versus temperature from 0 - 60^{o} (14, 15). The CMC of nonionic surfactants decreases with increasing temperatures (16). The magnitude of the temperature effect on the CMC of cationic surfactants appears to be smaller when compared to its effect on the anionic group. For CTAB, a value of 9.8×10^{-4}M is reported at 25^{o} (17) and 1×10^{-3}M at 60^{o}

(12, 18) while the CMC of sodium dodecyl sulphate is 8×10^{-3}M at 25^{o} and 1×10^{-2}M at 60^{o} (12).

(iii) Effect of salts on the CMC. In 1947 Corrin and Harkins (19) initiated a systematic experimental study of the effect of added electrolytes on the CMC of aqueous surfactant solutions. They established a log-log relationship between the change in the CMC and the concentration of the added salt, equation (1.15):

$$\log \text{CMC} = a \log m + b \quad \ldots\ldots\ldots\ldots\ldots\ldots \quad (1.15)$$

where m is the total molar concentration of the added salt and "a" and "b" are negative constants. The addition of salt, therefore, lowers the CMC of ionic surfactants. This is brought about through the shielding of repulsive interactions between the charged head groups. The constant "a" in equation (1.15) has been evaluated by Corrin (20) which leads to equation (1.16):

$$\log \text{CMC} = -\left(\frac{m}{n}\right) \log (\text{CMC} + Ca) + \text{Constant} \quad \ldots\ldots\ldots \quad (1.16)$$

where m is again the total molar concentration of the added salt, n is the number of micelles, $\frac{m}{n}$ represents the fraction of counterions bound to the micelle and Ca is the counterion concentration contributed by the added salt. In 1962, Tartar (21) using the data of Corrin and Harkins found that the CMC is a linear function of the "thickness of the ionic atmosphere", t, surrounding the micelle, equation (1.17):

$$\text{CMC} = a_1 t + b_1 \quad \ldots\ldots\ldots\ldots\ldots\ldots\ldots\ldots \quad (1.17)$$

where a_1 and b_1 are constants and t is the reciprocal of the Debye-Hückel function equation (1.18):

$$t = \left(\frac{DT}{\Sigma C_i Z_i^2} \cdot \frac{1000\ k}{4\pi\ Ne^2} \right)^{\frac{1}{2}} \quad \ldots\ldots\ldots\ldots\ldots \quad (1.18)$$

where D is the dielectric constant of the medium

T is the absolute temperature

k is the Boltzman constant

N is Avogadro's number

e is the electron charge

and C_i and Z_i refer to the concentration and valence number of ion species "i".

Equation (1.17) provides another relationship between the CMC and the added salts.

The addition of non-electrolytes such as urea (22) and dioxane (23, 24) have been found to increase the CMC. This is explained by the fact that these substances diminish the hydrophobicity of the surfactants via their effects on the structuring of the water and the lowering of its dielectric constant (11).

(iv) The effect of the hydrocarbon chain on the CMC. The number of carbon atoms constituting the hydrophobic part of a surfactant exerts an appreciable effect on the value of the CMC (11). It has been shown that the longer the chain the lower the value of the CMC and the relationship is represented by the empirical formula equation (1.19):

$$\log \text{CMC} = A - B\alpha \quad \ldots\ldots\ldots\ldots\ldots\ldots \quad (1.19)$$

where α is the number of carbon atoms and A and B are constants. The value of A is dependent on the type and

number of hydrophilic groups while the value of B is dependent on the number of ionic groups and approximates to log 2 for paraffin chain salts with one ionic group (11).

C. STRUCTURE OF THE MICELLE

The picture of the micelle which has evolved to date is one of a hydrocarbon core surrounded by a layer of polar or ionic head groups that separate the core from the surrounding aqueous environment. The hydrocarbon core is considered to be liquid-like in nature as evidenced by NMR (25), X-RAY (26), fluorescence depolarization (27) and other spectral techniques (11) and by the ability of surfactant solutions containing micelles to dissolve hydrocarbons and other hydrophobic substances which would be otherwise insoluble in water. The hydrocarbon chains in the core are generally regarded as disordered and restricted as a result of their close proximity giving the core of the micelle a viscosity several times higher than the corresponding liquid hydrocarbon (28). ESR measurements on solubilized dialkyl nitroxide radicals in sodium dodecyl sulphate show considerable mobility for the solubilizate and they indicate the liquid nature of the micellar core (29, 30). Their spectral lines are somewhat broader, however, than they are in aqueous solutions indicating that the local viscosity is high. On the other hand, the same nitroxide free radical, containing a steroid ring system, solubilized in 0.15M CTAB (29) gave a spectrum which correlated with that for the radical in hexane at -22^{o}, at which temperature hexane is solid, indicating a rigid micellar interior for the CTAB. These techniques, however, employ external probes and it is possible that the hydrocarbon chains in the vicinity of these probes are not in the same state as they would be in an additive-free micelle.

There is some evidence based on measurements by magnetic resonance of fluorinated surfactants that the outer part of the core contain water (31 - 33) as a result of entrapment during the aggregation process. This water has a lower dielectric constant than that of the water in the bulk phase, e.g. Stigter (34) quotes a figure of 2 for the hydrocarbon core boundary as compared to 78.5 for water. The proximity of the non polar micellar core and the large ionic concentration in the Stern layer plus the rough surface of the micelle caused by part of the hydrocarbon chain sticking through the interface between the core and the Stern layer (35) (See Figure 1.4) are some factors contributing to this difference between these two dielectric constants. The question of how far the water penetrates between the micellized hydrocarbon chains is far from resolved, however. A recent report by Stigter (34) emphasises the absence of water from the core of the micelle on the basis of comparing the CMC of various straight chain ionic surfactants in aqueous salt solutions with the CMC's of alkyl sulphates for the same alkyl chain length , ionic strength and temperature and concludes that the average location of the core-water interface is at a distance of 0.8 ± 0.4 Å above the α carbon atom of the hydrocarbon chain and that part of the head group, if sufficiently hydrophobic, would be included within the core. Stigter levels criticism at the assumptions made for the interpretation of the partial molar volume studies carried out by Corkill et al (36) who measured the effect of micellization on the partial molar volume of surfactants as a function of the alkyl chain length and concluded that in micelle formation the hydration of the methylene group adjacent to the hydrophilic group is retained. They assumed that all volume changes at the micelle surface were due to the concentration of ionic charges and that the exposure of the hydrocarbon core surface was much less than 4 ml/mole of micellized

surfactant. Stigter also criticises Clifford's interpretations from spin lattice relaxation studies (31) in which it was concluded that part of the alkyl chain in the micelle was exposed to water, on the grounds of the assumptions made concerning the micelle life time.

Surrounding the core of the ionic micelle is another region, consisting of the ionic head groups and a fraction of the associated counterions, known as the STERN LAYER (see Figure 1.4). The counter ions within this layer are considered to be hydrated (37). The Stern layer and the core are considered to form the kinetic micelle which moves as a unit under an applied EMF. The remaining counter ions are located outside the Stern surface in the Gouy-Chapman part of the electrical double layer. The thickness of this layer is determined by the concentration of the surfactant monomers and added salt in solution. The distribution of the counterions in this layer obeys the Boltzmann distribution law (equation 1.20) which can be expressed as:

$$n_x = n_a \cdot e^{-Ze\psi/kT} \qquad \ldots\ldots\ldots\ldots\ldots\ldots (1.20)$$

where n_x is the ion concentration at distance x from the stern surface,

n_a is the ion concentration at a long distance from surface i.e. in the bulk of the solution,

Z is the valency of the ion,

e is the electron charge,

ψ is the surface potential,

k is the Boltzmann constant,

and T is the absolute temperature.

So far the micelle has been shown to be an aggregated species presenting a hydrophilic surface to the solvent (see Figure 1.4).

This is by no means fixed, rigid entity however. Through temperature jump techniques(38, 39) NMR studies (40) and ultrasonic absorption measurements (41) estimates of the rate constant for the dissociation of one monomer from a micelle are put in the region of 10^2 to 10^9 sec^{-1}. Van Bureau and Gotz (42) showed that CTAB micelles have a breakdown time of less than 10^{-3} seconds. Jaycock and Ottewill (43) reported a half-life of approximately 10^{-2} seconds for the micelles of sodium dodecyl sulphate and dodecyl pyridinium bromide. The micelle must therefore be considered as an extremely complex dynamic entity which is continually breaking down and reforming.

To summarise then, an ionic micelle has three general structural regions, represented diagrammatically in Figure (1.4).

(1) The hydrocarbon core consisting entirely of portions of the hydrocarbon chain. It is assumed that the terminal $-CH_3$ groups are always contained in this core but one or more methylene groups may not be. It is also assumed that no solvent enters the core which resembles in its nature a droplet of liquid hydrocarbon. The radius of the core of a spherical micelle is limited by the maximum length of the hydrocarbon chain that actually constitutes part of that core.

(2) The Stern layer surrounding the core and consisting of the ionic head groups and a fraction of the associated counterions. The Stern layer contains a considerable amount of water and has a lower dielectric constant than the water in the bulk solution.

The core and the Stern layer together with a thin section of the diffuse layer up to the shear plane constitute the

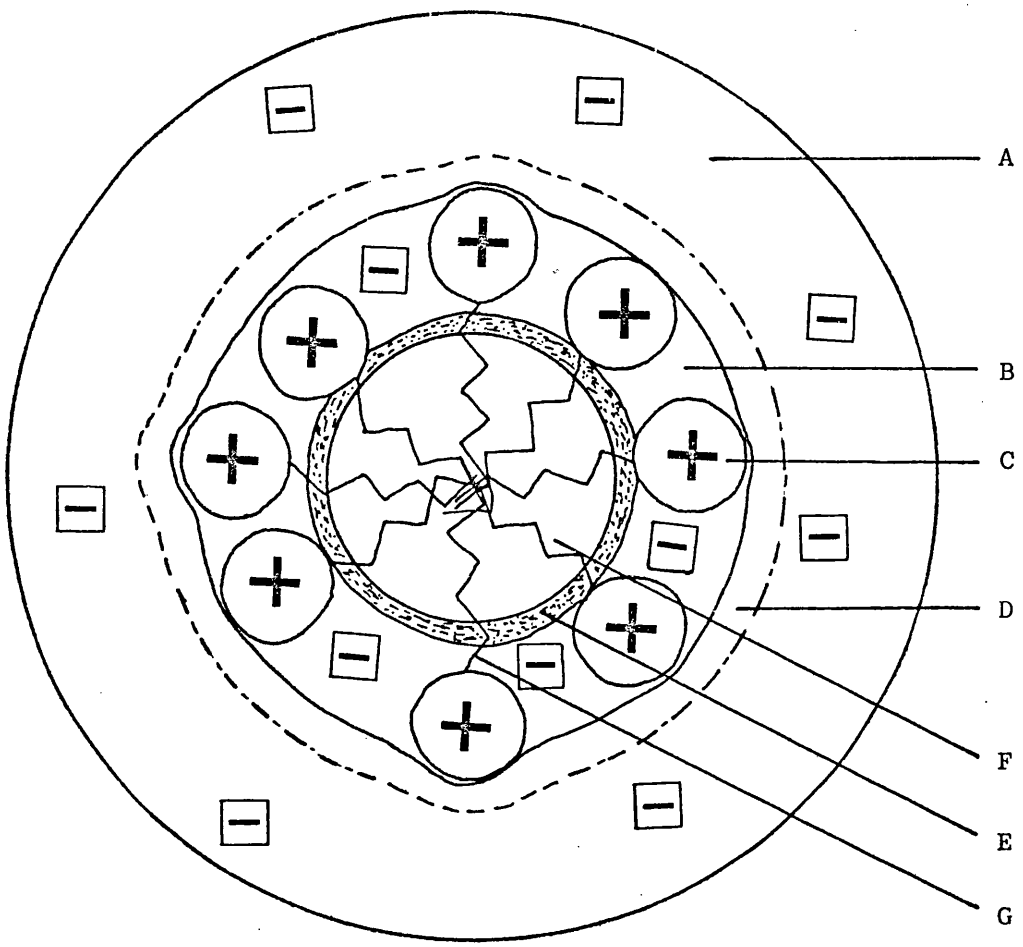

FIG.(1.4.) A SCHEMATIC REPRESENTATION OF A SPHERICAL CATIONIC MICELLE.

A. The Gouy-Chapman diffuse layer

B. The Stern layer

C. Surfactant Head Group

D. Shear plane

E. Core-Stern layer boundary

F. The Core

G. Methylene groups close to head present in Stern layer causing surface roughness.

kinetic micelle which moves as a unit under an applied EMF.

(3) The Gouy-Chapman layer contains the excess counterions required to neutralise the charge on the kinetic micelle. The thickness of this layer is determined by the charge at the Stern plane which depends on the concentration of the surfactant monomers and salts in the system.

D. THE SHAPE AND SIZE OF MICELLES

The shape and size of micelles have been studied by such techniques as light scattering (44,45), viscometry (44, 46 - 48), ultrasonic measurements (49), X-ray diffraction (11) and sedimentation (50). These studies have shown that micelles can be in the form of small spheres, ellipsoides or long cylinders or they may be arranged as a bilayer, that is, two parallel layers of surfactant molecules with the polar groups facing out, as shown in Figure (1.5). Both size and shape of micelles are found to vary with temperature, surfactant concentration, chain length and the presence of electrolytes

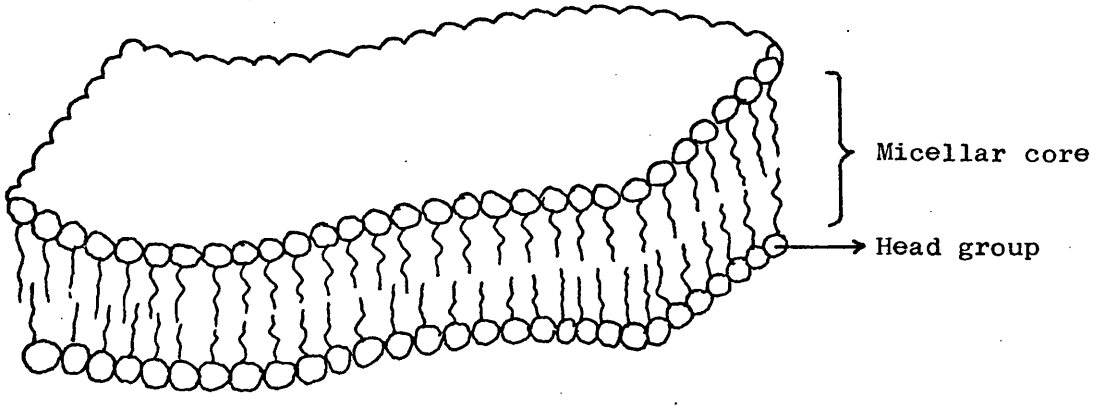

FIGURE (1.5). A SEGMENT OF SCHEMATIC BILAYER MICELLE

and other additives. The aggregation number, i.e. the number of monomers per micelle, is an indication of its size and one of the best methods for determining the aggregation number is by light scattering.

Ignoring their shape, micelles can be divided into two distinct kinds; small micelles with about 50 - 100 monomers and large micelles with over 1000 monomers. All surfactants with a single hydrocarbon chain can form both types and in many systems where the increase in size is not observed under dilute conditions a transition to much larger micelles has been observed at high surfactant concentrations by X-ray scattering (51).

The magnitude of the repulsive force between surfactant head groups influences micelle size as reflected by increasing ionic strength which decreases the repulsion between the ionic head groups and thus favours the formation of larger micelles. The aggregation number of dodecyl ammonium chloride is less than 100 in the absence of added electrolytes but at a concentration of 0.3M sodium chloride the aggregation number is about 10,000 (47). The change in aggregation number of dodecyl-trimethylammonium chloride is not so dramatic, being 40 in the absence of salt to about 75 in the presence of 0.3M sodium chloride. The presence of salt decreases the repulsion between the head groups more effectively when the head group is $-NH_3^+$ than when it is $-N(CH_3)_3^+$ because counterions can approach more closely to the site of the cation charge of $-NH_3^+$ group.

Tokiwa and Ohki (52) investigated the effect of the chain length on the size of the micelle in a homologous series of n-alkyl benzene sulphonates with chain length ranging from C_{10} to C_{15}. They found small, spherical and highly hydrated micelles with the lower

members of the series as compared to large and asymmetric micelles at the higher chain lengths.

Geometric considerations have been applied to the shape of micelles. Schott (53) states that applying simple geometry to experimentally determined micellar sizes would indicate the unlikelihood of spherical micelles forming in solutions of surfactants having a single normal alkyl chain as their hydrocarbon moiety. To illustrate this he calculated that for an n-dodecyl sulphate surfactant forming spherical micelles, 39% of the peripheral area is covered by the sulphate head groups leaving 61% of the hydrocarbon surface exposed to water which is brought about by the repulsion between the negatively charged head groups leaving voids which are filled with water. Tanford (54) using the same approach concludes that most of the common micelles must be ellipsoidal, rather than spherical, in shape as the aggregation numbers are too high to be consistent with a spherical shape. Tanford (28) also states that since the physical properties of the core resemble those of a droplet of liquid hydrocarbon, the volume of the core is calculable. For a given micelle containing "H" hydrocarbon chains the core volume V, in cubic Ångstroms, is given by equation (1.21):

$$V = (27.4 + 26.9\ n_c)H \quad \ldots\ldots\ldots\ldots\ldots\ldots\ldots\ldots \quad (1.21)$$

where (n_c) represents the number of carbon atoms of the hydrocarbon chain that are part of the core. The numerical values of equation (1.21) are based on volume measurements by Reiss-Husson and Luzzati (51). Tanford also calculates the maximum length, in Ångstroms, L_{max}, for a chain with (n_c) embedded carbon atoms as being, equation (1.22)

$$L_{max} = 1.5 + 1.265\ n_c \quad \ldots\ldots\ldots\ldots\ldots\ldots\ldots\ldots \quad (1.22)$$

The surface area per surfactant head group is $(\frac{s}{n})$, where (s) is the total surface area and (n) the aggregation number. Repulsion between head groups will increase $(\frac{s}{n})$ and when this becomes large enough there will be contact between the bulk water and the micelle core.

E. SIZE AND SHAPE OF CTAB MICELLES

The size of the CTAB micelle has been the subject of many studies, (Table 1.1).

Temperature ^{o}C	Concentration of added KBr (Molar)	Aggregation Number	Reference
25	-	95	44
"	-	61	48
30	-	80	55
"	0.003	80	55
"	0.013	169	56
"	0.025	270	55
"	0.025	288	57
"	0.178	2190	45
"	0.233	5000	45

TABLE (1.1). Aggregation Number of CTAB determined by light scattering in the presence of different concentrations of potassium bromide.

Ekwall (44) using light scattering, concludes that a CTAB micelle contains 95 surfactant monomers immediately above the CMC at 25^{o} whereas Hyde and Robb (48) quote 61-72. When a salt such as potassium bromide is added to the system higher values are obtained.

Viscosity and sedimentation data (50) and flow birefringence measurements (58) indicate that at high salt concentrations, rod-like micelles are formed. Ekwall (44) claims that CTAB micelles are very highly hydrated, having about 70 molecules of water associated with each surfactant molecule in the micelle. Granath (50) however, found the water of hydration for CTAB to be 40 molecules per molecule of surfactant in the presence of 0.2 to 0.4M sodium bromide.

At high salt concentrations the CTAB micelles become polydisperse (58, 59) varying in size about the average micellar molecular weight obtained from light scattering by as much as a factor of two (59). Granath (50) reports a micellar molecular weight of 1.2×10^6 g/mole for CTAB at 30^o in the presence of 0.2M sodium bromide and 2.23×10^6 g/mole for the same system in the presence of 0.4M sodium bromide. Through membrane osmometric studies at a concentration of 0.025M potassium bromide, Birdi (60) finds no evidence for polydispersity in the CTAB micellar system.

For a surfactant with a C_{16} straight hydrocarbon chain, the maximum aggregation number compatible with spherical shape is 84, as calculated by Tanford (28, 54). Applying this principle, it appears, from the data in table (1.1) that CTAB micelles are not spherical but ellipsoidal in shape even at very low concentrations and that they certainly deviate from sphericity in the presence of added salt.

Light scattering experiments by Debye and Anacker (45) show that surfactant micelles are relatively small in solutions of low ionic strength, but may become large enough in solutions of high ionic strength to scatter light dissymmetrically. Their dissymmetry data on CTAB in aqueous potassium bromide at a molarity above 0.15

indicated the micelles to be rod-like in shape.

F. ENERGETICS OF MICELLIZATION

At very low concentrations in water, ionic surfactants behave as strong electrolytes and are completely ionized. The proximity of the hydrophobic hydrocarbon chains of the surfactant and water therefore results in a high interfacial energy which causes the total free energy of the system to increase with surfactant concentration. Association of the hydrophobic hydrocarbon chains results in a decrease in the free energy of the system. Recent research (61) shows water to be highly structured as a result of hydrogen bonding, with unbound water molecules in the "cavities" of this structure. Addition of hydrocarbons results in increased structuring of the water which is entropically unfavourable. The transfer of a surfactant molecule from aqueous solution to micelle results in a reduction in the structuring of water in the vicinity of the hydrocarbon chain which increases its internal freedom and in energy being liberated through the attraction between adjacent chains. Mukerjee (62) concludes from thermodynamic data that the latter plays the major part in the free energy change per methylene group on transfer into a micelle.

Various approaches have been made to explain the mechanisms of micellization. They can be divided into two groups - the phase separation model and the law of mass action model.

(1) The Phase Separation Model. This model regards micellization as a phase separation which commences at the CMC and considers the CMC as the saturation concentration for the unaggregated surfactant monomers. For this model, if the micelle is composed of one species, then at constant temperature and pressure

the free energy of micellization is related to the CMC by the following equation (1.23)

$$\Delta G_m^o = RT \log_e CMC \quad \ldots\ldots\ldots\ldots\ldots\ldots\ldots \quad (1.23)$$

where ΔG_m^o is the free energy of micellization,

R is the gas constant,

T is the absolute temperature,

and CMC is expressed in mole fraction of monomers.

This model requires a sharp onset of the CMC, which would then have a single value. Careful determinations of the CMC, however, show it to be a relatively narrow region of concentrations (13, 63). The other conclusion arising from this model is that the activity of the surfactant monomers remains constant above the CMC. If this is so, application of the Gibbs equation (equation 1.24) where Γ is the surface excess of surfactant monomers and $\left(\frac{d\,\gamma}{d\,\log_e a}\right)$ is the change in surface tension with activity indicates that

$$\Gamma = -\frac{1}{nRT} \cdot \frac{d\,\gamma}{d\,\log_e a} \quad \ldots\ldots\ldots \quad (1.24)$$

(n = 1 for non-ionics and 2 for 1:1 ionic surfactants at low conc.) the surface tension must also remain constant with increasing total concentration of surfactant. Careful surface tension determinations, however, on highly purified sodium dodecyl sulphate (64) has indicated increasing activity of the monomers at concentrations above the CMC. Furthermore, premicellar dimerization has been shown by conductivity measurements. Bair and Kraus (65) found that a plot of equivalent conductivity against root concentration for hexadecyltrimethylammonium nitrate at concentrations immediately below the CMC exhibited a slope greater than that predicted for a 1:1 electrolyte

according to Debye-Hückel theory. The expected slope being 81.3 while that determined experimentally was 142.

(2) The Law of Mass Action Model. This model considers the aggregation process as a series of consecutive multiple equilibria. If we consider a cationic surfactant, S^+, of an aggregation number n and a counterion C^-, having a micelle M_n of a charge p, the reaction may be represented as follows:

$$nS^+ + (n-p)\ C^- \rightleftharpoons M_n^{p+}$$

Applying the law of mass action gives:

$$K_m = \frac{\left[M_n^{p+}\right]}{\left[S^+\right]^n \left[C^-\right]^{(n-p)}}$$

where K_m is the equilibrium constant for micellization.
The free energy of micellization per monomer is then given by equation (1.25):

$$\Delta G_m^o = -\frac{RT}{n} \log_e K_m \quad \ldots\ldots\ldots\ldots\ldots\ldots (1.25)$$

Using activities of the various species, Phillips (66) developed a more complete model and calculated the free energy of micellization per monomer, equation (1.26):

$$\Delta G_m^o = \frac{RT}{n}\left[\log_e 3 + 2\log_e n + (n-1)\log_e CMC + (n-p)\log_e (X + CMC)\right]$$

$$\ldots\ldots\ldots\ldots\ldots\ldots (1.26)$$

where p is the effective charge, in the presence of electrolytes, at the CMC,
and X is the concentration of added electrolyte.
When the aggregation number is high and X = 0, equation (1.26) approximates to equation (1.27):

$$\Delta G_m^o = (2 - \frac{p}{n})\ RT \log_e CMC \quad \ldots\ldots\ldots\ldots\ldots\ldots (1.27)$$

At high salt concentration ($\frac{p}{n}$) approaches zero and equation (1.27) compares with equation (1.23) developed for the pseudophase model.

The standard free energy change of micellization may be resolved into its enthalpic ΔH_m^o and entropic ΔS_m^o constituents by the conventional thermodynamic expression, equation (1.28):

$$\Delta G_m^o = \Delta H_m^o - T \Delta S_m^o \quad \ldots\ldots\ldots\ldots\ldots\ldots \quad (1.28)$$

The above considerations have been modified to account for the change in electrical free energy associated with the creation of the Gouy-Chapman diffuse layer during the formation of spherical micelles resulting in the following expression, equation (1.29):

$$\Delta G_m^o = -\frac{(\log_e fm)}{n} - \frac{(\log_e M_n)}{n} + \log_e f_s^+ + \log_e \left[S^+\right] - \frac{F_{el}}{RT} \quad \ldots\ldots \quad (1.29)$$

where fm is the activity coefficient for the micelle,

f_s^+ is the activity coefficient for the monomer,

and F_{el} is the electrical free energy of micelle formation.

The value of F_{el} can be evaluated using the tabulated functions provided by Loeb, Overbeek and Wiersema (67) for spherical charged particles of varying radius and surface potential.

In practice, activity coefficients are ignored since CMC values for ionic surfactants, especially in the presence of salt, are very small and $(\log_e fm)$ in equation (1.29) is divided by (n), which is usually large, becomes negligible and $\left[S^+\right]$ is taken as the CMC and equation (1.29) reduces to equation (1.30):

$$\Delta G_m^o = - RT \left(\frac{1}{n} \log_e M_n + \log_e CMC\right) - F_{el} \quad \ldots\ldots\ldots \quad (1.30)$$

Finally, a recent approach to the mechanism of micellization, based on ultrasonic relaxation studies, has been advocated by Rassing et al (68). It is based on the fundamental principles of Langmuir's adsorption theory and focuses on the exchange of monomers to and from micelles. The equilibrium is represented by the following scheme:

$$S^+ + [M]_1 \rightleftharpoons [M]_2$$

where S^+ is the monomer, in a cationic surfactant, and M_1 is a micelle having one monomer less than a micelle designated M_2. The micelle in this model is defined as "any aggregate containing more than one monomer". Adsorption theory is used to derive equation (1.31):

$$\frac{-d[S]}{dt} = k_1[S](1-\alpha)A - \underline{k}_1 \alpha A \quad \ldots\ldots \quad (1.31)$$

where $[S]$ is the monomer concentration,

A is the total possible surface area of all micelles in solution,

α is the fraction of the total micelle surface area covered by the monomer,

k_1 is the rate constant of monomers adsorbing onto the micelle surface,

$\underline{k}_1$ is the rate constant of the monomers desorbing from the surface of the micelle,

and $\frac{d[S]}{dt}$ is the change in monomer concentration with time.

The adsorption and desorption rates k_1 and $\underline{k}_1$ respectively, are related to the CMC according to the following relationship,

equation (1.32):

$$\frac{k_1 \alpha}{k_1(1-\alpha)} = [S] \approx \text{CMC} \quad \ldots\ldots\ldots\ldots\ldots (1.32)$$

It must be emphasised that the model is still in its infancy and reported here only for the sake of completion.

G. SOLUBILIZATION

Solubilization is a term used to describe the increase in solubility of a substance in a surfactant solution, usually above the CMC, over that in pure solvents. Thus the solubility of the dye Orange OT (1-O-tolyl-azo-2-naphthol) at 30° increases from 0.2 mg. per litre to 1650 mg. per litre as the concentration of dodecyl-ammonium chloride is raised from 0 to 0.5M (69). Solubilization is also physiologically important since it is involved in the transport of fats in the body through the action of bile salts.

From a structural viewpoint there are three possible sites in the micelle for solubilization - the hydrocarbon core for non-polar materials, the Stern layer for ionic substances and the micellar surface where the solubilized molecules are assumed to be adsorbed at the polar surfaces without actually penetrating the micelle. The effectiveness of a surfactant in solubilization will depend on its chain length and its charge type, the size of the head group (70) and the ionic environment of the solution, added electrolytes increasing solubilization.

The partition coefficient of additives between the aqueous bulk phase and the micellar phase can be determined by gel filtration chromatography (71), solubility measurements (71, 72), dialysis (72) or potentiometric studies if the solubilizate has a dissociable group (73).

The position of solubilizates in the micelle has been investigated by NMR (74), ESR (30), UV (75) and potentiometric measurements (73). These studies support generalizations outlined above but owing to the numerous parameters involved, solubilization patterns for any given system are difficult to characterise or predict. Standard works on solubilization are available (76, 77) and they offer critical discussions on observed solubility trends. It is important to mention that solubilization, like micelle formation, is a dynamic equilibrium process. NMR studies on solubilized benzene in the presence of sodium lauryl sulphate and dodecyltrimethylammonium chloride indicate a life-time in the micelle of 10^{-4} seconds or less for the solubilizate (74). Table (1.2) summarises the sites of solubilization of various sub-strates in CTAB micelles.

SUBSTRATE	SUGGESTED SITE OF SOLUBILIZATION	METHOD OF STUDY	REF.
Anthracene	Partly in the hydrocarbon core and partly near the head group.	U.V.	79
Testosterone	Partly in the hydrocarbon core and partly near the head group.	U.V.	80
Pyrene	Micellar Core	Fluores-cence	81
Isopropyl benzene	Orientated at the micelle-water interface	NMR	25
Cyclohexane	Micellar Core	NMR	25
Benzene	Micelle-water interface	NMR	25
Nitrobenzene	Orientated at micelle-water interface	NMR	25
Hexafluoro-benzene	Micellar Core	Conduct-ivity	78

TABLE (1.2) Suggested sites of solubilization of various substrates in CTAB micelles.

Eriksson and Gillberg (25) found that for benzene, N,N-dimethyl-aniline and nitrobenzene at low concentrations, these solubilizates were adsorbed at the micelle-water interface. For isopropylbenzene, however, their findings suggest that it is also adsorbed at the micelle-water interface but orientated in such a way that the isopropyl group is in a hydrocarbon environment and the benzene ring directed towards the hydrated polar region of the micelle.

Conductivity measurements have been carried out on solubilized benzene, cyclohexane, hexafluorobenzene, phenyl ethyl alcohol, m-cresol and various aliphatic alcohols in CTAB micelles (78). These measurements revealed that the equivalent conductivity of CTAB solutions increased with the addition of polar solubilizates, such as phenyl ethyl alcohol, and decreased, linearly, with an increase in the concentration of non-polar additives, such as ethyl benzene. The increase in conductivity was explained in terms of increased counterion dissociation from the CTAB micelles. The decrease was rationalised in two ways: either by assuming that the micelles solubilize hydrocarbons without any change in their ionisation and the only change in the system is a variation in the volume, and hence the mobility of the micelles or by assuming that the decrease in conductance involves a decrease in the degree of ionization of the micelles. The authors suggested that the latter could occur as a result of change in the dielectric environment of the charged groups of the surfactant brought about by the solubilization of the hydrocarbon in the micelle.

Benzene solubilized in CTAB produced conductivity behaviour intermediate between the results just discussed (78). Initial addition produced no change in equivalent conductivity followed by a linear

decrease as the concentration of benzene was increased. The authors offer no explanation for this behaviour.

Solubilization has been used to determine the CMC values of surfactants. Results obtained in this way should be viewed critically, since the presence of additives affects the value of the parameters for which they are employed to determine.

SECTION 3

MICELLAR CATALYSIS

A. INTRODUCTION

It is a well known phenomenon that the addition of surfactants brings about an alteration in the rates of many reactions (82-84). It is also established that such changes result from an association between the substrate and the surfactant micelle, since they are absent at concentrations below the CMC. The kinetic effects of micelles, generally, fit the simple rules put forward by Hartley for absorption of solutes into micelles (85). Hartley's work was on indicators and his rules state:

(1) If the dye is neutral in one form, positively charged micelles will shift the equilibrium to the alkaline side while micelles with negative charges cause a displacement to the acid side.

(2) If the indicator species both have the same charge as the micelles, no equilibrium effect is found.

(3) If both forms of the dye are opposite in charge to the micellar charge, any shift in equilibrium is due to other factors.

Applying these rules in relation to micellar catalysis, reaction (1.33) would be expected to shift to the right in the

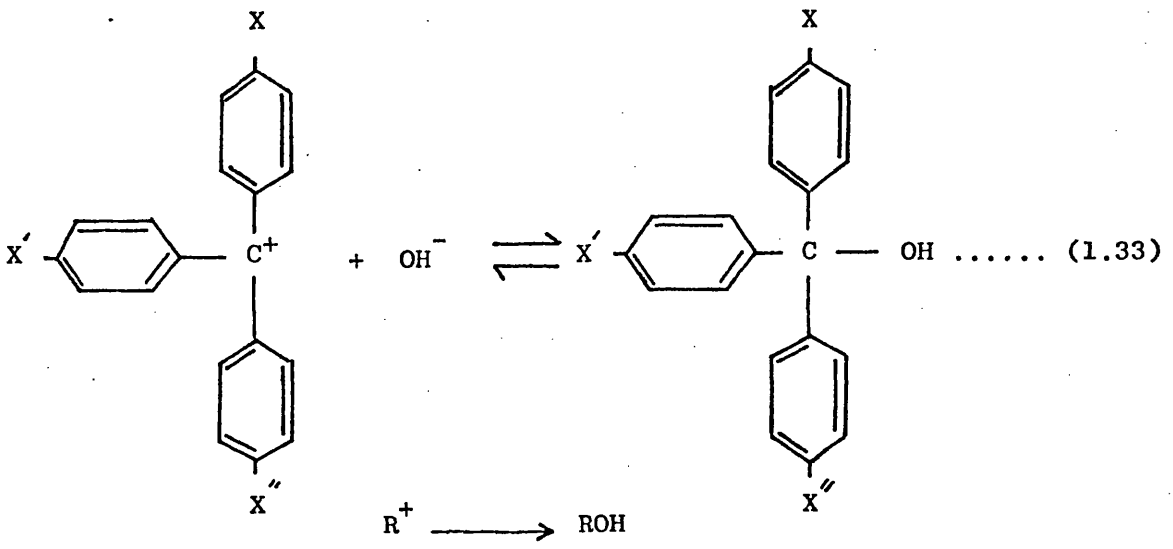

..... (1.33)

presence of CTAB micelles while sodium dodecyl sulphate micelles are supposed to shift the equilibrium to the left. With reaction (1.34), Hartley's rules predict no change in the equilibrium in the presence of anionic micelles. These predictions were found to be true (86).

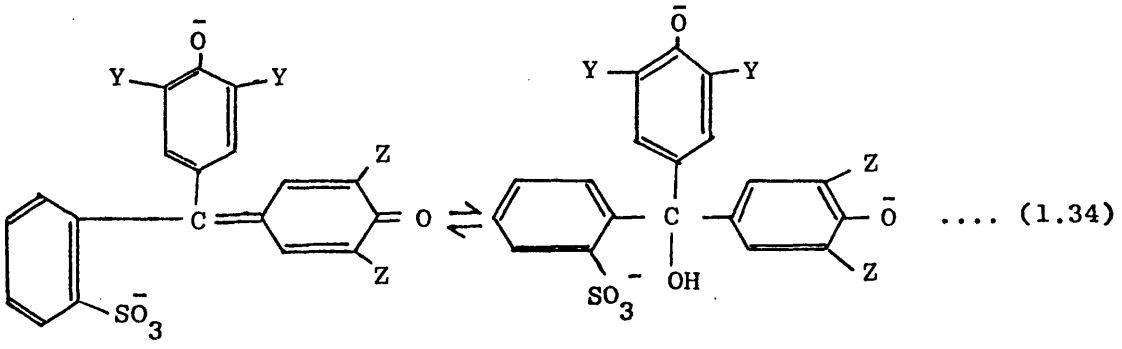

.... (1.34)

R^{2-} ⟷ R^{3-}

The first experimental data attributable to micellar catalysis was by Twitchell (87) in 1906. He observed the enhancement of the rate of hydrolysis of fat bodies in aqueous solutions at 100^{o} yielding fatty acids and glycerol upon the addition of stearosulphonic acid.

One of the first kinetic studies of micellar reactions were reported by Duynstee and Grunwald (86) who investigated the effect of cationic and anionic surfactants on the alkaline fading of stable triphenylmethyl dye cations, e.g. crystal violet, reaction (1.33). They found that the attack of the hydroxyl ion increased 4 to 5 fold in the presence of CTAB micelles. These findings stimulated an enthusiasm which has resulted in an increasing amount of work in this field over the past 20 years, culminating in the recent publication of several comprehensive reviews (82 - 84). These studies have shown the necessity of considering many variables when dealing

with micellar reactions including the nature and concentration of the surfactant, the nature of the substrate, the ionic environment of the reaction, pH, temperature, the nature of the solvent and the interaction constant of the reacting substrate molecule with the micelle and its site of association. Variations in these factors bring about modifications in the electrostatic and hydrophobic interactions between the micelles and the substrate and hence play an important part in the resultant micellar effect, namely enhancement or retardation of the reaction rate.

B. THE EFFECT OF CATIONIC SURFACTANTS ON REACTION RATES

In view of the multitude of work carried out on micellar catalysis, the following section will be restricted, as far as possible, to reactions relating to the micelles of cetyltrimethylammonium bromide (CTAB) and its homologues.

Cordes and his coworkers (88, 89) have investigated the effect of n-alkyltrimethylammonium halides (I)

$$R - \overset{+}{N} - (Me)_3 \; \overset{-}{X} \quad \ldots\ldots\ldots\ldots\ldots\ldots \quad (I)$$

(where R is a hydrocarbon chain of C_8 to C_{18} and X is a halide group) on the alkaline hydrolysis of a group of p-nitrophenyl esters (II),

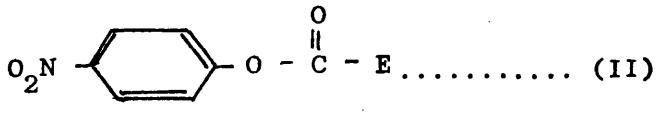

$$\ldots\ldots\ldots\ldots \quad (II)$$

where E was (CH_3-), (C_5H_{11}-) and ($C_{11}H_{23}$-). The reactions were followed spectrophotometrically in carbonate buffer at pH 10.07 and a temperature of 25°. They noted that:

(i) No rate enhancements occurred for any of the substrates below the CMC's of the surfactants.

(ii) For all the esters studied, the degree of catalysis increased as one moves from C_8 to C_{18} surfactants, i.e. as the length

of the surfactant's alkyl chain increases.

(iii) Catalytic effectiveness increased with increase in the length of the alkyl chain of the ester (E in II).

These observations illustrate the necessity of micelles for catalysis to take place. They also show the importance of the hydrophobic bonding between the alkyl chain of the ester and the alkyl chain of the surfactant.

The varying degrees of incorporation of the substrate into the micellar phase, i.e. the partition of the substrate between the micellar phase and the aqueous bulk phase has been determined by Cordes (89) using the gel filtration technique of Herries (71). He determined the partition coefficients for the acetate and hexanoate esters in the presence of tetradecyltrimethylammonium chloride and found them to be 33 M^{-1} and 1600 M^{-1} respectively. This indicates the importance of the hydrophobic interactions between the alkyl chains of the ester and the surfactant. This point is demonstrated further by the pronounced catalytic effect of CTAB micelles on reaction (1.33) page 35. In spite of the electrostatic repulsion between the two species, the catalysis is brought about by the incorporation of the dye into the micelle (83).

In reaction (1.33) however, in the presence of sodium dodecyl sulphate it is possible that ion-ion pair interactions could take place between the surfactant and the substrate causing the equilibrium to shift to the left. These interactions, coupled with suspect CMC values which are not determined in the kinetic environment make it necessary to view early reported sub-micellar catalysis (90) with caution.

A related group of compounds was also investigated by Menger

and Portnoy (90) who studied the effect of a cationic surfactant, n-dodecyltrimethylammonium bromide, on the base catalysed hydrolysis of a p-nitrophenyl acetate, mono-p-nitrophenyl dodecanedioate, p-nitrophenyl octanate and benzyl choline. The determinations were carried out in sodium-borate buffer at pH 10.49 and 25°. An increase in the rate of the hydrolysis was observed in the presence of all the cationic species and it was found to be substrate dependent being more pronounced as one moves from the shorter to the longer chain esters.

Another reaction that has been extensively investigated is the hydrolysis of the Schiff bases. The acid catalysed hydrolysis of benzylidene aniline (III) in boric acid-sodium borate buffer at

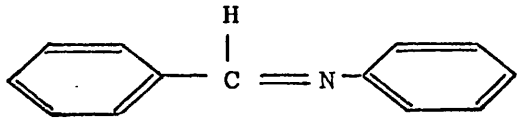

(III)

pH 9.0 and 25° was investigated in the presence of CTAB at concentrations above its CMC (91). Inhibition of the hydrolysis was observed and was directly proportional to the surfactant concentrations between the limits of 0.01 and 0.07M. The rate was reduced by a factor of 20 at 0.01M and by a factor of 128 at 0.07M. The retardation was explained in terms of changes brought about in the medium in the vicinity of the reaction site as a result of changes in the composition of the micelles, presumably their size. A later explaination for this retardation was in terms of electrostatic factors (92) involving the pH at the surface of the micelle as compared to the pH of the bulk phase and taking into account the electrokinetic or zeta potential ζ of the various CTAB concentrations. It is known

that the pH at the surface of a charged micelle is different from the pH in the bulk solution (93). Hartley and Roe (94) deduced that at 25°

$$pH_s = pH_b + \frac{\zeta}{60} \quad \ldots\ldots\ldots\ldots\ldots\ldots\ldots\ldots (1.35)$$

where pH_s and pH_b denote the pH of the surface and the bulk solution, respectively and ζ is zeta potential in millivolts. Crematy and Alexander (92) applied equation (1.35) to the findings of van Senden and Koningsberger (91) and obtained a pH_s of 10.3 and ζ + 78 mV for 0.01M CTAB while the corresponding values for 0.07M were found to be 11.1 and + 126 mV. They rationalised the decrease in rates with increase in CTAB concentration on the grounds of the increase in surface charge (high ζ potential and high pH_s) due to closer packing of the surfactant monomers in the micelle.

Winterborn et al (95) investigated the effect of CTAB on the base catalysed hydrolysis of a group of carboxylic acid esters. They found that the cationic surfactant caused an increase in the rate of hydrolysis of p-nitrophenyl acetate and ethyl-p-nitro-benzoate but a decrease in the rate of hydrolysis of ethyl-p-aminobenzoate and p-amino-phenyl acetate. The nature of the rate modification appeared to depend upon the combined inductive and mesomeric effect of the p-substituent on the benzene ring, influencing the orientation of the ester with respect to the micellar surface. In a later publication concerned with the investigations into the effect of 4.8×10^{-3}M CTAB on the base catalysed hydrolysis of eight p-substituted ethyl benzoates, the same authors (96) found that the nitro and cyano derivatives showed an increase in the rate whereas the acetyl, fluoro, hydrogen, methoxy, amino and diethylamino derivatives showed a decrease in the rate in the presence of the surfactant. They

explained their findings on the basis of a low dielectric constant at the micelle surface coupled with an increased hydroxyl ion concentration in accordance with electrostatic theory.

C. NATURE OF THE SURFACE ACTIVE AGENT

As surfactants exist in four major forms one would expect them to differ in their effect on the hydrolysis of esters depending upon the nature of the polar group. This difference in effect extends even to the members of a homologous series. Bunton et al (97) studied the effect of a series of quaternary ammonium salts on the nucleophilic aromatic substitution reactions using the following compounds (IV)

(IV) 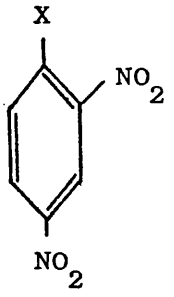 where X = F or Cl

The quaternary salts were:

Phenylcetyldimethylammonium bromide	V
2.4 dimethoxyphenylcetyldimethylammonium bromide	VI
2.4 dimethoxybenzylcetyldimethylammonium bromide	VII
Cetyltrimethylammonium bromide	VIII

Both neutral and anionic nucleophiles, as the attacking species, were considered. They observed that I, VI and VII were more effective than VIII as catalysts for the reactions of both F and Cl derivatives with aniline and hydroxide ions. They attributed the rate difference to the higher number of micelles in the case of

V, VI and VII as compared to VIII at a given concentration; variation in number of micelles being due to the different CMC values of these compounds, being -

2.7×10^{-4}M (V)
0.9×10^{-4}M (VI)
1.8×10^{-4}M (VII)
and 7.8×10^{-4}M (VIII)

They have also investigated a number of phosphate esters (97 - 103) of the general formula (IX) in relation to their hydrolysis

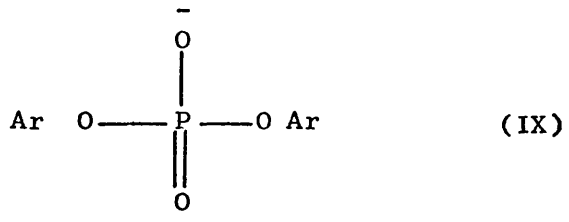

(IX)

and the reaction of these esters with other nucleophiles in the presence of CTAB and cetyltrimethylammonium chloride. They found that the latter was a more effective catalyst than CTAB in the nucleophilic aromatic substitution which was attributed to the higher number of micelles at a given concentration and the difference in their counterions affinity for the micellar surface where there is competition between them and hydroxide ions for binding sites.

D. NATURE OF THE SUBSTRATE

Prior to any alteration of the rate of hydrolysis of a substrate, it is essential that this substrate be incorporated into or onto the micelles. Such an incorporation for a given surfactant is dependent on the chemical nature of the substrate and its polarity. Indeed, some manifestations of micellar reactions can be interpreted in terms of electrostatic interactions and resemble other ion-molecule reactions. The hydroxide-ion catalysed hydrolysis of benzylidene

acetophenone (reaction 1.36) is catalysed by cationic micelles

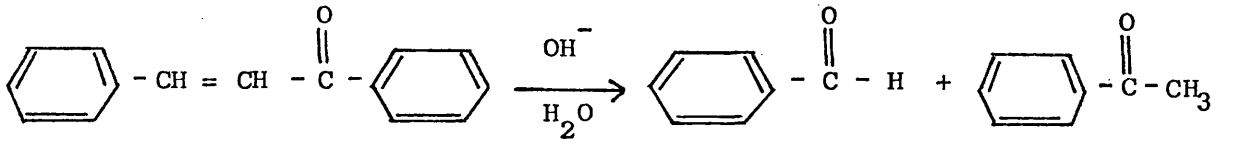

..... (1.36)

of CTAB (104). The dependence of the rate constant of this reaction on the cationic surfactant typifies that for other anion-molecule reactions.

Polar solutes are associated with the surface of the micelle and non polar solutes penetrate the micelle and reside in the hydrocarbon core. Riegelman (75) using U.V. spectroscopy and potassium laurate and dodecylamine hydrochloride solutions indicated four possible positions of association with a micelle. He found that ethyl benzene was solubilized in the core of the micelle, azobenzene in the outer layer of the core, o-nitroaniline in the Stern layer while dimethyl phthalate was adsorbed on the surface of the micelle. These various orientations bring about differences in the hydrolytic rates because of the difference in protection the micelle affords to the molecule.

E. SALT EFFECTS

Added electrolytes affect the CMC, the shape and the size of micelles and bring about alterations in the electrostatic environment of the micelle. It is through these alterations salts affect the catalytic behaviour of micelles in hydrolytic reactions. Cordes et al (105, 106) have observed that sodium dodecyl sulphate catalysed the hydrolysis of methyl orthobenzoate but the addition of inorganic cations inhibited such catalysis. The inhibition was found to increase with increasing ion size. They explained the inhibition

in terms of reduced sites in the Stern layer for the binding of the substrate. To study the inhibitory effects further, Cordes (89) used p-nitrophenyl hexanoate (X) in the presence of 9×10^{-3}M

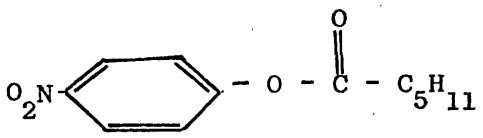

(X)

tetradecyltrimethylammonium chloride and 2×10^{-2}M triethylamine-ammonium chloride buffer. He found that the salts in their inhibitory effects followed a lyotropic series for anions; the order of effectiveness being -

$$F^- < SO_4^{2-} < Cl^- < Br^- < NO_3^-$$

It should be noted that although the SO_4^{-2} ion's size is bigger than the rest of the series by carrying double the charge, its surface charge density is higher than that of the larger mono-ions. The rate of hydrolysis in the presence of a sufficient concentration of bromide and nitrate ions is less than the rate in the absence of the surfactant altogether (105). In the reaction of the alkaline fading of triphenylmethane (86, 107) it was noticed that the fading reaction was also sensitive to added salts. Their inhibitory effectiveness in the presence of 0.01M CTAB was in the same order as above.

Cordes et al (108, 109) investigated the addition of cyanide ion to N-substituted 3-carbamoyl pyridinium ions, reaction (1.37):

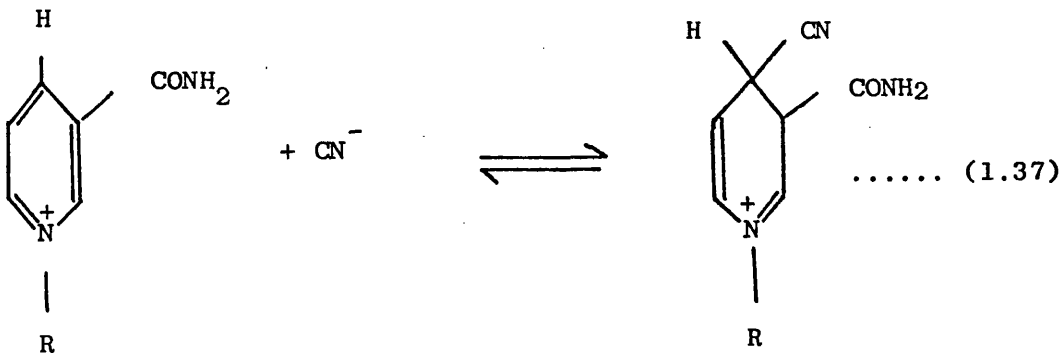

..... (1.37)

and found that CTAB and its lower homologues (C_{10} -C_{14}) increased the rate of addition and shifted the equilibrium to the right. Addition of inorganic salts inhibited this increase in the rate of addition. The inhibition was not as marked as that observed in the ester hydrolysis and the order of the series is somewhat different, being in this case:

$$F^- < NO_3^- < Cl^- < Br^-$$

Added salts also decreased the extent of catalysis of the reaction of hydroxide ion with 2,4 dinitrochloro and fluorobenzene by CTAB (110). The extent of the inhibition depended on the nature of the anions of the salt, being greater for anions with bulky organic residues. This is explained in terms of competition between the hydroxide ion and the anion for the cationic sites on the micelle making it more difficult for the hydroxide ion to attack the organic substrate which is incorporated into the micelle. The larger the ion the greater the exclusion of the hydroxide ion. This exclusion mechanism has been substantiated by a study on the hydrolysis of aryl phosphate monoester dianions (XI) (111)

$$X - OPO_3^{2-} \qquad \text{(XI)}$$

where X is either (XII) or (XIII) below:

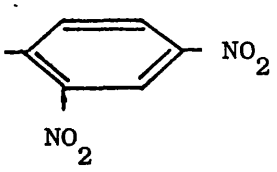

(XII)

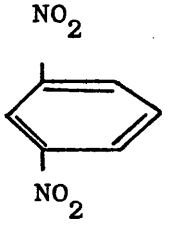

(XIII)

Competitive inhibition was cited as the reason for retardation of hydrolysis in the presence of CTAB with the anions of the added salts preventing the substrate from being incorporated into the micelle.

The reaction kinetics can be represented by the following scheme, (82)

$$M + S \underset{}{\overset{K}{\rightleftharpoons}} MS \xrightarrow{km} \text{Products}$$

$$S \xrightarrow{ko} \text{Products}$$

where M is the micelle, S is the substrate, MS is the micelle-substrate complex and ko and km are the rate constants for product formation in the bulk solvent and in the micellar phase respectively and K is the equilibrium constant for the association of the substrate with the micelle. From such a scheme equation (1.38) results (111):

$$\left(\frac{km - ko}{k_{obs} - ko}\right) = 1 + \frac{N}{K(C_D - CMC)} + \frac{K_I C_I N}{K(C_D - CMC)} \quad \ldots\ldots\ldots\ldots (1.38)$$

where C_D is the total concentration of the surfactant, N is the aggregation number, k_{obs} is the observed rate constant for the product formation, C_I is the concentration of the inhibiting ion and K_I is the binding constant for the inhibiting salt. A plot of $\left(\frac{km - ko}{k_{obs} - ko}\right)$ versus C_I enables the valuation of K_I. Using these equations, Bunton (111) obtained K_I values for the hydrolysis of compound (XII) and (XIII) above in the presence of 3×10^{-3}M CTAB at pH 9.0 and 25° ranging from 4 for NaCl to 2800 for sodium tosylate, $p\text{-}C_7H_7SO_3Na$. These results show that the extent of inhibition by added salts decreases markedly with increasing charge density of the anion, e.g. chloride ion is an ineffective inhibitor as compared with the bulkier tosylate.

Bunton investigated another interesting reaction to elucidate salt effects (112, 113). He examined the decarboxylation of the following compound (XIV) and observed positive salt effects for

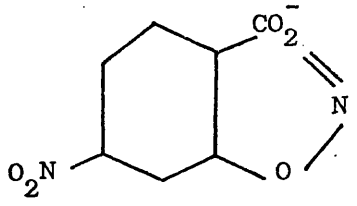

(XIV)

the micelle-catalysed decarboxylation rather than inhibition. The salts followed a lyotropic series in their effects. At a concentration of 2×10^{-2}M in ammonium buffer at pH 9.0 and 25°, CTAB produced a 100-fold rate enhancement. This rate increased in the presence of salts up to 0.8M salt concentration, the order of the effectiveness of the salts being

$$OH^- < F^- < Cl^- < Br^- < SO_4^=$$

Bunton explains these salt effects by postulating an increase in the size of the micelle which would bring the head groups closer together and thus enhances the binding of the molecules with the micelle.

It is thus clear that salts play an important role in the modifying effects of surfactants on reaction kinetics and particular notice must be paid to such conditions as buffer type, buffer strength and total ionic strength when carrying out comparative studies or evaluation of literature reports.

MATERIALS

AND

GENERAL METHODS

MATERIALS AND GENERAL METHODS

MATERIALS

CHEMICALS. The source and grade of the commercially obtained chemicals used are shown in Table (2.1).

CHEMICAL	SOURCE	GRADE
ACETIC ANHYDRIDE	BRITISH DRUG HOUSES	ANALAR
ACETONE	HOPKINS & WILLIAMS	CHROMATOGRAPHY
BENZENE	BRITISH DRUG HOUSES	MOLECULAR WEIGHT DETERMINATION
BORAX	"	ANALAR
CALCIUM CHLORIDE	"	"
CTAB	"	REAGENT GRADE
ETHER	"	ANALAR
ETHYL ALCOHOL	FISONS LTD.	ABSOLUTE B.P.
PHENOL	BRITISH DRUG HOUSES	ANALAR
POTASSIUM CHLORIDE	"	"
SODIUM BICARBONATE	"	"
SODIUM CARBONATE	"	"
SODIUM HYDROXIDE	"	"
SILVER NITRATE	"	"

TABLE (2.1) Source and grade of chemicals used.

Benzene was redistilled for surface tension and light scattering measurements. With the single exception of CTAB all other chemicals were used without further treatment. Buffer salts were kept in a dessicator at room temperature.

Purification of CTAB. The reagent grade CTAB was further purified according to the method given by Mukerjee and Mysels (114). The solid product was soxhlet extracted with petroleum spirit (B.pt. 40^{o} - 60^{o}) for 36 hours. It was then dried and shaken with ether and filtered. The solid product was redissolved in a minimum amount of hot ethanol. Cooling in the refrigerator gave a crystalline mass which was filtered off at room temperature with a slight loss as the solid partly redissolved in the ethanol. The moist crystalline mass which was left on the filter funnel was redissolved in ethanol. Anhydrous ether was then added which caused precipitation of some of the surfactant, which was redissolved by warming. Recrystallization, by cooling, gave a white crystalline product which was filtered off. This process was repeated three times. The final product was then dried in a vacuum oven at 50^{o} for 24 hrs. The purity of the sample was assessed in the following ways:

(i) Melting Point. This was found to be 232^{o} (literature value is 226 - 235^{o}) (86).

(ii) Surface Tension versus Log Concentration Plot. This method is commonly used, and generally accepted, as a criterion for purity (12). A plot of the surface tension of a series of surfactant concentrations in aqueous solutions against the logarithms of such concentrations is shown in Fig.(2.1), which shows the profiles before and after the recrystallization treatment. Table (2.2) gives the data used for these profiles.

The absence of a minimum in the profile of the recrystallized sample was taken as an indication of its purity.

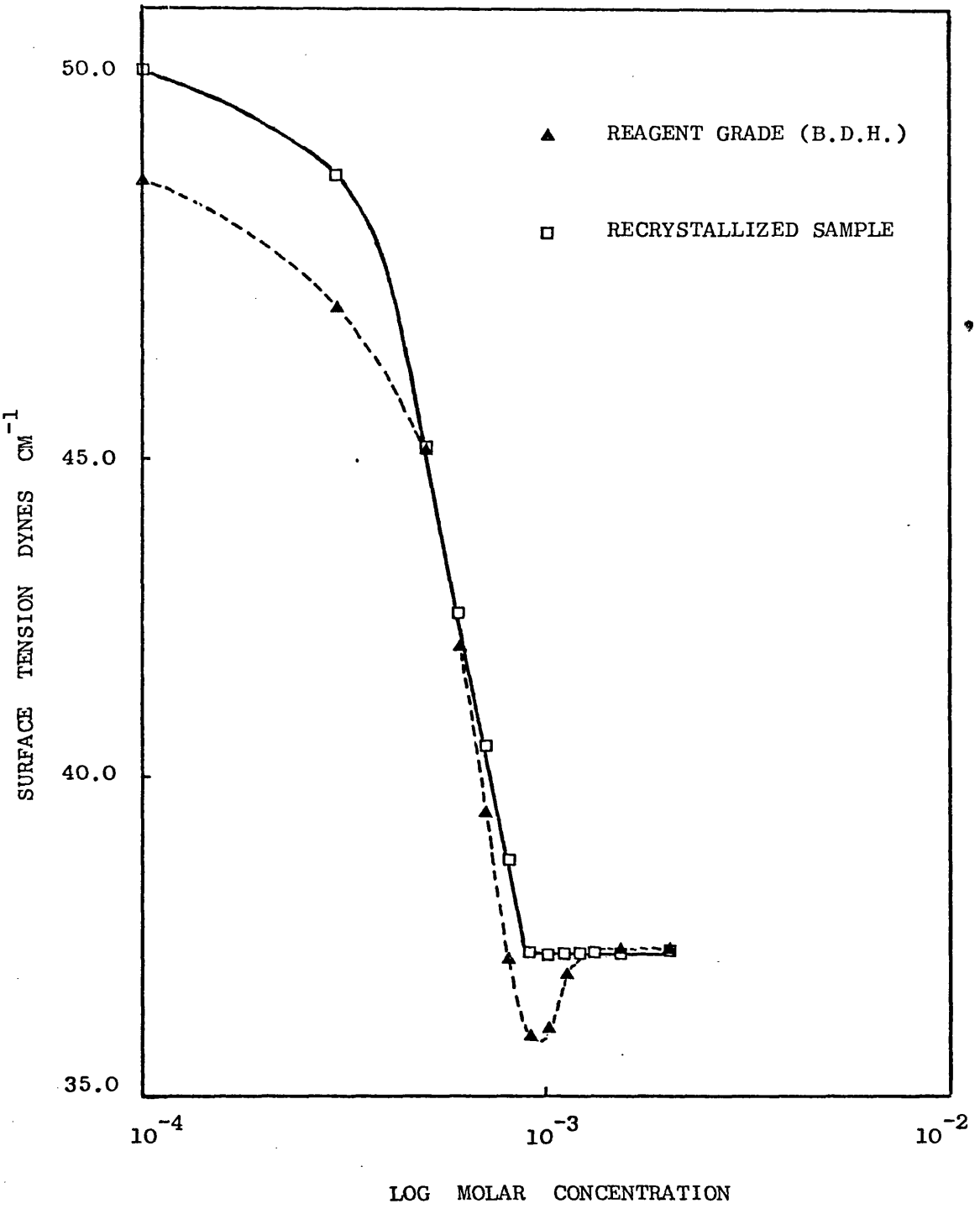

FIG. (2.1). A PLOT OF THE SURFACE TENSION AGAINST THE MOLAR CONCENTRATION OF CTAB IN WATER AT 30°.

MOLAR CONCENTRATION OF CTAB x 10^4	SURFACE TENSION IN DYNES CM^{-1}	
	BEFORE RECRYSTALLIZATION	AFTER RECRYSTALLIZATION
1.00	49.30	51.10
3.00	47.35	49.40
5.00	45.28	45.25
6.00	42.07	42.57
7.00	39.38	40.50
8.00	37.03	38.65
9.00	35.90	37.25
10.00	35.97	37.20
11.00	36.88	37.19
12.00	-	37.20
13.00	-	37.25
15.00	37.30	37.25
20.00	37.30	37.30

TABLE (2.2). Values of surface tension of CTAB solutions in water at 30° before and after recrystallization of the reagent grade.

(iii) Mass Spectrometry. A sample of the recrystallized CTAB was submitted to the PHYSICO-CHEMICAL MEASUREMENTS UNIT at HARWELL (DIDCOT - BERKS). Their analysis showed the highest mass at m/e 269. As it is known that the analysis leads to a loss of a (CH_3-Br) group, this figure indicated the sample to be predominantly $C_{16}H_{33}NMe_2$. From other peaks it was concluded that the sample contained less than 1% of other homologues.

(iv) Molecular Weight Determination. A Radiometer-Copenhagen assembly consisting of an ABU-1C Autoburette and a TTT-1d titrator, which recorded the volume of the titrant added automatically, was used for the potentiometric titration

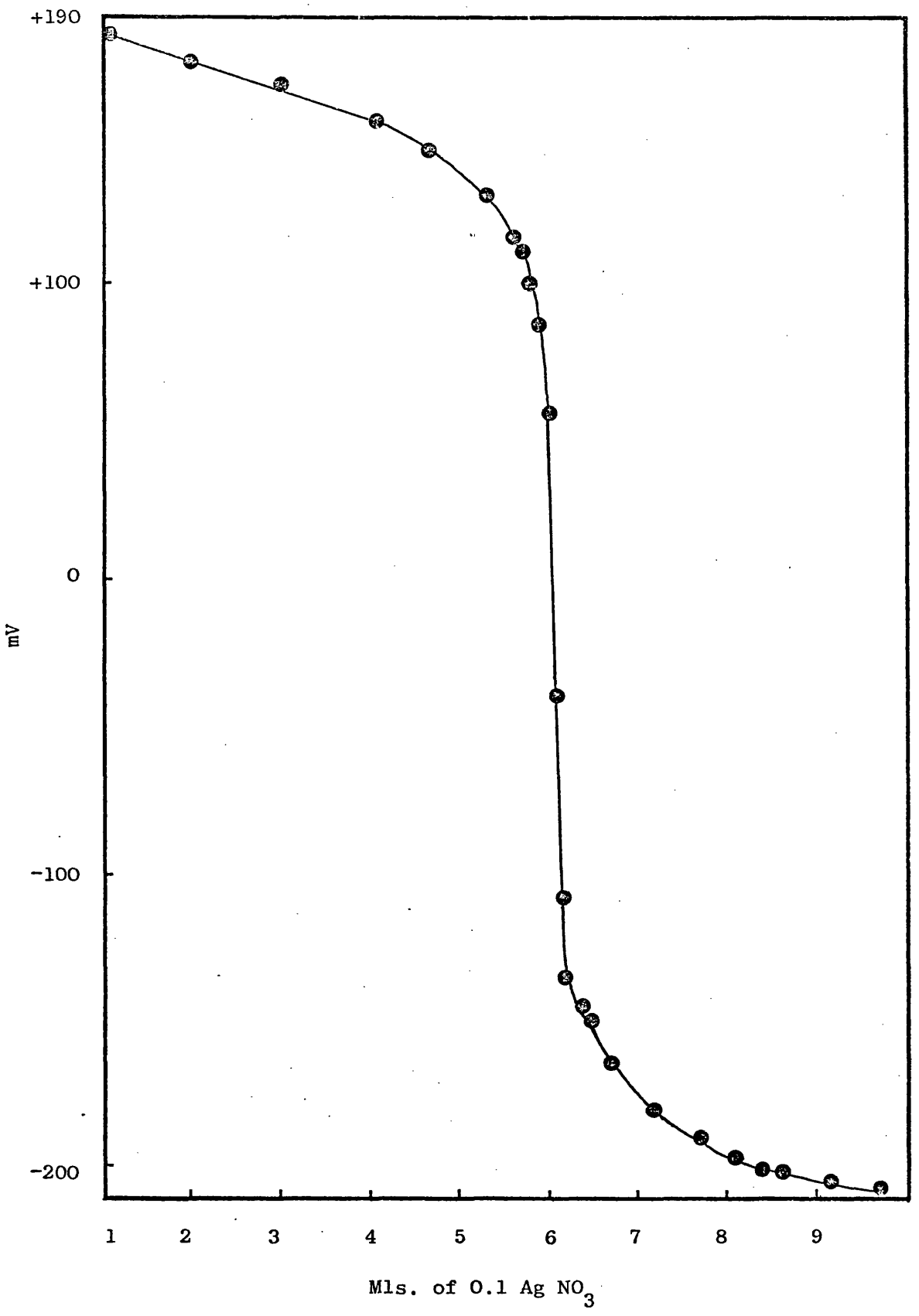

FIGURE (2.2). THE TITRATION OF CTAB AGAINST SILVER NITRATE SOLUTION FOR THE DETERMINATION OF MOLECULAR WEIGHT OF CTAB.

of an accurately weighed sample of CTAB with a standardized silver nitrate solution. The molecular weight obtained was 364.15 (lit. 364.46). The plot of the titration is shown in Fig.(2.2).

Synthesis of Phenyl Acetate. Phenyl acetate was synthesised according to the method given by Mann and Saunders (115), as indicated in the following scheme:

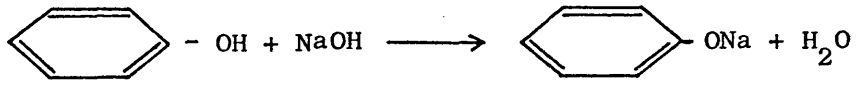

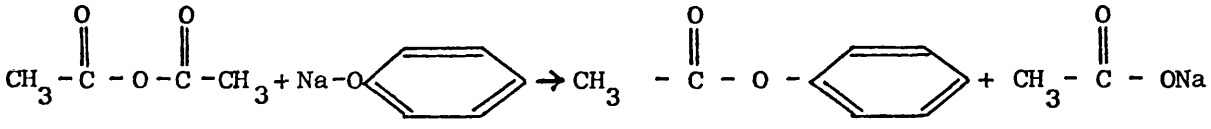

The crude product obtained was fractionally redistilled, under vacuum, and only the middle fraction collected, boiling at about 60°. The purity of the sample was assessed by determination of the boiling point and mass spectrometry. The latter showed a single peak at 136 confirming the purity of the sample. The boiling point was found to be 195.5° compared to the literature value of 196.0° (115). The ester was stored in the refrigerator in a blackened, stoppered flask and the refractive index (n_D^{30} = 1.5002) was determined at regular intervals to assess the purity and to ensure that hydrolytic processes did not take place.

Water. Water used throughout this work was double distilled from an all-glass still.

EQUIPMENT.

Glassware. Grade B glass was used throughout, with the exception of 1 ml. pipettes which were of grade A.

Spectrophotometers

(i) UNICAM SP600 with a wavelength range from 185 to 1000 nm.

(ii) UNICAM SP1800 with a wavelength range from 185 to 800 nm. This was fitted with an SP1805 programme controller and a UNICAM AR25 Linear recorder.

(iii) PERKIN-ELMER double beam 124 with a wavelength range from 100 nm. to 900 nm. fitted with a Perkin-Elmer 56 recorder.

pH Meters

(i) PYE DYNACAP pH-meter fitted with a PYE INGOLD 405 combined glass-calomel electrode and 622 thermal resistor. The expanded scale was readable to 0.002 pH units.

(ii) RADIOMETER 27 S.E. Copenhagen fitted with a PYE INGOLD 405 combined glass-calomel electrode and 622 thermal resistor. Scale as above.

pH-Stat.

A RADIOMETER pH-STAT assembly consisting of an ABU-1C Autoburette (2.5 ml.) and a TTT-1d Titrator-pH-meter which recorded the volume of the titre automatically.

Conductivity Meter

A WAYNE-KERR Autobalance Universal Bridge model B641.

Fraction Collector

An LKB RADI-RAC with a drop counter attachment and an LKB miniflow precision micropump type 4501.

Refractometers

(i) ABBÉ-"60" supplied by Bellingham and Stanley Ltd. fitted with a water heated prism block.

(ii) RAYLEIGH-HABER-LÖWE interference liquid refractometer for differential refractive index increments fitted with a temperature control jacket, 1 cm. two-compartment cell

supplied by Optex Ltd. and two matched thermometers.

Light Scattering Photometer

BRICE-PHOENIX model 2000 supplied by Phoenix Precision Instrument Co. fitted with a circular heating jacket as described by Trementozzi (116) and a W.P.A. moving coil GALVANOMETER with an 18 cm. scale bearing 10 divisions per cm. and a sensitivity of 925 mm./μA.

Melting Point Apparatus

Supplied by Gallenkamp Ltd.

Travelling Microscope

Supplied by Tool and Instrument Co.Ltd.

Balances

(i) OERTLING single pan balance model R20.

(ii) SARTORIUS type 2604 (used for density measurements).

Centrifuge

M.S.E. high speed model 18.

Thermocouple

Supplied by Light Laboratories - Brighton. This was used for temperature monitoring within the spectrophotometers, the light scattering photometer and the gel filtration column.

GENERAL METHODS

Cleaning of Glassware. Unless otherwise stated, all glass-ware was cleaned by soaking for at least 30 minutes in "chromic acid" mixture, washed five times with tap water, rinsed three times with freshly distilled water and finally once with double distilled water. The glass-ware was then dried in an oven and used only once

before subjecting it to the same treatment again. The same glassware was used throughout the entire experimental programme and, whenever possible, the same flasks were used for the same concentrations throughout.

Temperature Control.

(i) For surface tension measurements, solubility, gel filtration and pH-stat studies the heating and circulating of the water was effected by Techne heaters (Techne Ltd.) which maintained the temperature at $30^{\circ} \pm 0.05$. The water baths were well insulated and the surface of the water was covered with "All Pas" plastic balls to minimise evaporation and temperature fluctuations.

(ii) For viscosity, light scattering, refractive index, density and kinetic studies in the spectrophotometer the heating water baths were supplied by Laboratory Thermal Equipment Ltd. These baths maintained the temperature at $30^{\circ} \pm 0.005$ as determined by conductivity measurements on a Wayne Kerr Autobalance conductivity bridge, used in conjunction with a calibrated thermistor, over a period of 8 hours. The water circulation to the temperature jackets of the refractometer, the spectrophotometer and the light scattering photometer was effected by the pumping mechanism from the Techne heaters. The actual temperature within these instruments was monitored using a thermocouple immersed in a cuvette or a cell and connected to an electric thermometer. The latter was calibrated against a certified thermometer, supplied by Gallenkamp Ltd., which had a limit of accuracy of $\pm 0.02^{\circ}$ as certified by the British Standards Institution.

Preparation and Standardization of Buffers. The buffer used throughout this work was the Delory and King buffer (117). It consisted of anhydrous sodium carbonate and sodium bicarbonate. The ionic strength adjustment to 0.5M for all the studies was made with potassium chloride solution using the pK_a values for carbonic acid (pK_1 = 6.352 pK_2 = 10.329) given by Robinson and Stokes (3) after corrections for temperature using the equation given by the same authors.

The pH of the buffer solutions was determined on a Radiometer 27 S.E. or a Pye Dynacap pH-meters. These were calibrated, at 30°, using standard phthalate and borax buffers which were prepared according to Bates (118). The standard pH values for these buffers at various temperatures are given in Documenta Geigy (117). The response of the electrode for determinations involving surfactant solutions was noticed to diminish. The electrode was, therefore, washed with alcohol, dilute hydrochloric acid and copious amounts of distilled water after these determinations and was not used again until it gave the correct response using the standard buffer solutions.

A 2-litre stock solution of double strength buffer was always prepared and adjusted to an ionic strength of 0.832 with potassium chloride and the correct pH, with the dropwise addition of $^N/_{10}$ sodium hydroxide solution. Volumes added during this adjustment procedure were never greater than 4 mls.

Preparation and Standardization of Experimental Solutions. 50 mls. of the buffer stock solution was placed in a reaction vessel and appropriate volumes of CTAB and potassium chloride, from 0.2M stock solutions, were added. The vessel was then

stoppered and equilibrated to 30° and the pH of the solution was measured and, if necessary, adjusted by the dropwise addition of N/10 sodium hydroxide solution until the required pH was obtained. This solution was then made up to a volume of 96 mls. with double distilled water, in a previously calibrated flask. The volumes of CTAB and potassium chloride solutions were calculated in such a way that when 48 mls. of the 96 mls. solution were taken and 2 mls. of the ester solution were added, the final ionic strength would be 0.5M and the CTAB concentration would be the required one for that particular experiment. Table (2.3) gives four examples of making up the solutions as explained above.

Required Molar Concentration of CTAB	Volume of 0.2M CTAB mls.	Volume of 0.2M Potassium Chloride mls.	Volume of Double Strength Buffer (μ=0.832) mls.	Final Volume Adjusted with water mls.	Final Ionic Strength μ
4.0×10^{-3}	2.0	40.0	50.0	96.0	0.52083
1.0×10^{-2}	5.0	37.0	50.0	96.0	0.52083
4.0×10^{-2}	20.0	22.0	50.0	96.0	0.52083
8.0×10^{-2}	40.0	2.0	50.0	96.0	0.52083

Table (2.3). Volumes of constituent solutions for the preparation of standardized mixtures for kinetic and other studies. (See flow-chart page 76)

Surface Tension Measurements of Surfactant Solutions.

Introduction. In their compendium of the critical micelle concentration of aqueous surfactant systems, Mukerjee and Mysels (12) cited 71 methods for the determination of CMC. Surface tension and

electrical conductivity were, by far, the most used and most frequently quoted of these methods. The conductivity method has greater limitations, however, when dealing with systems containing high concentrations of electrolytes. For this reason the surface tension method was used for the CMC determinations and the conductivity method was utilized as a check procedure. For surface tension measurements, the Wilhelmy plate method was used (119).

Apparatus and Procedure. The apparatus was constructed by modifying an Oertling balance (119). The principal components of the assembly are shown, diagrammatically, in Fig. (2.3). A standard microscope cover glass, the plate, was attached to one of the pans with non-spun, monofilament nylon thread with a platinum hook. This allowed for the total submersion of the plate in "chromic acid" mixture for cleaning. It also allowed for the exact balancing of the free plate and the nylon thread by counterweights on the other balance pan. The plate, during actual determinations, was housed in a special glass container which had a wide mouth to allow the plate to enter without touching the sides. During determinations, the container was covered with a halved plastic petri dish which had a circular hole in the middle to allow for the free movement of the nylon thread. The container was mounted on a moveable rack and pinion arrangement that could be raised or lowered very smoothly. A beam of light could be focused onto a mirror, situated centrally on top of the fulcrum. Any slight movement of this mirror resulted in a large displacement of a light spot, with a central hair-line, received on a marked scale. The vertical position of the balance could be adjusted by

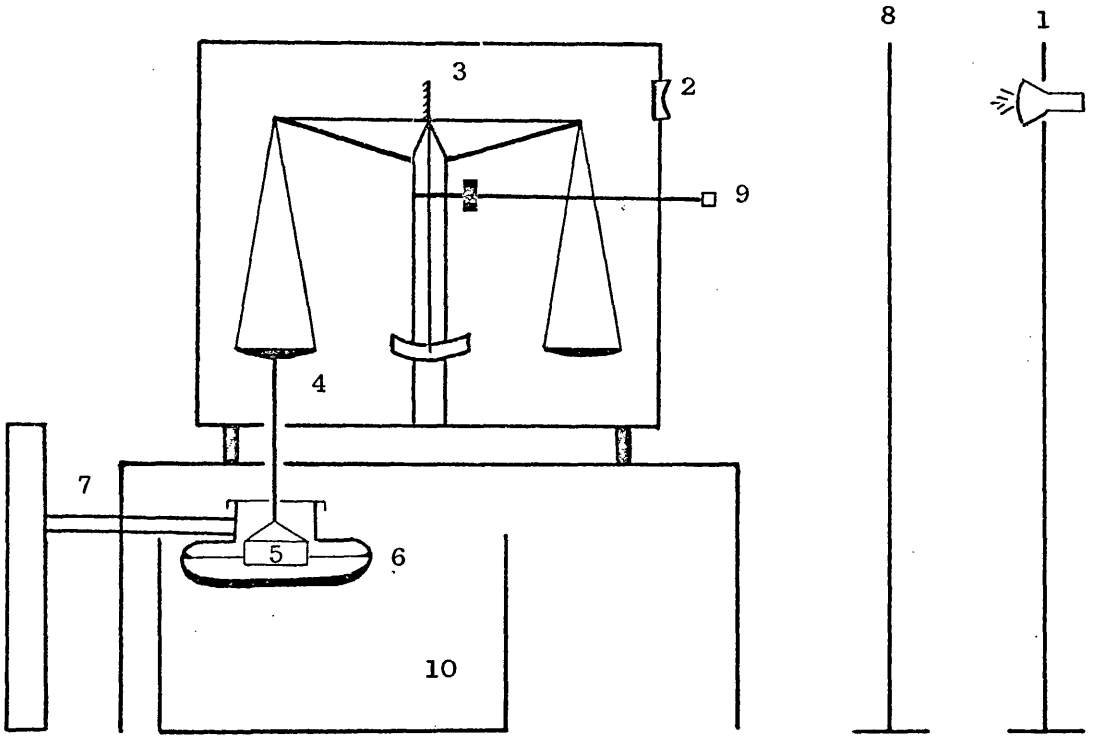

FIG. (2.3). SCHEMATIC REPRESENTATION OF THE WILHELMY BALANCE ARRANGEMENT FOR THE SURFACE TENSION MEASUREMENTS.

1. LIGHT SOURCE
2. A LENSE
3. MIRROR AT CENTRE OF FULCRUM
4. NON-SPUN NYLON THREAD
5. GLASS COVER SLIP
6. SPECIAL GLASS FLASK WITH COVER
7. RACK AND PINION
8. SCALE FOR RECEIVING THE LIGHT SPOT
9. CHAIN WEIGHT ARRANGEMENT
10. WATER BATH

levelling screws on the legs of the balance and checked by a built-in spirit level. The horizontal position of the plate, on the other hand, was checked by its reflected image in the solution which acted as a mirror.

The surface tension is given directly by the downward force acting upon the periphery of the wetted plate. The zero position of the plate was noted from the position of the light spot. The balance beam was then clamped in this zero position. The solution was then raised, gently, until the plate just touched the surface of the solution. The balance beam was then released. As a result the plate sank into the solution and the light spot was displaced upwards on the scale and away from the zero position. Counter-weights were then placed on the other balance pan until the light spot was slightly above the zero position. The final fine weight adjustment needed to bring thespot back to zero position was made by adding weights from a chain weight attached to a circular scale mounted on the column of the balance. This enabled the accurate addition of 0.5 mg. at a time. The final total weight was recorded. This was repeated three times for each determination and the average of the three readings was taken as the weight necessary to bring the plate to the zero position. The surface tension was then calculated from the following relationship (2.1):

$$\gamma = \frac{wg}{2(L + t)} \qquad \text{(2.1)}$$

where γ is the surface tension in dynes cm^{-1}.

w is the weight, in grammes, necessary to bring the plate to the zero position.

g is the acceleration of gravity, taken as 981 $cm.sec^{-2}$

L is the width of the plate in cms.

and t is the thickness of the plate in cms.

The thickness and the width of the plate were determined using a travelling microscope.

Determination of Accuracy of the Method. The apparatus was tested using liquids with well known surface tension values, namely water and benzene. The water was a freshly double distilled sample that was boiled and cooled. Table (2.4) shows the determined and literature values:

Liquid	Temperature	Determined Surface Tension dynes cm^{-1}	Literature dynes cm^{-1}	Reference
Water	25^{o}	71.88	71.97	120
	30^{o}	71.20	71.18	120
Benzene	30^{o}	27.49	27.56	120

Table (2.4). Determined and literature values of surface tension of water and benzene.

EXPERIMENTAL

EXPERIMENTAL

DETERMINATION OF CMC OF CTAB

By Surface Tension. Prior to any surface tension determinations on the surfactant solutions, the volumetric flasks and the special glass containers were allowed to "age" by preparing the appropriate solutions and leaving them standing in the flasks and the containers, which were covered with aluminium foil, for a period of 24 hours. These solutions were then discarded and fresh ones were made up and transferred from the volumetric flasks to the special containers, covered again, and were allowed to stand in the water bath for at least three hours to allow for surface ageing (9) and temperature equilibration. The CMC of CTAB was then determined under the experimental conditions. The data are given in Table (2.5) and a representative diagram of the surface tension against the logarithm of the molar concentration is given in Fig.(2.4).

By Conductivity. A conductivity cell with a cell constant of 50.47 cm^{-1}, as described by Winterborn (121) was used in conjunction with a Wayne-Kerr Autobalance Universal bridge B641. The conductivity bridge had a discrimination of 0.01% of the maximum of all ranges between 20 p Ω^{-1} and 500 p Ω^{-1}. The cell was held in the water bath, at 30^{o}, for at least 30 minutes for temperature equilibration prior to any determinations. The CTAB solutions were prepared using a stock buffer solution and previously aged volumetric flasks. The cell was rinsed with a continuous stream of freshly distilled water for at least half an hour, then three times with the solution whose conductivity was to be measured. The cell

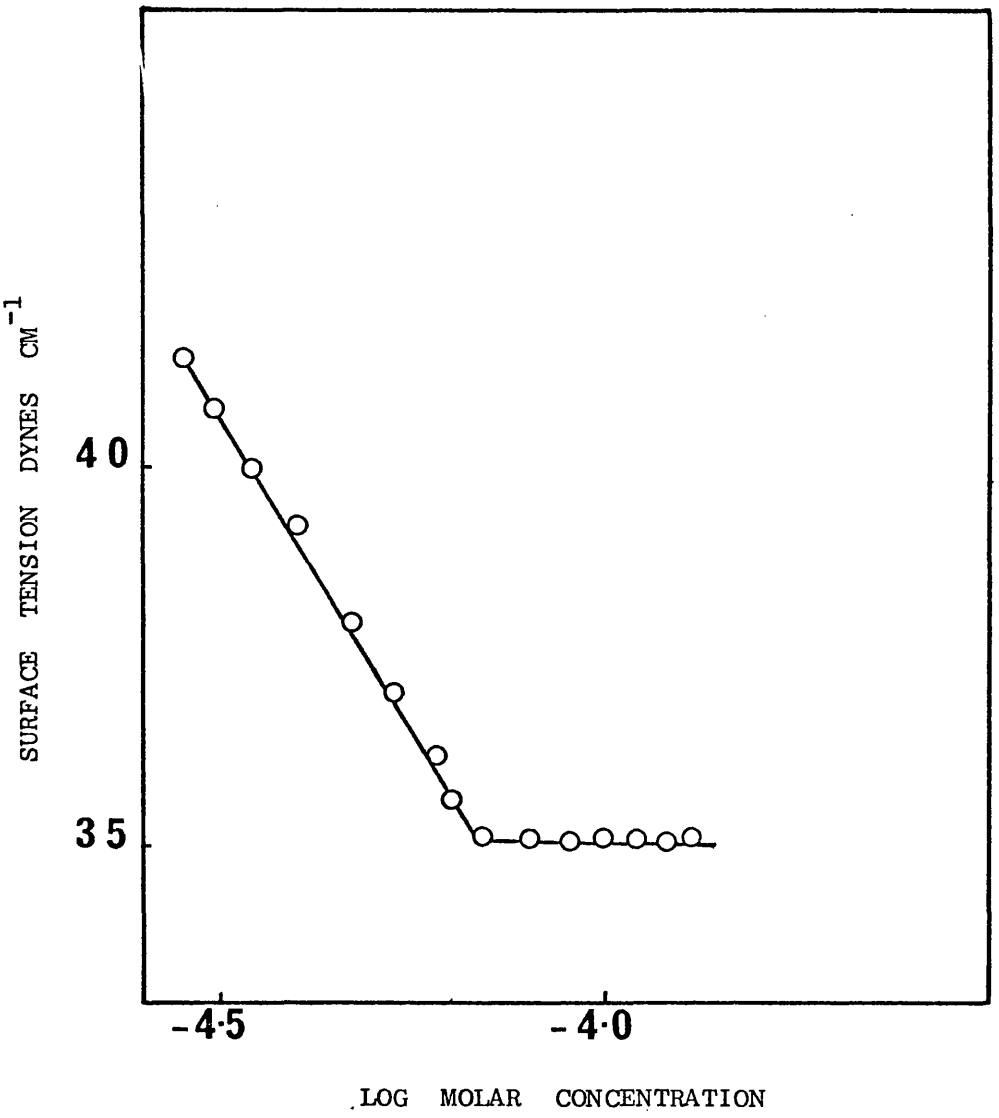

FIG. (2.4). A PLOT OF SURFACE TENSION AGAINST THE LOG MOLAR CONCENTRATION OF CTAB IN CARBONATE-BICARBONATE BUFFER AT pH 9.2 AND IONIC STRENGTH OF 0.5M AT 30°.

was then stoppered and placed in the water bath and the terminals of the conductivity bridge connected to the electrodes. Readings were then taken after temperature equilibration. Three readings were taken for every solution by introducing a fresh portion of the same solution and repeating the procedure. The average conductivity value of the three readings for each CTAB solution was then plotted against the molar concentration of CTAB. The CMC was then taken from the point of intersection of the two linear portions of the curve below and above this region. Fig.(2.5) shows such a plot for the conductivity of CTAB solutions in carbonate-bicarbonate buffer in the presence of phenyl acetate.

The CMC of CTAB was determined for each condition of the kinetic and physical studies. The results are shown in Table (2.5).

CONDITIONS	METHOD OF DETERMINATION	CMC (Molar)
Water	Surface Tension	9.00×10^{-4}
Water + Potassium Chloride	Surface Tension	7.00×10^{-5}
Carbonate-Bicarbonate Buffer and Potassium Chloride		
pH 8.0	Conductivity	7.02×10^{-5}
pH 9.2	Surface Tension	7.00×10^{-5}
pH 9.8	Surface Tension	7.00×10^{-5}
pH 10.2	Surface Tension	7.05×10^{-5}
Buffer + Potassium Chloride at pH 9.2	Conductivity	7.05×10^{-5}
Buffer + Ester + Potassium Chloride at pH 9.2	Conductivity	6.90×10^{-5}

Table (2.5). The CMC of CTAB at 30^{o} under the conditions used for kinetic and physical studies - all at ionic strength 0.5M, except the first system.

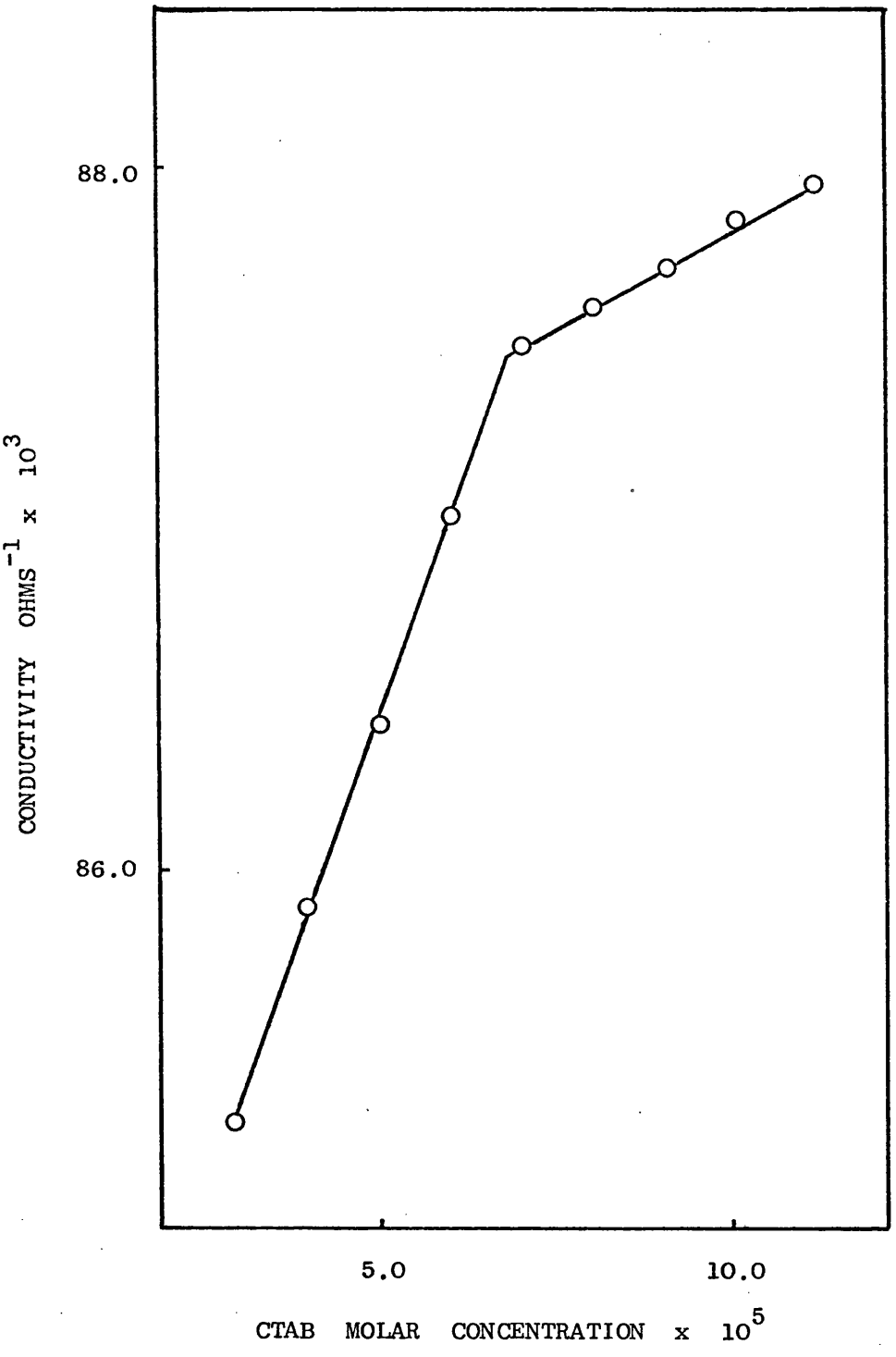

FIG. (2.5). A PLOT OF CONDUCTIVITY AGAINST MOLAR CONCENTRATION OF CTAB IN CARBONATE-BICARBONATE BUFFER AT pH 9.2 AND 30° IN THE PRESENCE OF 8 x 10^{-4}M PHENYL ACETATE.

It can be seen that in the presence of buffer and salt the CMC decreased from 9.00×10^{-4}M to 7.00×10^{-5}M but changing the pH did not seem to affect its value. For the purpose of this study the CMC in water was taken as 9.0×10^{-4}M and the CMC in buffer solutions and salt solutions with an ionic strength of 0.5M was taken as 7.00×10^{-5}M, which is the mean of all values, with a standard error of 7.8×10^{-7}.

KINETIC STUDIES ON THE HYDROLYSIS OF PHENYL ACETATE

Determination of Assay Method for the Hydrolysis Studies

Introduction. In order to be able to accurately measure the rate of hydrolysis of an ester it is essential that an assay process be available which unequivocally will allow a true estimate to be made of the amount of the ester degraded. In general, this means that either the ester or all of its degradation products must be assayed accurately by one of the many physical assay procedures available. The most convenient and commonly used is the spectrophotometric technique.

The extent of absorption of light at any given wavelength is governed by the Beer-Lambert relationship which can be expressed as (2.2).

$$A = \log \frac{I_o}{I} = abc \quad \ldots\ldots\ldots\ldots\ldots\ldots\ldots (2.2)$$

where I_o is the intensity of the incident light,

I is the intensity of the transmitted light,

$\log \frac{I_o}{I}$ is the absorbance or optical density, A,

a is the extinction coefficient,

b is the length of the light path,

and c is the concentration of solute in grammes per litre.

If c is expressed in moles per litre, the Beer-Lambert relationship can be written as, equation (2.3)

$$D = A_m C L \quad \ldots\ldots\ldots\ldots\ldots\ldots\ldots\ldots (2.3)$$

where D is the optical density at a fixed wavelength, usually the wavelength of maximum absorbance (λ_{max}),

Am is the molar extinction coefficient,

and L is the path length of the light through the solution, i.e. the length of the cuvette.

When a mixture of two components exists in a solution, the relative contribution of each to the observed optical density has to be assessed. In the system under study one of the components is the ester, phenyl acetate, and the second component which might absorb at the wavelength and is the degradation product phenol . As a result of hydrolysis 1 mole of the ester results in 1 mole of phenol according to the following scheme:

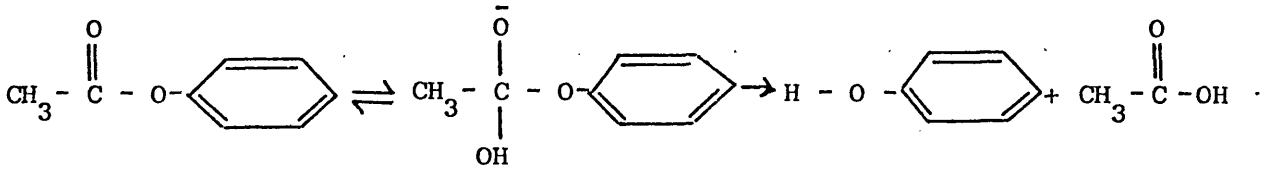

and therefore, the relative contributions of phenol and phenyl acetate to the observed optical density have to be determined.

Preliminary experiments showed that at the λ_{max} of the ester phenol was also absorbing and it was decided, therefore, to follow the rate of hydrolysis by the measurement of phenol production by absorbance measurements at the λ_{max} of the phenol. This requires determination of the ester contribution to the observed optical density.

Contribution of Phenyl Acetate to the Observed Optical Density at the λ_{max} of Phenol. The following set of determinations were carried out:

(i) A solution of 8×10^{-4}M phenol was prepared in buffer at a given pH, and an ultraviolet absorption spectrum obtained on the SP1800.

(ii) A solution of 8×10^{-4}M phenyl acetate in buffer at the same pH as above was then prepared and again a U.V. spectrum was obtained on the SP1800. The time interval from the moment of adding the ester to the buffer solution until it reached the λ_{max} of phenol was noted (t_1) and the optical density at this wavelength was also noted (d_1).

(iii) A solution of 8×10^{-4}M phenyl acetate was then prepared as above and the hydrolysis in buffer at the same pH was then followed at the λ_{max} of phenol, obtained in (i) above, and the result was recorded on the SP1800. The chart speed on the recorder was set at a fast rate and the scale on 0 - 0.2. The optical density (d_2) corresponding to (t_1) was then noted.

Upon repeating the above procedure for the various conditions used, it was found that the amount of absorbance (d_1) obtained in the absorption spectrum was always equal to the absorbance (d_2) caused by phenol during hydrolysis of the ester at time (t_1). Furthermore, extrapolation of the straight line, obtained in (iii) above, to zero time always passed through the zero optical density indicating that the ester did not absorb at the λ_{max} of phenol. Two U.V. Spectra of phenol and phenyl acetate in the absence and presence of CTAB are shown in Fig. (2.6) and Fig. (2.7) respectively.

Since the ester does not contribute to the observed optical density at the λ_{max} for phenol the percentage residual concentration of the ester at any given time can be determined from O.D. measurements of phenol applying the following equation (2.4).

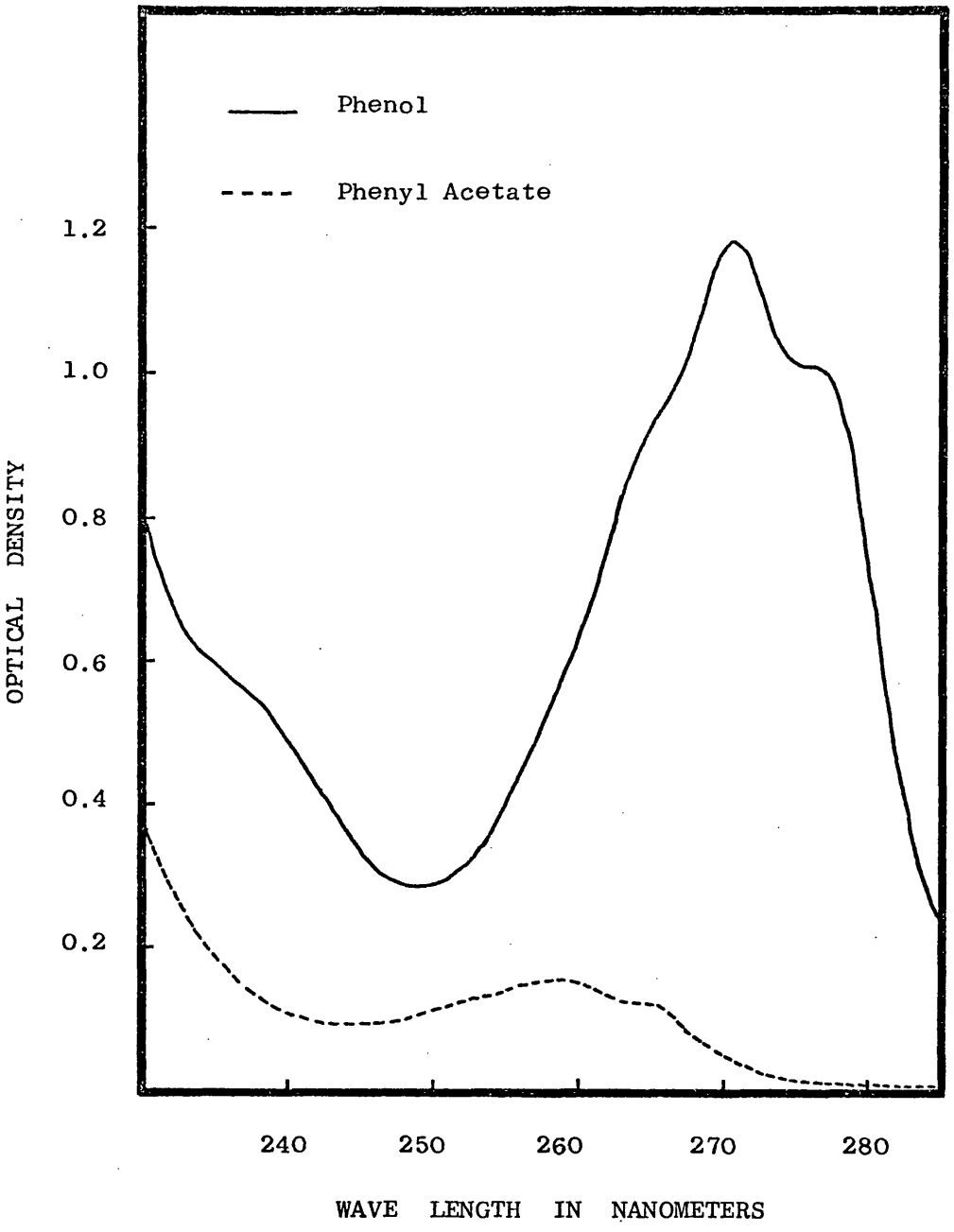

FIG.(2.6). THE ABSORPTION SPECTRA OF PHENOL AND PHENYL ACETATE IN CARBONATE-BICARBONATE BUFFER AT pH 9.2, BOTH AT 8×10^{-4}M.

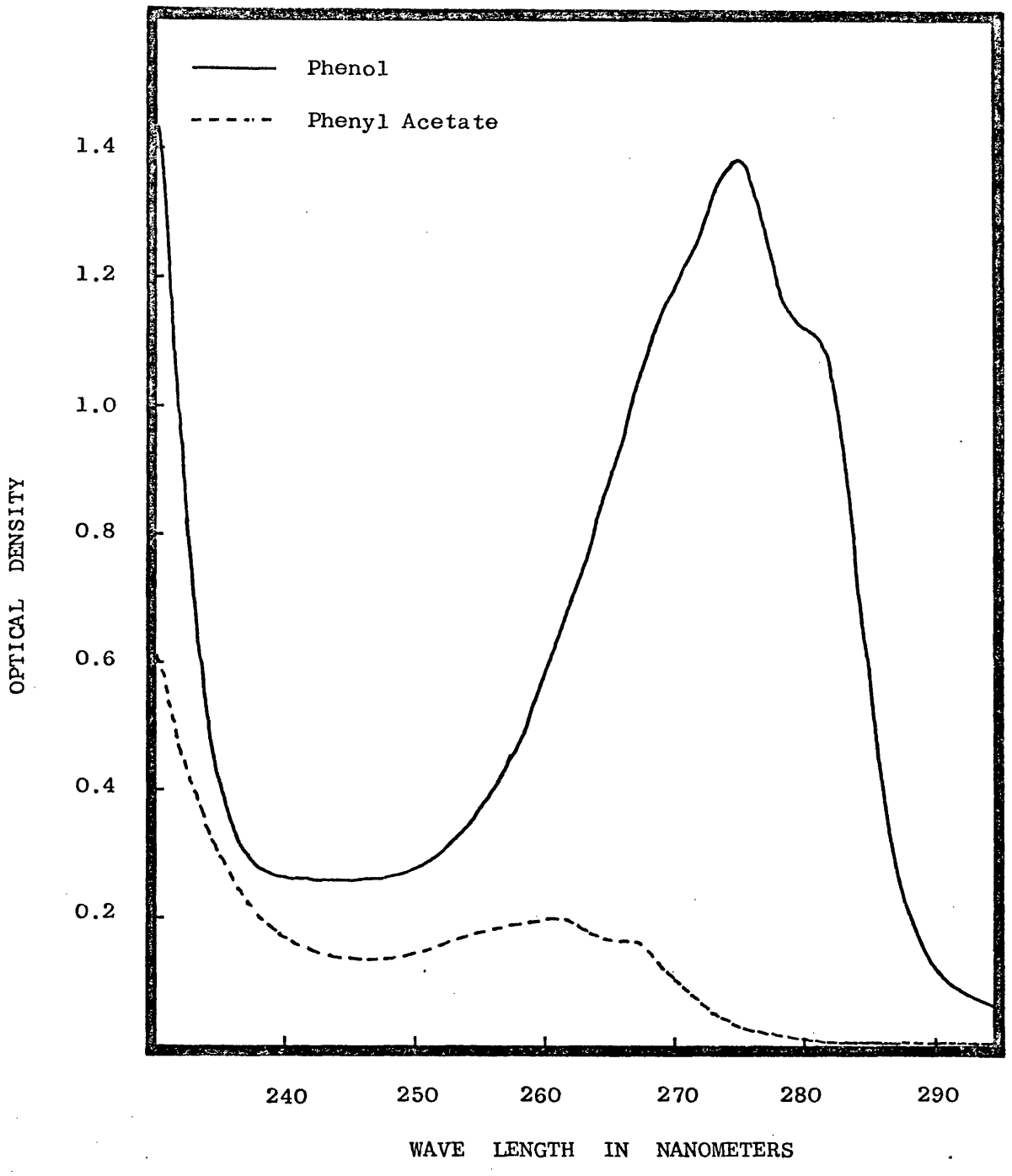

FIG. (2.7). THE ABSORPTION SPECTRA OF 8×10^{-4}M OF PHENOL AND PHENYL ACETATE IN CARBONATE-BICARBONATE BUFFER AT pH 9.2 IN THE PRESENCE OF 4×10^{-2} CTAB.

$$x = \left(\frac{D_c - D_t}{D_c}\right) \times 100 \quad \ldots\ldots\ldots\ldots\ldots\ldots\ldots\ldots \quad (2.4)$$

where x is the percentage residual concentration of the ester at time t,

D_c is the optical density at the completion of hydrolysis,

and D_t is the optical density at time t.

Determination of the λ_{max} of Phenol. The λ_{max} of phenol was determined, from U.V. spectra, for all experimental conditions and it was found that the λ_{max} and the A_m values were affected by the presence of CTAB as shown in Fig. (2.8). For this reason, λ_{max} for every experimental condition was obtained prior to the actual spectrophotometric assay. These values are given in Table (2.6).

Molar Concentration of CTAB x 10^3	λ_{max} (nanometers)			
	pH 8.0	pH 9.2	pH 9.8	pH 10.2
-	271.5	271.0	278.0	288.0
3.0	-	-	-	-
4.0	271.5	272.0	278.0	288.0
6.0	272.0	274.0	278.0	289.0
8.0	273.0	274.0	277.0	289.0
10.0	274.0	274.0	277.0	289.0
15.0	274.0	274.0	-	283.0
20.0	275.0	275.0	276.0	283.0
40.0	275.0	275.0	275.0	282.5
60.0	275.0	275.5	275.0	282.5
80.0	276.0	276.0	274.0	282.0

TABLE (2.6). λ_{max} of Phenol in CTAB solutions at different pH values of Carbonate Bicarbonate Buffer at 30° $\mu = 0.5$

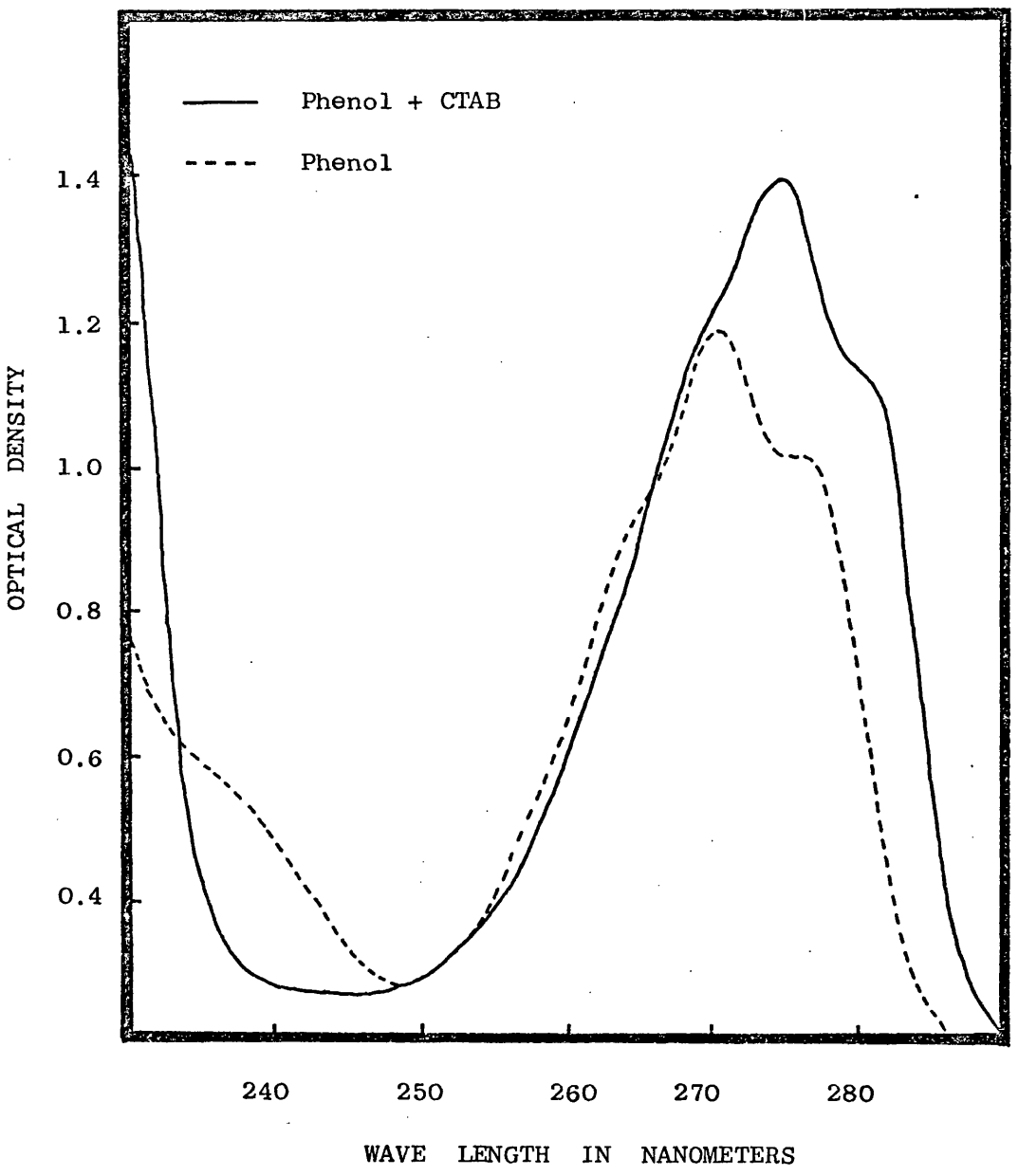

FIG. (2.8). ABSORPTION SPECTRUM OF 8 x 10^{-4}M PHENOL IN CARBONATE-BICARBONATE BUFFER AT pH 9.2 IN THE PRESENCE (____) AND ABSENCE (---) OF 4 x 10^{-2}M CTAB.

General Method. After preparation and standardization of the buffer solution 48 mls. were taken and 2 mls. from a stock solution of 0.02M phenyl acetate, were added and the time noted. The solution was then quickly mixed and optical density measurements were obtained at intervals throughout the experimental period. In the case of high pH studies, the optical density was continuously recorded with the solution being held in a 1 cm. cuvette in the SP1800, while at low pH's samples were withdrawn from a flask held in the water bath, at regular intervals. A summary of the assay procedure is given in the flow chart. The hydrolysis was usually followed down to a percentage residual concentration of below 50% and the pH was checked at the end of every experiment. This was always found to be within $\pm$ 0.001 of the pH value at the start of the experiment.

Determination of the Precision of Experimental Procedure. Two determinations for the ester hydrolysis were performed at 30^{o} and pH 9.8 in the absence of CTAB and two in the presence of the highest CTAB concentration used, 8×10^{-2}M. The data are given in Table (2.7) and shown graphically in Fig. (2.9), plotted according to first order kinetics with percentage residual concentration, on a log scale, against time, on a linear scale. For the sake of clarity only alternate points from (1) and (2), in each case, are drawn.

A computerised least squares regression analysis gave the rate constant, the intercept, standard deviation of the slope and intercept and the correlation coefficient. These values, together with calculated and tabulated t-Test values at a 0.05 probability level, are given in Table (2.8). It can be seen from

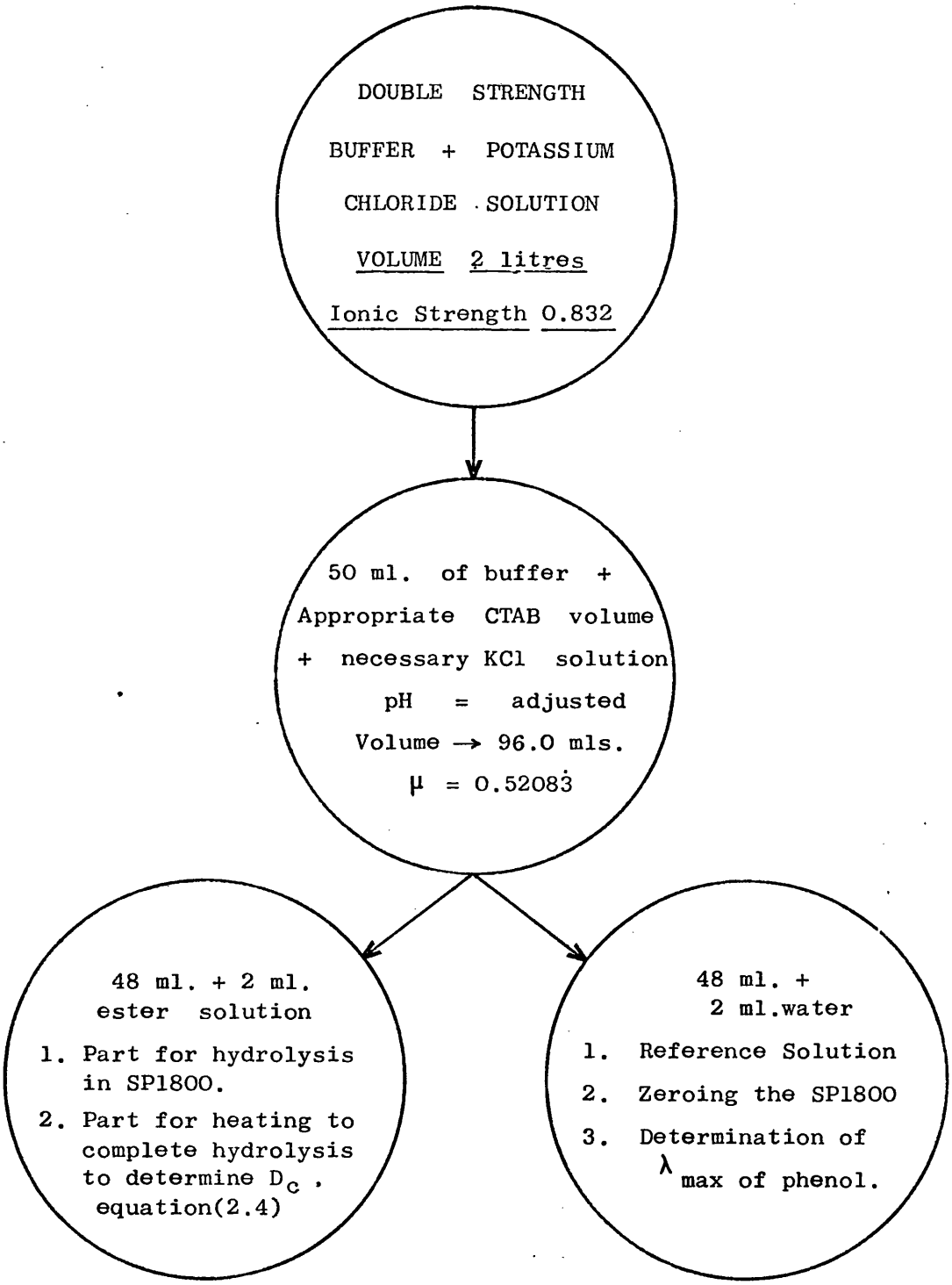

FLOW CHART FOR THE ASSAY PROCEDURE

FOR KINETIC STUDIES

WITHOUT CTAB					IN PRESENCE OF 8 x 10^{-2}M CTAB				
Time in minutes	1.		2.		Time in minutes	1.		2.	
	O.D.	% Residual concentration	O.D.	% Residual concentration		O.D.	% Residual concentration	O.D.	% Residual concentration
5.0	0.070	94.017	0.070	94.017	10.0	0.07	94.309	0.060	95.041
10.0	0.150	87.179	0.149	87.265	20.0	0.132	89.268	0.122	90.087
15.0	0.220	81.197	0.220	81.197	30.0	0.188	84.715	0.183	85.122
20.0	0.285	75.641	0.283	75.812	40.0	0.241	80.407	0.236	80.813
25.0	0.345	70.512	0.345	70.512	50.0	0.292	76.260	0.290	76.423
30.0	0.405	66.385	0.401	65.726	60.0	0.340	72.358	0.338	72.520
35.0	0.455	61.111	0.450	61.538	70.0	0.385	68.699	0.383	68.862
40.0	0.505	56.838	0.500	56.838	80.0	0.431	64.959	0.428	65.203
45.0	0.548	53.162	0.545	53.419	90.0	0.474	61.463	0.470	61.789

TABLE (2.7). Optical density and % residual concentration for the hydrolysis of 8 x 10^{-4}M Phenyl Acetate in Carbonate-Bicarbonate buffer at pH 9.8 and 30^{o} in the absence and presence of 8 x 10^{-2}M CTAB.

the high correlation coefficient values that a good fit to first order kinetics is obtained.

	WITHOUT CTAB		IN PRESENCE OF 8×10^{-2}M CTAB	
	1.	2.	1.	2.
RATE CONSTANT (MIN^{-1})	1.41490×10^{-2}	1.42596×10^{-2}	5.32687×10^{-3}	5.37353×10^{-3}
CORRELATION COEFFICIENT	0.99988	0.999938	0.999976	0.999983
STANDARD DEVIATION OF SLOPE	0.82072×10^{-4}	0.59832×10^{-4}	0.1176×10^{-4}	0.9777×10^{-4}
t-test(p=0.05)				
CALCULATED	1.09		0.473	
TABULATED	2.145		2.145	

TABLE (2.8). Values of various parameters obtained from computerised least squares regression analysis for the hydrolysis of phenyl acetate in the presence and absence of CTAB together with t-test values for duplicates.

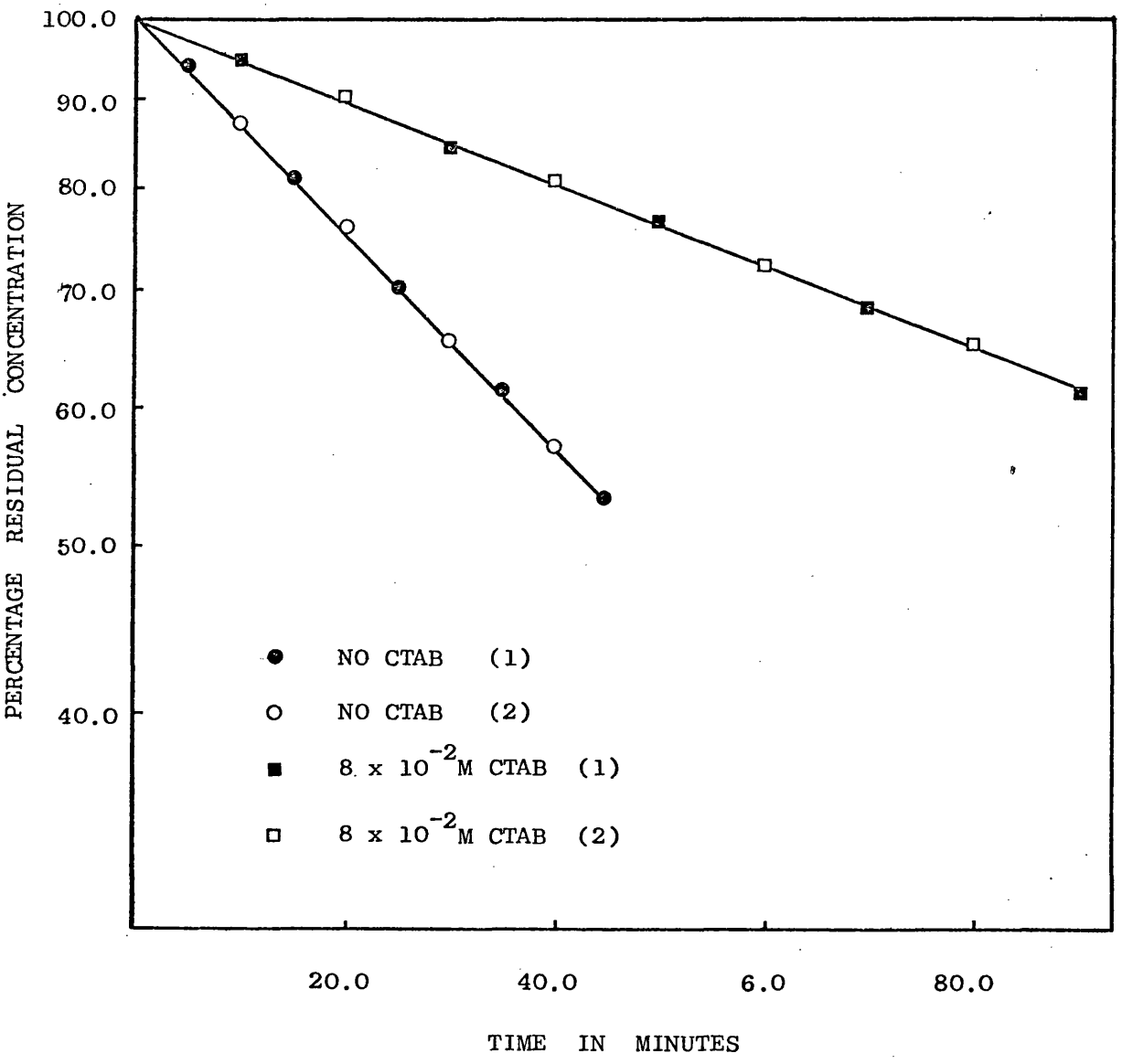

FIG. (2.9). PERCENTAGE RESIDUAL CONCENTRATION AGAINST TIME FOR THE HYDROLYSIS OF 8×10^{-4}M PHENYL ACETATE IN CARBONATE-BICARBONATE BUFFER AT pH 9.8 AND 30^{o} IN THE ABSENCE AND PRESENCE OF 8×10^{-2}M CTAB.

THE EFFECT OF CTAB ON THE RATE OF HYDROLYSIS OF PHENYL ACETATE AT pH 9.2, 9.8 and 10.2.

The effect of a series of concentrations of CTAB, above the CMC, on the hydrolysis of 8×10^{-4}M phenyl acetate in carbonate-bicarbonate buffer at 30° was determined at pH's of 9.2, 9.8 and 10.2. The concentrations of CTAB used at each pH are given in Table (2.9).

pH	Molar Concentrations of CTAB used $\times 10^2$
9.2	0.3, 0.4, 0.6, 0.8, 1.0, 2.0, 4.0, 6.0, 8.0
9.8	0.4, 0.6, 0.8, 1.0, 1.5, 2.0, 4.0, 6.0, 8.0
10.2	0.4, 0.6, 0.8, 1.0, 1.5, 2.0, 4.0, 6.0, 8.0

TABLE (2.9). The range of CTAB concentrations used for kinetic studies at a given pH.

The hydrolysis at pH 9.8 and 10.2 were carried out on a single sample in a 1 cm. cell housed in the SP1800 spectrophotometer and maintained at 30°. The hydrolysis at pH 9.2, being a lot slower, was carried out in a stoppered flask maintained at 30° by immersing it in a constant temperature bath. Samples were withdrawn at regular intervals from the flask and their optical densities determined in the usual manner on the SP1800. At the end of the determinations, the solutions were subjected to an elevated temperature to determine the optical density corresponding to total hydrolysis (D_c in equation (2.4)). This was always found to be equal to the value obtained from a solution of phenol. Representative optical density readings and percentage residual concentrations obtained for pH 10.2 in the absence of CTAB and in the presence of 6×10^{-3}M, 2×10^{-2}M,

NO CTAB			6×10^{-3}M CTAB			2×10^{-2}M CTAB			4×10^{-2}M CTAB			8×10^{-2}M CTAB		
Time in minutes	O.D	% Residual concentration	Time in minutes	O.D	% Residual concentration	Time in minutes	O.D.	% Residual concentration	Time in minutes	O.D	% Residual concentration	Time in minutes	O.D	% Residual concentration
2.0	0.103	93.007	5.0	0.168	87.509	5.0	0.111	91.494	5.0	0.091	93.037	5.0	0.067	94.733
4.0	0.191	87.033	10.0	0.316	76.506	10.0	0.235	81.992	10.0	0.183	85.977	10.0	0.130	89.844
6.0	0.280	80.991	15.0	0.443	67.063	15.0	0.345	73.563	15.0	0.261	80.000	15.0	0.192	85.000
8.0	0.359	75.628	20.0	0.558	58.513	20.0	0.445	65.900	20.0	0.339	74.023	20.0	0.250	80.469
10.0	0.433	70.604	25.0	0.655	51.302	25.0	0.520	60.153	25.0	0.412	68.429	25.0	0.307	76.016
12.0	0.500	66.056	30.0	0.740	44.981	30.0	0.600	54.023	30.0	0.479	63.295	30.0	0.358	72.031
14.0	0.576	61.507	35.0	0.815	39.405	35.0	0.670	48.659	35.0	0.542	58.467	35.0	0.406	68.281
16.0	0.626	57.502	40.0	0.880	34.572	40.0	0.730	44.061	40.0	0.596	54.330	40.0	0.452	64.688
18.0	0.685	53.496				45.0	0.790	39.464	45.0	0.650	50.192	45.0	0.493	61.484
20.0	0.737	49.966				50.0	0.840	35.632	50.0	0.698	46.513	50.0	0.538	57.969
22.0	0.787	46.572				55.0	0.885	32.184	55.0	0.744	42.989	55.0	0.576	55.000
24.0	0.832	43.517												
26.0	0.876	40.530												

TABLE (2.10). Optical densities and percentage residual concentration for the hydrolysis of 8×10^{-4}M phenyl acetate in presence and absence of CTAB at pH 10.2 and 30^{o}.

NO CTAB			6×10^{-3}M CTAB			2×10^{-2}M CTAB			4×10^{-2}M CTAB			8×10^{-2}M CTAB		
Time in minutes	O.D	% Residual concentration	Time in minutes	O.D	% Residual concentration	Time in minutes	O.D.	% Residual concentration	Time in minutes	O.D	% Residual concentration	Time in minutes	O.D	% Residual concentration
2.0	0.103	93.007	5.0	0.168	87.509	5.0	0.111	91.494	5.0	0.091	93.037	5.0	0.067	94.733
4.0	0.191	87.033	10.0	0.316	76.506	10.0	0.235	81.992	10.0	0.183	85.977	10.0	0.130	89.844
6.0	0.280	80.991	15.0	0.443	67.063	15.0	0.345	73.563	15.0	0.261	80.000	15.0	0.192	85.000
8.0	0.359	75.628	20.0	0.558	58.513	20.0	0.445	65.900	20.0	0.339	74.023	20.0	0.250	80.469
10.0	0.433	70.604	25.0	0.655	51.302	25.0	0.520	60.153	25.0	0.412	68.429	25.0	0.307	76.016
12.0	0.500	66.056	30.0	0.740	44.981	30.0	0.600	54.023	30.0	0.479	63.295	30.0	0.358	72.031
14.0	0.576	61.507	35.0	0.815	39.405	35.0	0.670	48.659	35.0	0.542	58.467	35.0	0.406	68.281
16.0	0.626	57.502	40.0	0.880	34.572	40.0	0.730	44.061	40.0	0.596	54.330	40.0	0.452	64.688
18.0	0.685	53.496				45.0	0.790	39.464	45.0	0.650	50.192	45.0	0.493	61.484
20.0	0.737	49.966				50.0	0.840	35.632	50.0	0.698	46.513	50.0	0.538	57.969
22.0	0.787	46.572				55.0	0.885	32.184	55.0	0.744	42.989	55.0	0.576	55.000
24.0	0.832	43.517												
26.0	0.876	40.530												

TABLE (2.10). Optical densities and percentage residual concentration for the hydrolysis of 8×10^{-4}M phenyl acetate in presence and absence of CTAB at pH 10.2 and 30^{o}.

4×10^{-2}M and 8×10^{-2}M CTAB are given in Table (2.10) and shown graphically in Fig.(2.10). For each pH, the calculated values of the rate constants and their associated standard error, together with the calculated and tabulated t-test values for the duplicates, are given in Tables (2.11 -.2.13). The Bartlett test values in Tables 2.11 and 2.13 indicate the results to be significantly different. This is attributable, however, to the very low standard deviations associated with the slopes. t-Tests performed on paired values show them not to be significantly different.

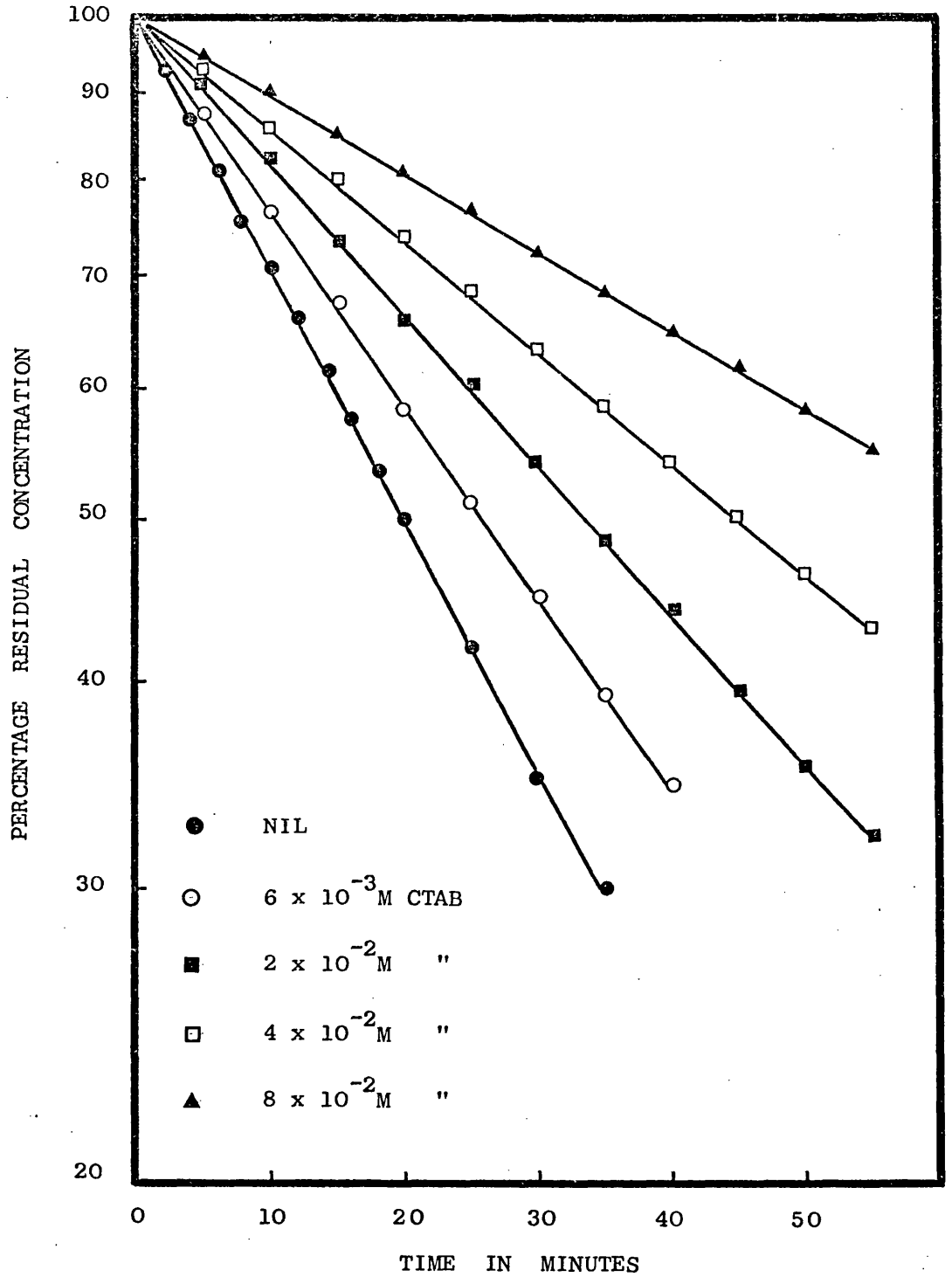

FIG. (2.10). THE EFFECT OF INCREASING CTAB CONCENTRATION ON THE HYDROLYSIS OF 8×10^{-4}M PHENYL ACETATE AT 30°C IN CARBONATE-BICARBONATE BUFFER AT pH 10.2 AND IONIC STRENGTH 0.5

TABLE (2.11). The effect of CTAB on the hydrolysis of 8×10^{-4} M phenyl acetate at pH 9.2 and 30°.

Molar concentration of CTAB	Rate Constant Minutes^{-1} $\times 10^3$	Standard Deviation of the Slope $\times 10^5$	t-Test		Average Rate Constant Minutes^{-1} $\times 10^3$
			Calculated	Tabulated	
NIL	3.73962 3.65606 3.70577 3.75126	0.61814 0.98919 1.54493 0.17959	42.60*	7.82*	3.71318
4×10^{-3}	3.24398 3.24522	0.80330 0.82909	0.107	2.086	3.24460
6×10^{-3}	3.08688 3.08390	0.55494 0.62516	0.357	2.086	3.08539
8×10^{-3}	2.93943 2.94268	0.70325 0.68845	0.33	2.086	2.94105
1×10^{-2}	2.83526 2.81927	0.60160 1.25982	1.145	2.086	2.82726
1.5×10^{-2}	2.51234 2.55246	0.58930 7.58320	0.527	2.12	2.53241
2×10^{-2}	2.34008 2.35217	0.42972 1.05136	0.184	2.11	2.35112
4×10^{-2}	1.78008 1.77997	0.37995 0.26001	0.024	2.145	1.78003
6×10^{-2}	1.46073 1.46332	0.14989 0.26732	0.847	2.145	1.46203
8×10^{-2}	1.24842 1.25936	0.30348 0.61255	1.60	2.12	1.25389

* THESE FIGURES REFER TO BARTLETT TEST

TABLE (2.12). The effect of CTAB on the hydrolysis of 8×10^{-4}M phenyl acetate at pH 9.8 and 30°.

Molar concentration of CTAB	Rate Constant Minutes^{-1} x 10^3	Standard Deviation of the Slope x 10^4	t-Test		Average Rate Constant Minutes^{-1} x 10^2
			Calculated	Tabulated	
NIL	1.414893 1.42596	0.8207 0.598	1.09	2.145	1.42043
3×10^{-3}	1.25155 1.24808	0.52375 0.52375	0.417	2.120	1.24982
4×10^{-3}	1.2104 1.2124	0.07637 0.8723	0.228	2.120	1.21140
6×10^{-3}	1.1475 1.14113	0.4467 0.2655	1.226	2.110	1.14432
8×10^{-3}	1.093668 1.098598	0.5076 0.2634	0.862	2.080	1.09613
1×10^{-2}	1.071466 1.068929	0.1814 0.2515	0.818	2.110	1.07020
2×10^{-2}	0.901681 0.913717	0.3998 0.3854	2.168	2.228	0.90770
4×10^{-2}	0.703262 0.711247	0.2773 0.3564	1.768	2.131	0.70726
6×10^{-2}	0.629994 0.630021	0.1958 0.8641	0.003	2.110	0.63000
8×10^{-2}	0.5326865 0.5373530	0.1176 0.9777	0.473	2.090	0.53285

TABLE (2.13). The effect of CTAB on the hydrolysis of 8×10^{-4}M phenyl acetate at pH 10.2 and 30°.

Molar concentration of CTAB	Rate Constant Minutes^{-1} x 10^2	Standard Deviation of the Slope x 10^4	t-Test		Average Rate Constant$_{-1}$ Minutes x 10^2
			Calculated	Tabulated	
NIL	3.44859 3.45393 3.50055	1.11775 0.77737 0.80974	20.67*	5.99*	3.46769
4×10^{-3}	2.83149 2.80250	1.13320 6.50505	0.439	2.12	2.81699
6×10^{-3}	2.65428 2.66527	0.52114 0.56957	1.424	2.101	2.65977
8×10^{-3}	2.56849 2.54545	0.24882 0.54074	3.87	2.10	2.55700
1×10^{-2}	2.47516 2.50031	6.79063 0.56831	0.369	2.145	2.48912
1.5×10^{-2}	2.26280 2.28174	0.41645 0.28529	3.75	2.13	2.27227
2×10^{-2}	2.08054 2.11576	0.85923 0.50624	3.53	2.11	2.09815
4×10^{-2}	1.53493 1.54392	0.34725 0.33678	1.859	2.11	1.53942
6×10^{-2}	1.24248 1.22950	1.29121 2.68268	0.436	2.23	1.23599
8×10^{-2}	1.08324 1.08533	0.18625 0.21093	0.744	2.06	1.08428

* THESE FIGURES REFER TO BARTLETT TEST

HYDROLYSIS OF PHENYL ACETATE AT pH 8.0

The range covered by Delory and King's carbonate-bicarbonate buffer is from pH 9.2 to pH 10.2 and it was found that the buffers capacity at pH 8.0 was very low. It was therefore decided to use a pH-stat method to maintain the pH value when carrying out the hydrolysis at pH 8.0.

The pH-stat assembly consisted of a 2.5 ml. autoburette which held the titrant, N/10 hydrochloric acid. The titrator-pH-meter was fitted with an automatic temperature compensator and had a scale readable to 0.002 pH unit. The reaction vessel was a 250 ml. round bottom flask with three outlets - one for a Pye Ingold 405 combined glass-calomel electrode and one for the delivery tube from the titrator. The third outlet was stoppered during the hydrolysis and opened only for samples to be withdrawn with a pipette at regular intervals. The reaction vessel was kept in a water bath, maintained at a temperature of $30^{o} \pm 0.05$. The solution within the vessel was continuously stirred with a magnetic stirrer to ensure the immediate dispersion of the added titre. The optical densities of the withdrawn samples were read on a Perkin Elmer double beam spectrophotometer at the λ_{max} of phenol at pH 8.0 and the given CTAB concentration.

Determination of the Accuracy of the pH-stat Procedure. The pH-stat technique was assessed by determining the rates of hydrolysis of phenyl acetate at pH 9.2 and 10.2 at 30^{o} in the absence and presence of CTAB and comparing them with the previously obtained values. These results are given in Table (2.14) together with the calculated and tabulated t-test values at a probability level of 0.05.

pH	Molar concentration of CTAB	Rate constant $_{-1}$ Minutes previously determined	Standard deviation of slope	Rate constant $_{-1}$ Minutes pH-stat determined	Standard deviation of slope	t-test	
						Calculated	Tables
9.2	NIL	3.70577×10^{-3}	0.15449×10^{-4}	3.70621×10^{-3}	0.20188×10^{-4}	0.017	2.2
	8×10^{-3}	2.94268×10^{-3}	0.68845×10^{-5}	2.99817×10^{-3}	0.30870×10^{-4}	1.75	2.2
10.2	NIL	3.50055×10^{-2}	0.80974×10^{-4}	3.48803×10^{-2}	0.87216×10^{-2}	1.05	2.13
	8×10^{-3}	2.54545×10^{-2}	0.54074×10^{-4}	2.55206×10^{-2}	0.16779×10^{-3}	0.375	2.13

TABLE (2.14). Rate constants of the hydrolysis of 8×10^{-4}M phenyl acetate at pH 9.2 and 10.2 in carbonate-bicarbonate buffer at 30° as determined with pH-stat assembly in presence and absence of CTAB.

The values obtained confirm that the two pH meters were not giving significantly different measurements.

The Effect of CTAB on the Hydrolysis of Phenyl Acetate at pH 8.0.

The effect of a series of concentrations of CTAB, above its CMC, on the hydrolysis of 8×10^{-4}M phenyl acetate, in carbonate-bicarbonate buffer at 30° was determined at pH 8.0 using the pH-stat assembly to maintain the system at this pH. 200 mls. of the solution was prepared as before, 96 mls. of this were placed in the reaction vessel and the delivery tube, from the titre, and the electrode were introduced and the magnetic stirrer activated. After temperature equilibration and when the solution reached a pH of 8.0, 4 mls. of phenyl acetate, from a 0.02M stock solution, were introduced and the timing started. Samples were withdrawn at regular intervals and their optical densities

determined. The maximum volume of N/10 hydrochloric acid added during the longest experiment was 1.2 mls.

Results. The data obtained were plotted according to first order kinetics with percentage residual concentration, on a log scale, against time, on a linear scale. Table (2.14) shows the rate constants, at the various CTAB concentrations, obtained from least squares regression analysis. Because the reaction was very slow, duplicates were not made on all the determinations in the presence of the surfactant. The concentrations for which duplicate determinations were made are shown in the table, together with the associated standard error and the calculated and tabulated t-test values at a probability level of 0.05.

TABLE (2.15). The effect of CTAB on the hydrolysis of 8×10^{-4} M phenyl acetate at pH 8.0 and 30°.

Molar concentration of CTAB x 10^3	Rate Constant Minutes^{-1} x 10^4	Standard Deviation of the Slope x 10^6	t-Test		Average Rate Constant Minutes^{-1} x 10^4
			Calculated	Tabulated	
NIL	2.56411 2.54822	1.89375 0.32418	0.827	2.15	2.55616
3.83	2.24601	0.41977	-	-	2.24601
5.76	2.11974 2.13075	0.56276 1.00152	0.960	2.18	2.12525
7.68	2.01291	0.81329	-	-	2.01291
9.60	1.90787 1.92678	0.41885 1.14470	1.550	2.18	1.91733
14.40	1.72159	1.37890	-	-	1.72159
19.20	1.56055 1.56763	0.66649 1.36781	0.465	2.18	1.56409
38.40	1.19170	0.57723	-	-	1.19170
57.60	0.98338 0.98455	0.56379 0.99808	0.103	2.18	0.98397
76.80	0.83985	0.92050	-	-	0.83985

DETERMINATION OF PARTITION COEFFICIENT

Introduction. Many interpretations of micellar reactions rely on the tentative assumption that a surfactant solution can be visualised, on a phase change model, as having two compartments - a bulk solvent phase, usually aqueous, and a micellar phase. The rates of reactions in the micellar phase differ from those in the bulk phase due to an association of the substrate with micelles. A measure of such an association is the partition coefficient of the substrate between the micelles and the aqueous bulk phase. This can be represented by the following relationship, equation (2.5).

$$K_p = \frac{[C_m]}{[C_w]} = \frac{n_m}{n_w} \left(\frac{1-V}{V} \right) \quad \ldots\ldots\ldots\ldots\ldots (2.5)$$

where K_p is the partition coefficient,

$[C_m]$ is the concentration of the substrate in the micellar phase,

$[C_w]$ is the concentration of the substrate in the aqueous phase,

n_m is the number of moles of substrate, per unit volume, in the micellar phase,

n_w is the number of moles of substrate, per unit volume, in the aqueous phase,

and V is the volume fraction of the micellar phase.

The partition coefficient can be determined, experimentally, by solubility (71, 72) equilibrium dialysis (72), molecular sieve (71) and kinetic (121) measurements. For the purpose of this study, solubility, gel filtration and kinetic data have been utilized to determine the partition coefficient of phenyl acetate between the CTAB micelles and the aqueous bulk phase.

Determination of the Partial Specific Volume. A knowledge of the partial specific volume, $\bar{v}$, is necessary for calculations of

partition coefficient, K_p, from gel filtration chromatography, solubility and kinetic data. The partial specific volume is the increase in volume, at constant temperature and pressure, of a system caused by the addition of one gramme of solute to a large volume of the system without an appreciable change in the concentration. It is obtained by plotting the reciprocal of the density (specific volume) against the weight fraction of the surfactant, which is the weight of the surfactant divided by the total weight of the solution under study. Such a plot results in a linear relationship between the specific volume and the weight fraction above the CMC. It is noticed, however, that a break in this linear relationship is obtained if a phase change or a change in the shape of the micelles takes place (122). This fact has been utilized to determine the CMC of surfactants (12).

Method. Density measurements were made using a Lipkin bicapillary pycnometer having a capacity of approximately 10 mls. (123), modified to enable suspension from a five place balance via a cross bar connecting the two limbs. The method used for calibrating the pycnometer and for determining the density values was the standard method given by the American Society for Testing and Materials (A.S.T.M. D941 - 55). The height of the meniscus in each limb of the pycnometer was measured from a reference point at the bottom of each limb using a travelling microscope. For each determination the pycnometer was weighed before equilibration in a thermostated bath at $30^{\circ} \pm 0.005$. After fifteen minutes equilibration, the heights of the menisci were measured with the pycnometer still in the bath. It was then removed, wiped with a damp wash-leather, to prevent interference from static charges during weighing, and

re-weighed. The density values used to calculate the specific volumes were, in all cases, the average of three determinations on the same solution.

Results and Treatment of Results. Data were obtained for CTAB in carbonate-bicarbonate buffer at pH 9.2, in the presence of enough potassium chloride to adjust to an ionic strength of 0.5M, in the presence and absence of 8×10^{-4}M phenyl acetate. Table (2.16) gives the data for such a determination in the absence of the ester and Fig.(2.11) shows the plot of these data.

WEIGHT FRACTION OF CTAB x 10^3	DENSITY (AVERAGE OF 3 DETERMINATIONS)	SPECIFIC VOLUME
1.80	1.019070	0.981287
2.80	1.019079	0.981278
3.50	1.019083	0.981274
4.53	1.019096	0.981262
7.44	1.019124	0.981235
10.00	1.019165	0.981195
14.00	1.019230	0.981133
21.46	1.019347	0.981020
28.53	1.019457	0.980914

TABLE (2.16). Date for partial specific volume of CTAB micelles in carbonate-bicarbonate buffer at pH 9.2 and 30° $\mu = 0.5$

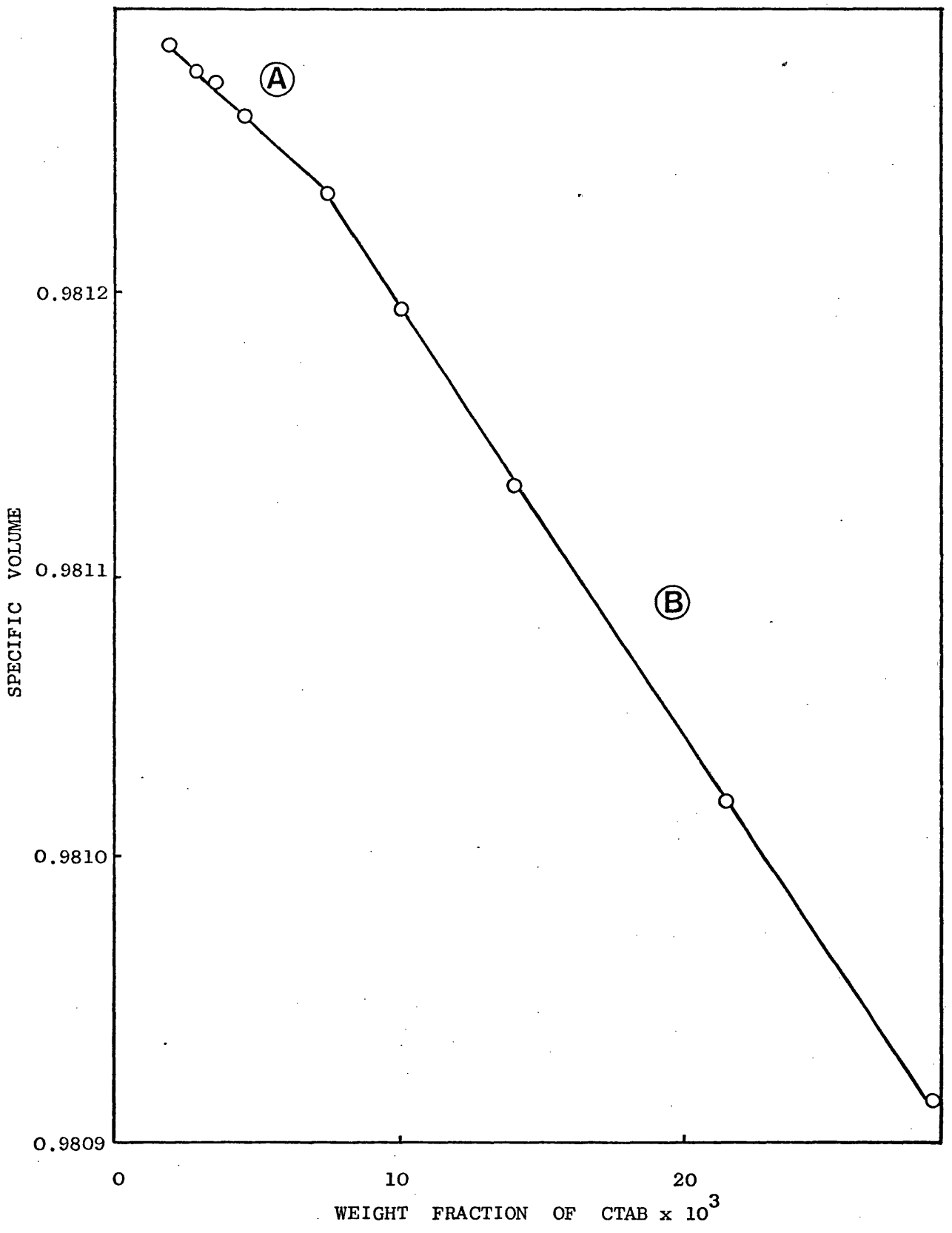

FIGURE (2.11). SPECIFIC VOLUME AGAINST WEIGHT FRACTION FOR CTAB IN CARBONATE-BICARBONATE BUFFER AT pH 9.2 AND 30°.

The linear portions of the plots were submitted to a least squares regression analysis. The partial specific volume, $\bar{v}$, was then obtained by the summation of the slope and the intercept values which gives the value of $\bar{v}$ when x = 1. It was noticed that a break occurred in the region of 7×10^{-3} weight fraction, in the system without the ester. The break suggests a change in the micellar shape and its absence in the system containing the ester suggests that the latter stabilizes the shape of the micelles as had been found by other workers (121). The partial specific volume was calculated from both linear portions before and after the break. These are denoted as A and B respectively. The results are given in Table (2.17) together with the calculated $\bar{v}$.

Conditions	Slope	Intercept	Partial Specific Volume
Carbonate-Bicarbonate Buffer at pH 9.2 and Ionic Strength of 0.5	A) -0.005038	A) 0.991498	A) 0.98646
	B) -0.007675	B) 0.991513	B) 0.98380
Carbonate-Bicarbonate Buffer at pH 9.2 and 8×10^{-4}M Phenyl Acetate Ionic Strength 0.5	-0.000801	0.98089	0.980089

TABLE (2.17). Slope and intercept values from specific volume-weight fraction plots of CTAB at 30^{o} in the presence and absence of phenyl acetate.

Since all the systems investigated contained 8×10^{-4}M phenyl acetate, the value for the partial specific volume, for the purpose of calculations in this thesis, was taken as 0.980.

Partition Coefficient by Solubility Measurements. The partition coefficient can be determined from solubility measurements (71, 72). Assuming ideal behaviour, K_p can be determined using the following equation (2.6).

$$\left[C_T\right] = \left[C_w\right] + \left[C_w\right](K_p - 1)\,\bar{v}\,C_m \quad \ldots\ldots\ldots \quad (2.6)$$

where $\left[C_T\right]$ is the total concentration of the substrate,

$\left[C_w\right]$ is the concentration of the solute in the aqueous (non-micellar) phase,

$\bar{v}$ is the partial specific volume of the surfactant in the micelles,

C_m is the concentration of micelles, in grams per ml., calculated from (C-CMC), where C is the concentration of surfactant in grams per ml and the CMC is also expressed in grams per ml.

From equation (2.6) above a plot of $\left[C_T\right]$ against C_m should be linear with a slope of $\left[C_w\right](K_p - 1)\,\bar{v}$

$$\therefore \quad \text{Slope} = \left[C_w\right](K_p - 1)\,\bar{v} \quad \ldots\ldots\ldots\ldots\ldots \quad (2.7)$$

$$\therefore \quad K_p = \left(\frac{\text{Slope}}{\left[C_w\right]\bar{v}}\right) + 1 \quad \ldots\ldots\ldots\ldots\ldots \quad (2.8)$$

The value of $\left[C_w\right]$ is obtained from the intercept of such a linear plot.

Method. A series of 25 ml. solutions of CTAB, of the same concentration range used in the kinetic studies, containing 2 mls. of phenyl acetate and enough potassium chloride for an ionic strength of 0.5M were prepared using freshly distilled, boiled and cooled water. The solutions were then transferred to pyrex centrifuge tubes which were then stoppered and mounted in a perspex jig and immersed in a thermostated shaking water bath held at $30^{\circ} \pm 0.1$. The tubes were

left to shake for one week (a time that was shown to be sufficient, from preliminary experiments, for the attainment of equilibrium). The suspensions were then centrifuged and the "oily" layer of the ester sank to the bottom. The tubes were then returned to a water bath, held at 30°, without disturbing the bottom layer. After temperature equilibration, the supernatant was filtered, while still in the bath, by sucking the solution, using a filter pump, through glass tubes with No.3 sintered glass filters. Dilutions were then made of the clear solutions obtained and optical densities were determined at the λ_{max} of the ester (261 nm.) on an SP600 spectrophotometer.

Results and Treatment of Results. From a previously determined "extinction coefficient", the amount of ester solubilized in each solution was determined, in grams per ml. This was then plotted against the concentration of micelles C_m . The data are given in Table (2.18) and shown graphically in Fig.(2.12).

CTAB Molar Concentration x 10^3	CTAB concentration $g.ml^{-1} \times 10^3$	Micellar concentration $g.ml^{-1} \times 10^3$	Optical Density	Ester Solubilized $g.ml^{-1} \times 10^3$
-	-	-	0.060	4.0341
3.0	1.0934	1.0234	0.066	4.4375
4.0	1.4580	1.3880	0.070	4.7064
6.0	2.1870	2.1170	0.073	4.9081
8.0	2.9160	2.8460	0.076	5.1098
10.0	3.6450	3.5750	0.080	5.3788
20.0	7.2870	7.2190	0.095	6.3873
40.0	14.5780	14.5080	0.140	9.4128
60.0	21.8680	21.7980	0.180	12.1020
80.0	29.1570	29.0870	0.220	14.7920

TABLE (2.18). Solubility data of phenyl acetate in aqueous solutions of CTAB at 30° and ionic strength 0.5M.

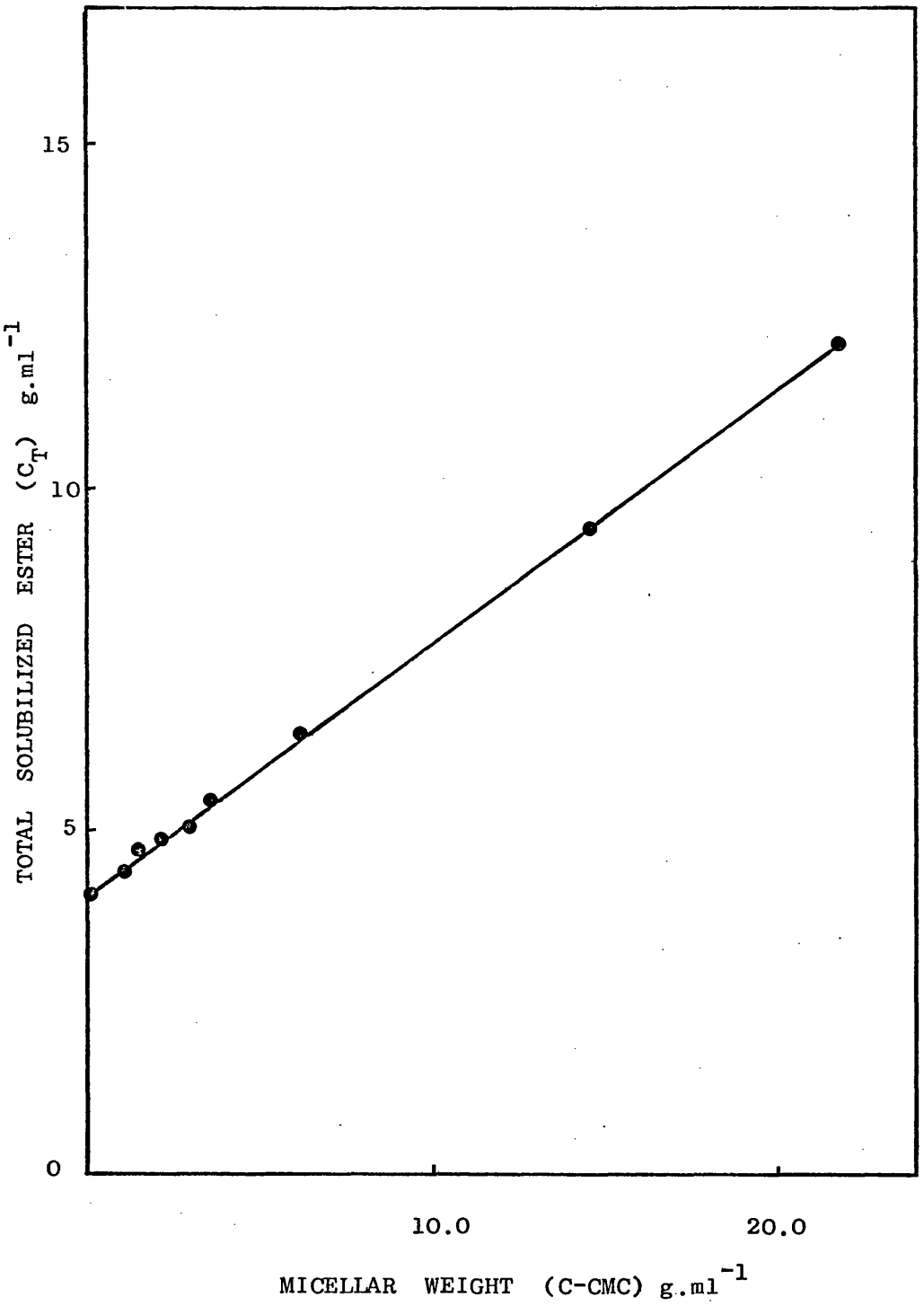

FIG. (2.12). TOTAL WEIGHT OF PHENYL ACETATE SOLUBILIZED (C_T) IN g.ml^{-1} AGAINST MICELLAR WEIGHT IN g.ml^{-1} OF CTAB AT 30° AND IONIC STRENGTH 0.5M.

The data were submitted to a least squares regression analysis from which the slope and intercept were obtained and the K_p calculated. This was found to be 94.16.

Determination of Partition Coefficient by Gel Filtration.

Gel filtration is a type of partition chromatography in which substances are separated largely on the basis of their molecular size. If a mixture of low-molecular-weight substances (‹ 4000) and high-molecular-substances (› 5000) moves through a gel column, the former are slowed down as a result of their penetration into the gel while the latter flow faster down the column. Surfactant micelles with molecular weights much larger than these figures would be expected to move on a gel bed in the same fashion as macromolecules and thus emerge first from a gel column. When a third component of low molecular weight is added to a gel column containing surfactant micelles, the emergence of this component will depend on its degree of interaction with the micelles. This fact has been utilised for the determination of the partition coefficient of various substrates between micellar and aqueous phases (71, 124-126). The column and material used in this study is SEPHADEX, a cross-linked dextran, produced in the form of uniformly sized beads. On contact with suitable solvents, these beads swell to an extent dependent upon their degree of cross-linkage and it is this swelling that controls the pore size of the swollen beads and the sizes that can or cannot penetrate the gel bed. In order to include molecular sieving and micellar partitioning effects, Herries et al (71) modified equations previously introduced by Martin and Synge (127) for partition chromatography and thus enabled the calculation of partition coefficients from gel filtration data. For a solute introduced into a column of a Sephadex

previously equilibrated with a solution containing the same concentration of surfactant as that in the mixture under investigation, above the CMC under the prevailing conditions, and where the substrate is eluted with the same concentration of surfactant the relationship is found to be -

$$\frac{Vi}{Ve - Vo} = \frac{\bar{v}\,(K_p - 1)}{k' K_D} C_m + \frac{1}{k' K_D} \quad \ldots\ldots\ldots (2.9)$$

where Vi is the imbibed volume, defined as the volume of solvent in the swollen gel, the product of the dry gel weight and the water regain weight per gram of dry gel assuming unit density for water. Vo is the external volume for the column of swollen gel and is equal to the elution volume for a solute known to be completely excluded from the gel particles. Ve is the elution volume for the solute, $\bar{v}$ is the partial specific volume of the surfactant in the micelle and C_m is the concentration of micelles in grams per ml. and equals (C-CMC). K_D is the "molecule sieving" constant which is the ratio of solute concentration in imbibed liquid to concentration in non-micellar portion of external liquid. $k' = \frac{(k\,Vg + Vi)}{Vi}$ where k is a proportionality constant between the solute adsorbed per unit volume of gel matrix and the equilibrium concentration of monomer solute in the liquid, Vg is the volume of the gel.

Dividing equation (2.9) by Vi results in equation (2.10) -

$$\frac{1}{Ve - Vo} = \frac{\bar{v}\,(K_p - 1)}{k' K_D\, Vi} C_m + \frac{1}{k' K_D Vi} \quad \ldots\ldots\ldots (2.10)$$

A plot of $\frac{1}{Ve - Vo}$ against the concentration of micelles in gm. per ml. would result in a linear relationship and the ratio of slope to intercept from such a plot would equal $\bar{v}\,(K_p - 1)$ enabling the partition

coefficient, K_p, to be evaluated, providing the partial specific volume of the surfactant in the micelles is known.

Method. 10g. of Sephadex 25/80, with an exclusion limit of 5000, were allowed to swell for 6 hours at room temperature in a potassium chloride solution of ionic strength 0.5M. The slurry so produced was introduced into a jacketed glass column of 1 cm. internal diameter and a height of 33 cms. fitted with a sintered glass plate and a teflon nozzle at the bottom. The column was maintained at a temperature of $30^{o} \pm 0.1$ as checked by the insertion of a thermocouple into the centre of the gel. After the column had then been filled with the Sephadex gel, a filter paper disc was placed on the top of the gel to prevent its disturbance when the sample solutions were introduced. A delivery tube from a reciprocating piston pump, delivering a constant volume of 50 ml. $hour^{-1}$ was then connected to the top of the column, the pump having been flushed first with 100 mls. of the 0.5M potassium chloride solution. The column was then allowed to be washed with this solution overnight to ensure even packing. It was then ready for use.

Determination of the External Volume (Vo). The interstitial volume of the column was determined using a 0.2% solution of Dextran Blue 2000, with a molecular weight of 2×10^{6}, in a 0.5M potassium chloride solution eluted with a 0.5M potassium chloride solution. An automatic fraction collector, fitted with a drop counter, was employed. A 2 ml. sample of the 0.2% solution of Dextran Blue in the eluent was applied to the top of the column, using a pipette, after allowing the eluant to just drain into the surface of the bed. When the sample had also drained into the bed the outlet of the column was drained and the teflon nozzle fitted, a few mls. of eluent were

introduced onto the surface of the bed and the delivery tube from the pump was then fitted to the top of the column. The effluent solution was then collected in tared tubes. When the blue band of the Dextran neared the outlet, the fraction collector was started and a series of eight-drop fractions were collected. After weighing, the fractions were diluted and assayed by measurement of their absorbance at 250 nm. on an SP600 spectrophotometer. The data obtained were plotted as optical density versus fraction number from which the elution fraction was obtained. The optical density values lying on a straight line on the ascending limb of such a plot were joined and the mid point of that line was then determined. The elution volume, which is the external volume in this case, was the total volume of the individual fractions from the commencement of collection to, and including the mid-point fraction. The Vo value used in the calculations to follow was the average of three determinations.

Determination of Elution Volumes (Ve) for the Ester in the Presence of CTAB. 500 mls. of the eluent solution containing the required concentration of CTAB was prepared and made up to an ionic strength of 0.5M with potassium chloride. The pump was flushed for 2 hours with this solution. The delivery tube from the pump was then connected to the top of the column and 100 mls. of the surfactant solution was allowed to pass through the column. 2 ml. samples of an 8×10^{-4}M phenyl acetate in 0.5M potassium chloride solution was then introduced onto the top of the column. The same procedure used for fraction collections for the determination of Vo was then followed. Optical densities were read, after dilutions, at a wavelength of 261 nm. and elution volumes were determined in the same manner, as above, from the points of inflexion on the ascending limb of the

optical density versus fraction number plots.

Results and treatment of Results. Fig. (2.13) shows the elution profiles plotted as optical density against effluent volume for the elution of 8 x 10^{-4}M phenyl acetate in CTAB solutions in water adjusted to an ionic strength of 0.5M with potassium chloride. Fig.(2.14) shows a plot of $\frac{1}{Ve - Vo}$ against concentration of CTAB micelles in grams per ml. at 25° and 30° ± 0.1. The straight lines were submitted to a least squares programme from which the slope and the intercept were obtained. Table (2.19) shows these values together with calculated partition coefficient values.

Temp.	Slope	Standard deviation of slope	Intercept	Standard deviation of intercept	$\bar{v}(K_p - 1)$	K_p
25°	5.14179	9.05696×10^{-2}	4.412835×10^{-2}	8.3858×10^{-4}	116.519	119.4
30°	5.19745	4.30069×10^{-2}	4.46937×10^{-2}	3.2677×10^{-4}	116.29	119.18

TABLE (2.19). Values of the slope and intercept for plots of $\frac{1}{Ve - Vo}$ against C_m in $g.ml^{-1}$ together with the $\bar{v}(K_p - 1)$ and K_p values at 25° and 30° ± 0.1. for 8 x 10^{-4}M phenyl acetate in CTAB solutions at an ionic strength of 0.5M.

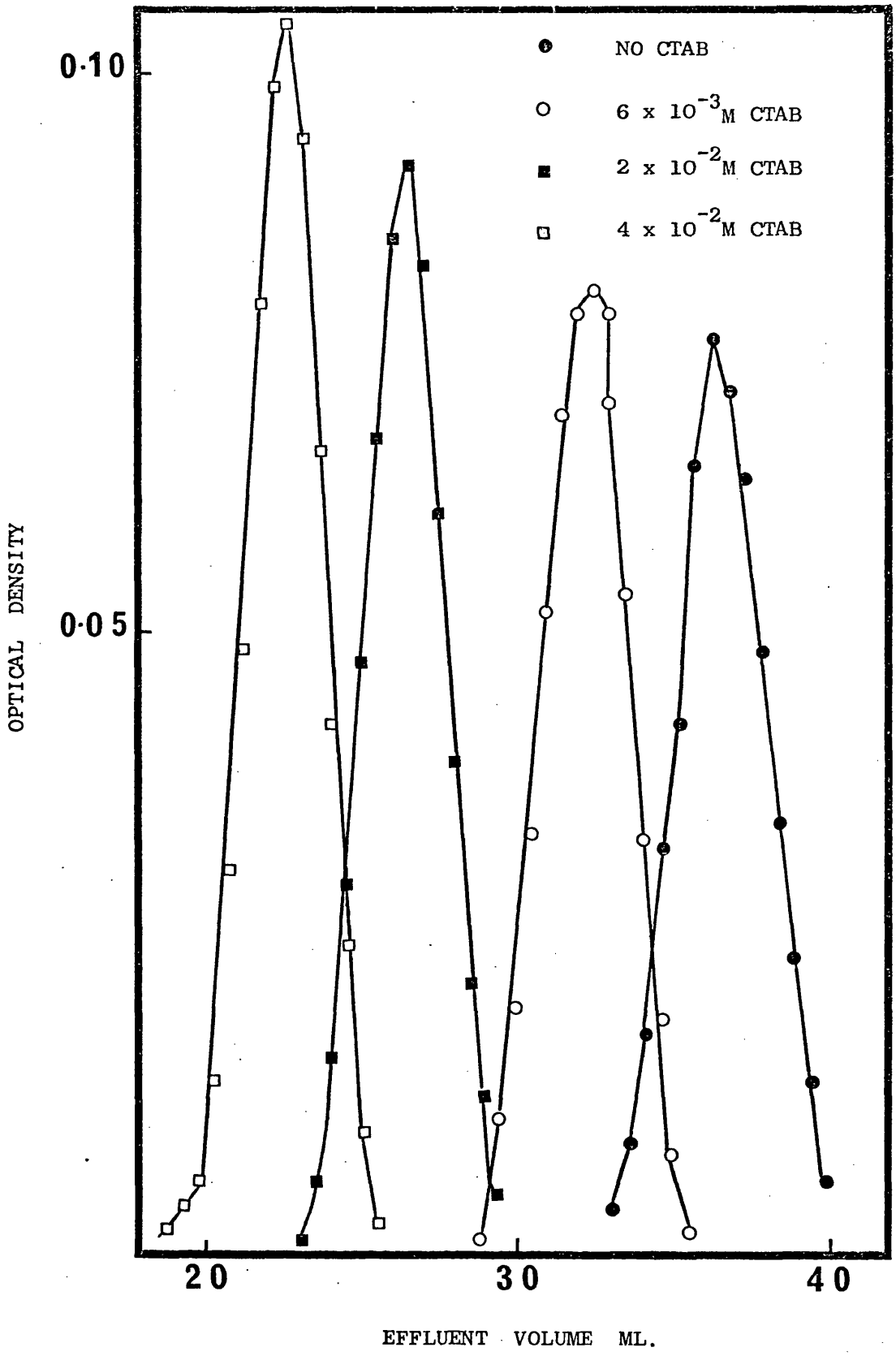

FIG. (2.13). PROFILES TO SHOW THE EFFECT OF CTAB CONCENTRATION ON THE ELUTION OF PHENYL ACETATE FROM A COLUMN OF DEXTRAN GEL (SEPHADEX G25/80).

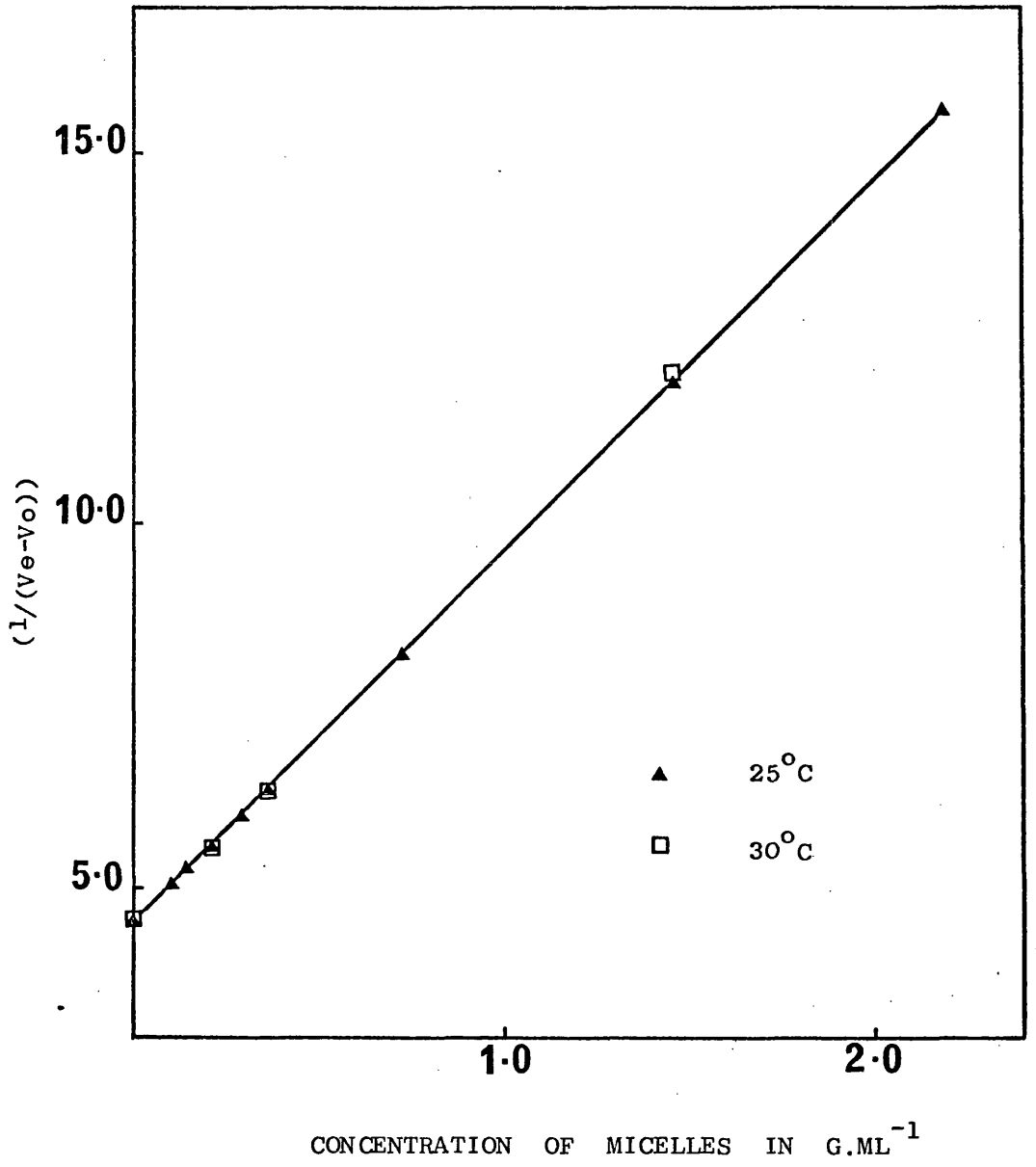

FIG. (2.14). A PLOT OF $^{1}/(Ve-Vo)$ AGAINST CONCENTRATION OF CTAB MICELLES IN $G.ML^{-1}$ FOR PHENYL ACETATE AT 25°C AND 30°C.

VISCOSITY MEASUREMENTS

Viscometry is one of the simpler experimental techniques which can be used to determine the size and shape of molecules.

The influence of introducing colloidal, spherical, non-interacting particles on the viscosity of a pure liquid was first quantified by Einstein who concluded that the viscosity of a very dilute ideal suspension of non-interacting spheres would be given by equation (2.11).

$$\eta = \eta_o (1 + 2.5 \phi) \quad \ldots\ldots\ldots\ldots\ldots (2.11)$$

where η_o is the viscosity of the solvent,

η is the viscosity of the suspension,

and ϕ is the volume fraction occupied by the suspended particles and = $\frac{\text{Volume of particles}}{\text{Total volume of suspension}}$

In real systems involving the addition of macromolecules to a solvent additional terms have to be added to allow for assymetry and solvent-solute interactions. Under these circumstances, if the volume fraction, ϕ, is replaced by a concentration term, c, the viscosity can be described by a power series, equation (2.12).

$$\eta = \eta_o (1 + ac + bc^2 + \ldots) \quad \ldots\ldots\ldots\ldots (2.12)$$

where a and b are constants allowing for the solvent-solute interactions and assymetric particles.

Neglecting terms higher than c^2 in equation (2.12) and rearrangement gives the Huggins equation (2.13).

$$\frac{\left(\frac{\eta}{\eta_o} - 1\right)}{c} = [\eta] + k[\eta]^2 c \quad \ldots\ldots\ldots\ldots (2.13)$$

where c is the concentration in $g.ml^{-1}$.

$[\eta]$ is the concentration intrinsic viscosity,

k is a constant that can be determined experimentally and known as Huggins Constant,

η / η_o is the relative viscosity,

and $(\frac{\eta}{\eta_o} - 1)$ is the specific viscosity $\eta_{sp} = (\eta_{rel} - 1)$.

In micellar systems, the solution at the CMC is considered to be the solvent and the concentration term in equation (2.13) reverts to the concentration of the micelles C_m where (C_m = c-CMC) in grams per ml., and equation (2.13) becomes equation (2.14).

$$\frac{\eta_{sp}}{(c-CMC)} = [\eta] + k[\eta]^2(c-CMC) \quad \ldots\ldots\ldots\ldots\ldots \quad (2.14)$$

and a plot of $\frac{\eta_{sp}}{C_m}$ against C_m would result in a linear relationship with an intercept $[\eta]$, and a slope $k[\eta]^2$ from which Huggins constant can be evaluated. Both can provide an indication of the shape and extent of hydration of the colloidal particle; solid spherical particles characteristically have a value for k of 2.0 Rod like macromolecules have values up to 0.8 and random coils have values about 0.4.

The concentration intrinsic viscosity has been related both empirically (128) and theoretically (129) to the viscosity average molecular weight, which approximates to the weight average molecular weight, by equation (2.15).

$$[\eta] = a M^{\beta} \quad \ldots\ldots\ldots\ldots\ldots\ldots \quad (2.15)$$

where a and β are constants for a given macromolecule-solvent system and temperature. The value of β generally lies between

0 and 2 and is again dependent on the shape and the solvation of the macromolecule.

The volume intrinsic viscosity $[\eta]_\phi$ can be calculated from using equation (2.16).

$$[\eta]_\phi = \frac{[\eta]}{\bar{v}} \quad \ldots\ldots\ldots\ldots\ldots\ldots (2.16)$$

where $\bar{v}$ is the partial specific volume when c is in $g.ml^{-1}$.

For non-hydrated spheres $[\eta]_\phi$ has a value of 2.5 which increases with the degree of hydration and assymetry.

Experimental. The kinematic viscosity of a liquid is defined in terms of density and dynamic viscosity by equation (2.17).

$$v = \frac{\eta}{\rho} = Ct - \beta/t \quad \ldots\ldots\ldots\ldots\ldots\ldots (2.17)$$

where v is the kinematic viscosity,

η is the dynamic viscosity,

ρ is the density of the solution,

t is the time in seconds,

and C and β are constants for a particular viscometer.

Most U-tube viscometers require the introduction of an exact volume of liquid. This complication is avoided by the use of the suspended-level viscometer, which has the added advantage of lessening the hydrostatic head during viscosity measurements.

The β/t term in equation (2.17) can be ignored when surfactant solutions are used with capillary viscometers, such as the suspended level, due to the negligible hydrostatic head correction and by choosing suitably long flow times (130) and equation (2.17) becomes equation (2.18).

$$v = \frac{\eta}{\rho} = Ct \quad \ldots\ldots\ldots\ldots\ldots\ldots (2.18)$$

Equation (2.18) is used for the determination of viscometer constants using liquids of known viscosities and for checking known constants.

Treatment of Apparatus and Solutions. The viscometers used were cleaned with "chromic acid" mixture for at least half an hour, washed with distilled water and then rinsed with running distilled water, sucked through by a water pump, for at least half an hour. The viscometers were then dried with acetone and a stream of filtered air, under pressure.

The solutions were prepared in the usual way, in volumetric flasks previously aged, and then passed through a 0.22μm millipore filter, boiled in several changes of double distilled water to remove any wetting agents, discarding the first 10 mls. in case of contamination or adsorption of solute onto the filter discs.

Viscosity Determinations. Viscosity measurements were carried out at $30^{o} \pm 0.05$ in a glass sided, thermostatically controlled, water bath. The temperature fluctuations were monitored by a thermocouple which touched the bulb of the viscometer. The viscometer was then suspended in the bath from a holder which could be levelled to ensure that the viscometer capillary was always vertical. Flow times were measured with a Heuer stop watch graduated to 0.05 seconds. The procedure for measurements was according to the British Standard 188 - 1957 (130). The flow time used for the determination of the viscosity was the average of three readings, all of which fell within the permitted range of $\pm$ 0.2%. The solutions were left in the water bath to equilibrate to the temperature of $30^{o} \pm 0.05$ for at least 30 minutes prior to any flow time determinations.

Calibration of Viscometers. Three suspended level viscometers were used, two had known calibration constants which were used to check the technique by determination of the viscosity of double distilled, boiled and cooled water for which the viscosity and the density at 30^{o} were taken as 0.7975 cps. and 0.995646 $g.ml^{-1}$, respectively (120). The data in Table (2.20) which was calculated ignoring the β/t term in equation (2.17) shows this was satisfactory and water was therefore used to calibrate the remaining unknown constant. The β/t term was also ignored in all subsequent measurements.

Viscometer No.	Flow time (seconds)				Certified Constant$_1$ cs sec^{-1} x 10^4	Calculated Constant cs sec^{-1} x 10^4	Calculated Viscosity of water cp
	t_1	t_2	t_3	$t_{average}$			
1	872.2	872.2	872.3	872.23	9.181	-	0.7973
1	991.4	991.5	991.4	991.43	8.079	-	0.7975
1	1031.1	1031.1	1031.4	1031.28	-	7.7669	-

TABLE (2.20). Data for the calibration and determination of viscometer constants.

Viscosity Determinations of Surfactant Solutions. Viscosities were determined for the following four systems:

CTAB in water

CTAB in water adjusted to an ionic strength of 0.5 with potassium chloride

CTAB in carbonate-bicarbonate buffer at pH 9.2 and ionic strength of 0.5

and CTAB in carbonate-bicarbonate buffer at pH 9.2 and ionic strength of 0.5 in the presence of 8×10^{-4}M phenyl acetate.

The concentration range of surfactant covered was the same as that in the kinetic studies.

Treatment of Results. Relative viscosities were calculated from equation (2.18) ignoring the densities of the solutions and are shown in tables (2.21 - 2.24). The error in the approximation was found to be negligible; when density corrections using values obtained by interpolation of the data given in Table (2.16) were made, the relative viscosities were changed only in the fifth decimal place.

The data are represented graphically in diagram (2.15) according to equation (2.14) and in diagram (2.16) as η_{rel} against the % concentration of CTAB. Figure (2.17) represents the results according to equation (2.14) at a higher CTAB concentration than that used in this study and shows the sudden rise in reduced specific viscosity after an almost parallel line to the x-axis.

TABLE (2.21). Viscosity data for CTAB in water at 30°C.

CTAB Concentration $g.ml^{-1} \times 10^3$	(c-CMC) $g.ml^{-1} \times 10^3$	Average Flow time (seconds)	Viscometer Constant cs $sec^{-1} \times 10^4$	η_{rel}	Reduced Specific Viscosity
0.32801 (CMC)	-	1033.90	7.767	1.00000	-
1.45784	1.12983	891.50	9.181	1.01929	17.073
2.18676	1.85875	1065.87	7.767	1.03097	16.662
2.91568	2.58767	912.70	9.181	1.04353	16.822
3.64460	3.31659	1092.03	7.767	1.05627	16.966
4.37572	4.04551	1099.50	7.767	1.06349	15.694
5.83136	5.50335	938.57	9.181	1.07311	13.285
7.28920	6.96119	953.03	9.181	1.08964	12.877
10.20488	9.87687	974.34	9.181	1.11400	11.542
14.57840	14.25039	1014.23	9.181	1.15961	11.200
21.86760	21.53959	1069.23	9.181	1.22250	10.330
29.1568	28.82879	1125.20	9.181	1.28649	9.938

TABLE (2.22). Viscosity data for CTAB in water adjusted to ionic strength 0.5 at 30^{o}.

CTAB Concentration $g.ml^{-1} \times 10^{3}$	(c-CMC) $g.ml^{-1} \times 10^{3}$	Average Flow time (seconds)	Viscometer Constant cs $sec^{-1} \times 10^{4}$	η_{rel}	Reduced Specific Viscosity
0.02551 (CMC)	-	862.30	9.181	1.00000	-
1.45784	1.43233	1019.60	7.767	1.00032	0.22341
2.18676	2.16125	863.47	9.181	1.00136	0.62927
2.91568	2.89017	1023.70	7.767	1.00434	1.50164
3.64460	3.61908	869.07	9.181	1.00785	2.16906
4.37352	4.34010	1030.30	7.767	1.01081	2.49073
5.83136	5.80585	875.57	9.181	1.01539	2.65077
7.28920	7.26369	1040.60	7.767	1.02091	2.87870
10.20488	10.17937	888.97	9.181	1.03093	3.03850
14.57840	14.55289	1067.77	7.767	1.04757	3.26877
21.86760	21.84209	925.77	9.181	1.07361	3.37010
29.15680	29.13129	948.40	9.181	1.09985	3.42759

TABLE (2.23). Viscosity data for CTAB in carbonate-bicarbonate buffer at pH 9.2, μ = 0.5 at 30°.

CTAB Concentration $g.ml^{-1} \times 10^3$	(c-CMC) $g.ml^{-1} \times 10^3$	Average Flow time (seconds)	Viscometer Constant cs $sec^{-1} \times 10^4$	η_{rel}	Reduced Specific Viscosity
0.02551 (CMC)	-	873.47	9.181	1.00000	-
1.45784	1.43233	1003.70	8.079	1.01117	7.79848
2.18676	2.16125	1046.45	7.767	1.01353	6.26027
2.91568	2.89017	1049.13	7.767	1.01612	5.57753
3.64460	3.61908	889.80	9.181	1.01870	5.16706
4.37352	4.34401	892.70	9.181	1.02202	5.06905
5.83136	5.80585	1018.70	8.079	1.02628	4.52647
7.28920	7.26369	1065.20	7.767	1.03169	4.36280
10.20488	10.17937	911.50	9.181	1.04354	4.27728
14.57840	14.55289	1051.20	8.079	1.05902	4.05555
21.86760	21.84209	1123.63	7.767	1.08827	4.04128
29.15680	29.13129	974.43	9.181	1.11559	3.96790

TABLE (2.24). Viscosity data for CTAB in carbonate-bicarbonate buffer at pH 9.2, μ = 0.5 at 30° in the presence of 8 x 10^{-4}M phenyl acetate.

CTAB Concentration $g.ml^{-1} \times 10^3$	(c-CMC) $g.ml^{-1} \times 10^3$	Average Flow time (seconds)	Viscometer Constant cs $sec^{-1} \times 10^4$	η_{rel}	Reduced Specific Viscosity
0.02551 (CMC)	-	878.85	9.181	1.00000	-
1.45784	1.43233	1006.45	8.079	1.00773	5.39680
2.18676	2.16125	887.60	9.181	1.00996	4.60844
2.91568	2.89017	889.90	9.181	1.01257	4.34923
3.64460	3.61908	1014.30	8.079	1.01559	4.30772
5.83136	5.80585	898.00	9.181	1.02179	3.75311
7.28920	7.26369	1026.40	8.079	1.02771	3.81487
10.20488	10.17937	912.28	9.181	1.03804	3.73697
14.57840	14.55289	925.30	9.181	1.05285	3.63158
21.86760	21.84209	1076.60	8.079	1.07797	3.56971
29.15680	29.13129	970.30	9.181	1.10406	3.57210

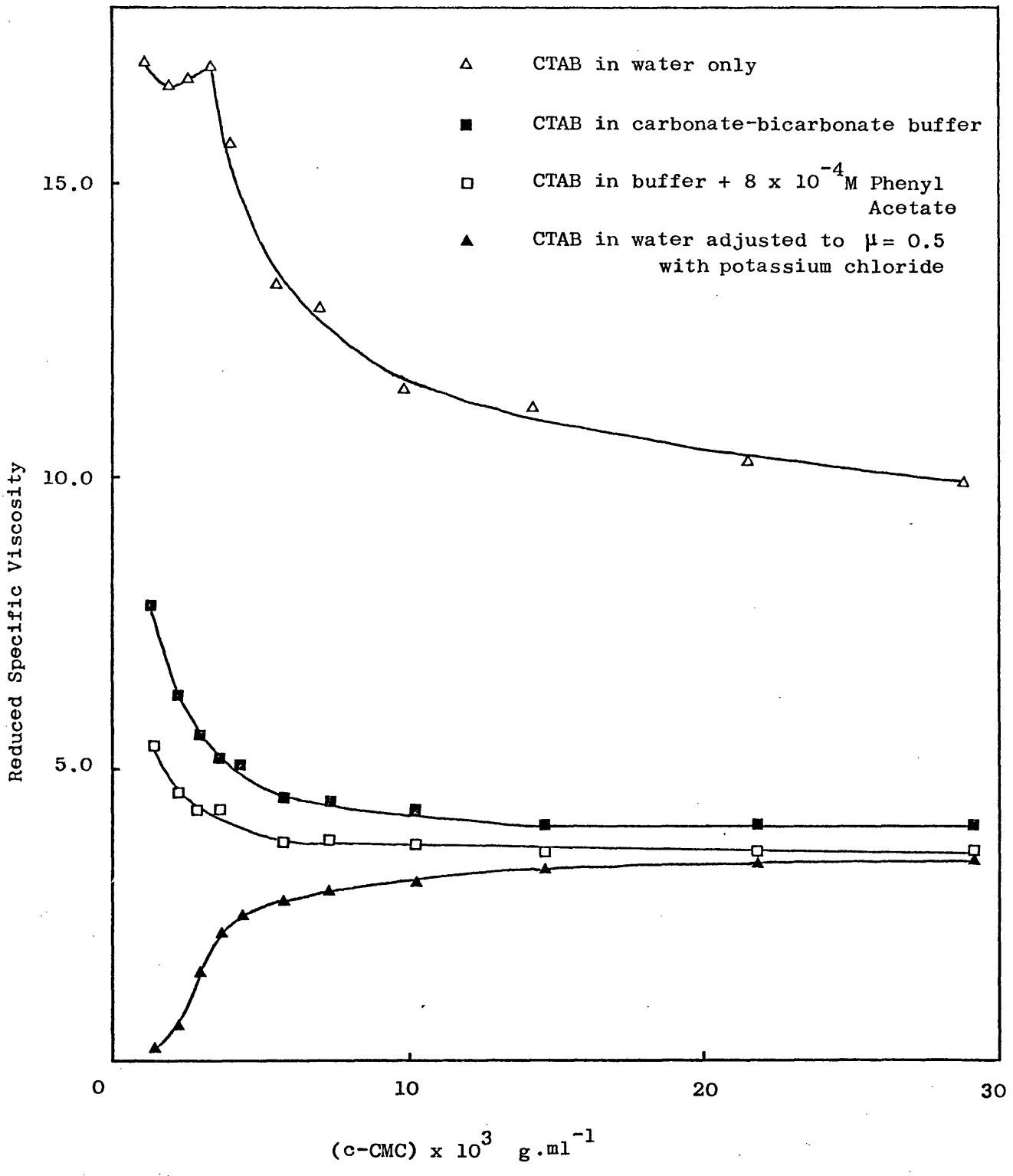

FIGURE (2.15). REDUCED SPECIFIC VISCOSITY AGAINST MICELLAR WEIGHT IN GM. ML^{-1} FOR CTAB IN ALL SYSTEMS INVESTIGATED AT 30^{o}.

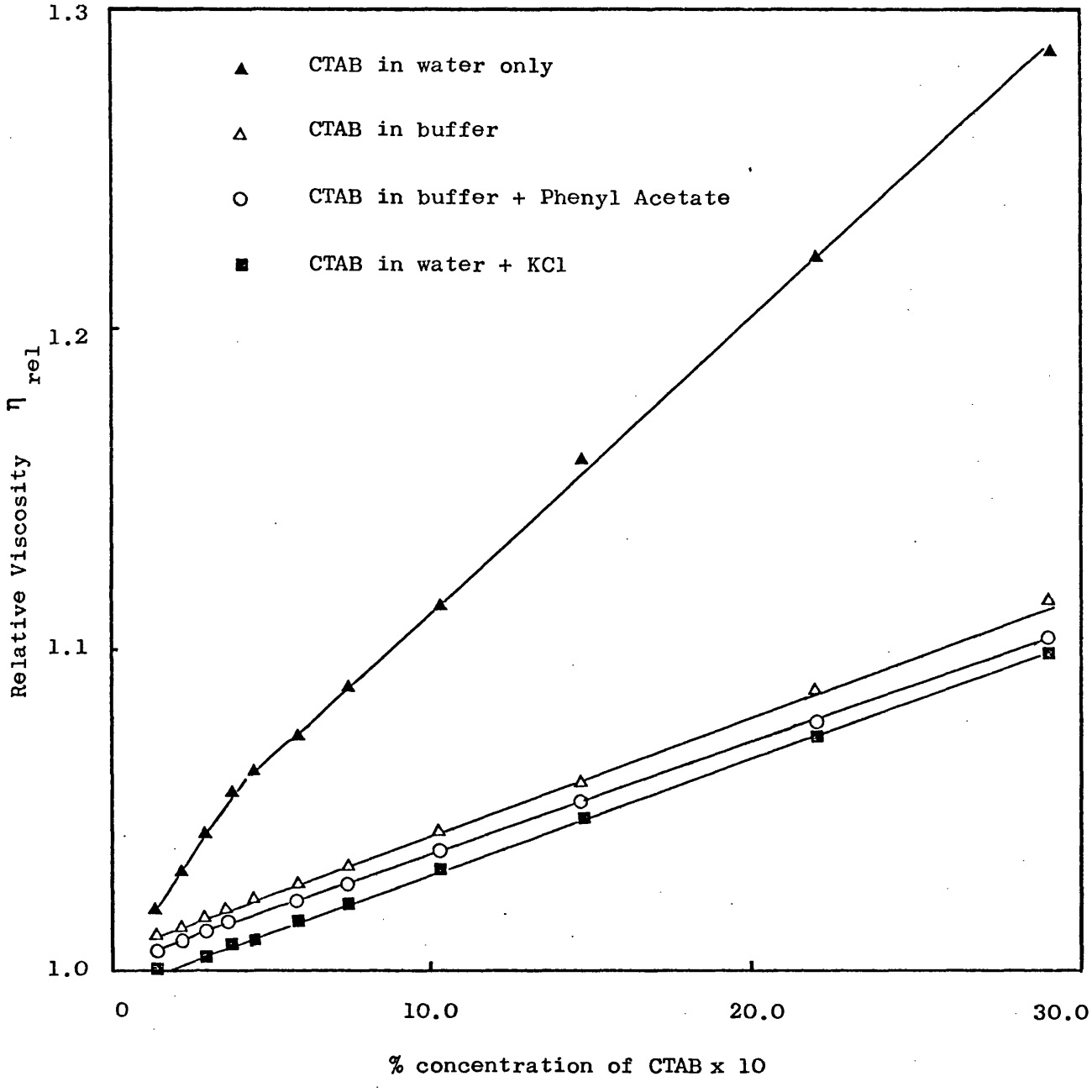

FIGURE (2.16). RELATIVE VISCOSITY AGAINST % CTAB CONCENTRATION FOR ALL THE SYSTEMS INVESTIGATED AT 30^{o}.

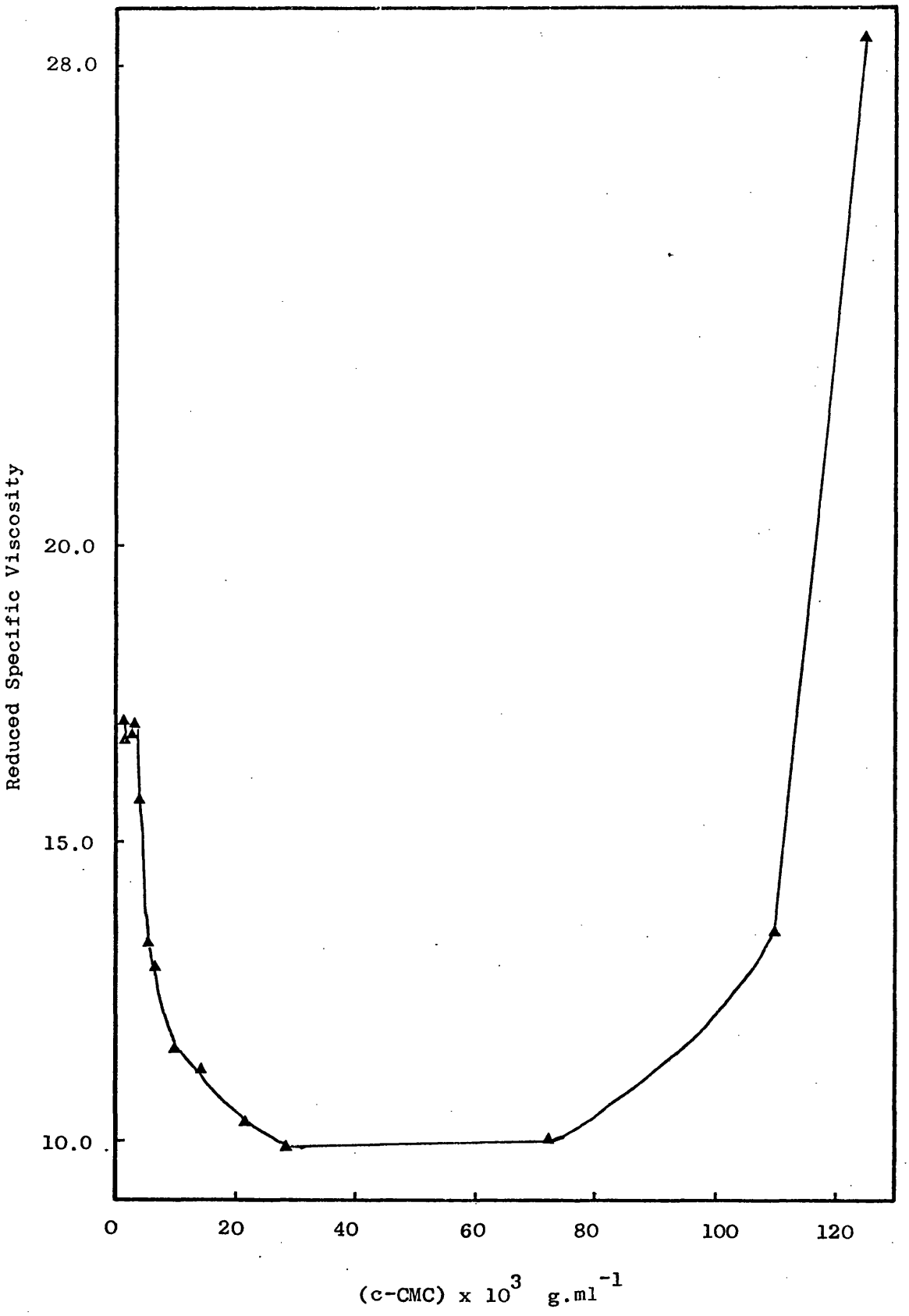

FIGURE (2.17). REDUCED SPECIFIC VISCOSITY AGAINST MICELLAR WEIGHT IN $g.ml^{-1}$ FOR CTAB IN WATER AT 30°.

LIGHT SCATTERING STUDIES

Light scattering provides an almost ideal technique for the characterization of physical properties of colloidal dispersions. It allows the examination of these systems without disturbing the natural state of the particles under observation, and as such it has been utilized for the evaluation of molecular weights and for the determination of particles shape and charge.

General Theory. The scattering of light by solutions can be treated from two points of view: scattering by ideal systems obeying Rayleigh theory and scattering by non-ideal systems to which the fluctuation theory can be applied. The former assumes the molecules in solution to be independent, isotropic and small compared to the wavelength of incident light, λ , with a radius less than $\frac{\lambda}{20}$. The light scattering results from the interactions of the oscillating electric field of the incident light wave with the electrons and nuclei in the molecules, setting them into forced oscillation so they become a source of secondary radiation. Rayleigh (131) showed that the intensity of light (I_θ) scattered by a medium at any angle θ at a distance (r) from the scattering particle is given by equation (2.19).

$$\frac{I_\theta r^2}{I_o} = \frac{8\ \pi^4 n_o^4 v\ a^2}{\lambda^4} (1 + \cos^2\theta) \quad \ldots\ldots\ldots (2.19)$$

where I_o is the intensity of the incident light,

a is the polarisability of the molecules, representing the ease of dipole formation,

λ is the wavelength of the incident light,

v is the number of molecules per unit volume,

n_o is the refractive index of the medium,

θ is the angle between the line of sight and the direction of propagation of the primary beam,

The term $\frac{I_\theta r^2}{I_o}$ is known as the Rayleigh ratio, R_θ

When traversing a medium, light loses intensity due to scattering by particles in its path. The decrease in $\log_e$ of the intensity (I) with path length (x), $-d \log_e I/dx$, is called the turbidity. If I_θ, the intensity of the scattered light from the particles, is known as a function of r and θ, the turbidity τ can be calculated by integrating I_θ over the surface of a sphere of radius r, which gives equation (2.20).

$$\tau = \frac{8\pi}{3} \frac{I_\theta r^2}{I_o} = \frac{16\pi}{3} R_{90} \quad \ldots\ldots\ldots \quad (2.20)$$

where R_{90} is Rayleigh's ratio at an angle of 90^o to the incident beam.

In the case of a solution, scatter arises from both solute and solvent particles. The excess turbidity (τ') is equal to the total turbidity minus the turbidity of the solvent (τ_o).

The polarisability of the solute molecules α , is given by equation (2.21) (ref. 132).

$$\alpha = \frac{n^2 - n_o^2}{4\pi v n_o^2} \quad \ldots\ldots\ldots\ldots\ldots\ldots \quad (2.21)$$

where n is the refractive index of the solution,

n_o is the refractive index of the pure solvent,

and v is the number of molecules per unit volume.

If $n \simeq n_o$ and v is replaced by $\frac{Nc}{M}$, where N is Avogadro's number and M is the molecular weight of the molecules in solution, and c is the molar concentration, equation (2.21) becomes

$$\alpha = \frac{2n_o(n-n_o)M}{4\pi c N n_o^2} = \frac{(n-n_o)M}{2\pi N c n_o} = \left(\frac{dn}{dc}\right)\frac{M}{2\pi N n_o} \quad \ldots (2.22)$$

The term (dn/dc) is known as the refractive index increment for the solution and is equal to (n-no)/c as the change in refractive index difference between solution and solvent, with concentration, is linear.

Substituting for α in equation (2.19) and combining equations (2.19 and 2.20) we obtain equation (2.23).

$$\tau' = \left[\frac{32\ \pi^3 n_o^2}{3N\ \lambda_o^4}\left(\frac{dn}{dc}\right)^2\right] Mc \quad \ldots\ldots\ldots (2.23)$$

where τ' is the excess turbidity measured at 90^o. The brackets contain an expression which is a constant for a particular system and is usually denoted by the symbol H and thus

$$\tau' = HMc \quad \ldots\ldots\ldots (2.24)$$

which is the relationship between the excess turbidity and the weight average molecular weight for a dilute solution of macromolecules behaving ideally. The solvent in surfactant solutions is usually taken as the solution at the CMC and the excess turbidity is then the turbidity of the solution minus the turbidity at the CMC

$$\tau' = \tau_{solution} - \tau_{CMC} \quad \ldots (2.25)$$

The premise of ideality and the assumption of random positions of the particles with respect to one another does not prevail in liquids and non-ideal solutions and the total scattering cannot be obtained by summing up of scattering intensities of the individual particles. To overcome this problem, light scattering from solutions can be viewed in terms of fluctuations in concentrations of one component with respect to another (133). The tendency for these fluctuations to occur will depend upon the osmotic work, provided by thermal agitation, required to produce the concentration gradient. Debye (134) using the fluctuation theory showed that

$$\tau' = \frac{32\ \pi^3 n_o^2 cRT}{3\ \lambda^4 N \left(\frac{dP}{dc}\right)} \left(\frac{dn}{dc}\right)^2 \quad \ldots\ldots\ldots\ldots\ldots (2.26)$$

where P is the osmotic pressure of the colloidal solution and c is the concentration in $g.ml^{-1}$.

For ideal solutions $\left(\frac{dP}{dc}\right)$ is equal to $\frac{RT}{M}$ and τ becomes proportional to M. For non-ideal solutions, use is made of the relationship derived by Debye (134) using the fluctuation theory

$$\frac{P}{RT} = \frac{c}{M} + Bc^2 \quad \ldots\ldots\ldots\ldots\ldots\ldots (2.27)$$

where B is the second virial coefficient and is a measure of the deviation from ideality in the van't Hoff osmotic pressure law. Differentiating equation (2.27) and substituting in equation (2.26) for $\frac{dP}{dc}$ leads to equation (2.28)

$$\frac{Hc}{\tau'} = \frac{1}{M} + 2Bc \quad \ldots\ldots\ldots\ldots\ldots (2.28)$$

Equation (2.28) can be transformed into equation (2.29)

$$\frac{H(c-CMC)}{T - T_{CMC}} = \frac{1}{M} + 2B\,(c-CMC) \quad \ldots\ldots\ldots\ldots (2.29)$$

where T is the turbidity of the solution,

T_{CMC} is the turbidity of the solution at the CMC,

c is the concentration in $g.ml^{-1}$.

and CMC is the critical micelle concentration in $g.ml^{-1}$.

A plot of $\frac{H(c-CMC)}{T - T_{CMC}}$ versus (c-CMC) would result in a straight line with an intercept giving the reciprocal of the molecular weight of the solute and a slope of 2B. The constant B gives information on the shape and degree of hydration of the particles in the solution and their charge. For ionic surfactants (135) the relationship of the slope to the effective charge is according to equation (2.30)

$$p' = \sqrt{\frac{2B\,x}{1/M}} \quad \ldots\ldots\ldots\ldots\ldots\ldots (2.30)$$

where x is the concentration of the surfactant at the CMC in $g.ml^{-1}$.

Depolarisation. The equations derived so far assume that the scattering particles are optically isotropic. Most molecules are, however, optically anisotropic and when irradiated, the light scattered at 90^{o} will exhibit a small horizontal component in addition to the vertical one. This effect is known as DEPOLARIZATION and when anisotropic effects are present the value of scattered light is greater than the theoretical value of an equivalent number of isotropic molecules, resulting in a higher excess turbidity. It is necessary in such cases, therefore, to apply a correction for this additional scattering, since the molecular weight is related

only to that part of the scattering due to fluctuations in concentration. This correction was worked out by Cabannes (136) who showed that the correction factor involves only the depolarization ratio, ρ_u, which is defined as

$$\rho_u = \frac{H_u}{V_u} \quad \ldots\ldots\ldots\ldots\ldots\ldots\ldots\ldots \quad (2.31)$$

where H_u is the horizontally polarized and V_u the vertically polarized components of the scattered unpolarized incident light.

The correction factor known as Cabannes' factor (C_F) is equal to

$$\left[\frac{6 - 7\rho_u}{6 + 6\rho_u}\right] \quad \ldots\ldots\ldots\ldots\ldots\ldots \quad (2.32)$$

Applying this correction to equation (2.24) gives equation (2.33)

$$M = \frac{\tau}{Hc}\left[\frac{6 - 7\rho_u}{6 + 6\rho_u}\right] = \frac{\tau}{Hc} \cdot C_F \quad \ldots\ldots\ldots \quad (2.33)$$

Dissymmetry. If the scattering molecules or particles are greater than $\lambda/20$ there will be a greater intensity of light scattered in the forward direction than in the backward direction. Therefore, the ratio i_{45}/i_{135}, known as the dissymmetry, will be greater than unity which is the value for spherical scatterers of a radius less than $\lambda/20$. Dissymmetry does, therefore, give valuable information concerning the shape of particles in a system. This is one of the reasons for ensuring dust free solutions when carrying light scattering determinations, since dust can cause large values of dissymmetry.

Light Scattering in Surfactant Solutions. The equations derived so far are not wholly applicable to the case of charged colloidal particles in a salt solution where a three component system exists with the fluctuations of colloid and salt being interdependent due to the interactions of the various charged species. Prins and Hermans (137) and Princen and Mysels (138) applied the general fluctuation theory of light scattering by multiple component systems to ionic surfactant solutions containing added inorganic electrolytes. These authors derived equation (2.35) which is known as the (PHPM) equation.

$$\frac{H\,(c-CMC_1)}{(\tau-\tau_{CMC})} = \frac{g}{M_n}\left[1+\frac{c-CMC_1}{2M_n}\left(\frac{p^2+p-pg}{CMC_2+x}\right)\right] \quad \ldots (2.35)$$

where H is the system constant shown in equation (2.23)

c is the total surfactant concentration in $g.ml^{-1}$.

CMC_1 is the critical micelle concentration in $g.ml^{-1}$.

τ is the turbidity of the solution,

τ_{CMC} is the turbidity of the solution at the CMC

p is the micellar charge,

M_n is the micellar weight = nM_1 where n is the aggregation number and M_1 is the molecular weight of the surfactant,

CMC_2 is the critical micelle concentration in $moles/ml^{-1}$.

x is the concentration of added salt in $moles/ml^{-1}$.

and g is an abbreviation for the following expression

$$g = \frac{(CMC_2+x)^2}{(CMC_2)^2 d_1 + 2(CMC_2)d_2 x + d_3 x^2} \quad \ldots\ldots\ldots (2.36)$$

where $d_1 = 1 - p/n + p^2/4n^2 + p/4n^2$

$d_2 = 1 - p/2n - fp/2n + fp^2/4n^2 + fp/4n^2$

and $d_3 = 1 - fp/n + f^2p^2/4n^2 + f^2p/4n^2$

f = is the ratio of the molar refractive index increments of the added inorganic electrolyte to that of the surfactant in the system.

According to these equations, a plot of $H\,(c-CMC_1)/{}^{T} - {}^{T}_{CMC}$ against $(c-CMC_1)$ yields a straight line with an intercept (A) equal to g/Mn and a slope (B) which could be evaluated according to equation (2.37)

$$B = \frac{A\,(p^2 + p - AnM_1p)}{2\,nM_1\,(CMC_2 + x)} \qquad \ldots\ldots\ldots\ldots\ldots (2.37)$$

Solving for p gives equation (2.38)

$$p = \frac{BM_1\,(CMC_2 + fx) + \sqrt{2B(CMC_2 + x)}}{A\,(1 - \frac{AM_1E}{2})} \qquad \ldots (2.38)$$

in which $E = \frac{CMC_2 + fx}{CMC_2 + x}$

and $n = \frac{1}{2}\left(pE + \frac{1}{AM_1}\right) + \frac{1}{2}\sqrt{\left(pE + \frac{1}{AM_1}\right)^2 - (p^2 - p)E^2}$

$\ldots\ldots\ldots\ldots\ldots (2.39)$

and thus the charge p and the aggregation number n can be evaluated.

EXPERIMENTAL

Treatment of Equipment. When carrying out light scattering measurements, it is essential the solutions be dust free. This can be achieved by ultrafiltration of the solutions and by careful cleansing of equipment. To this aim all the glass apparatus was thoroughly cleaned by treatment with "chromic acid" mixture followed by washing with distilled water and then inverted and flushed with a steam jet for at least fifteen minutes followed by condensing acetone vapour. This treatment was applied to the lower parts of the filtering apparatus (see diagram 2.18).

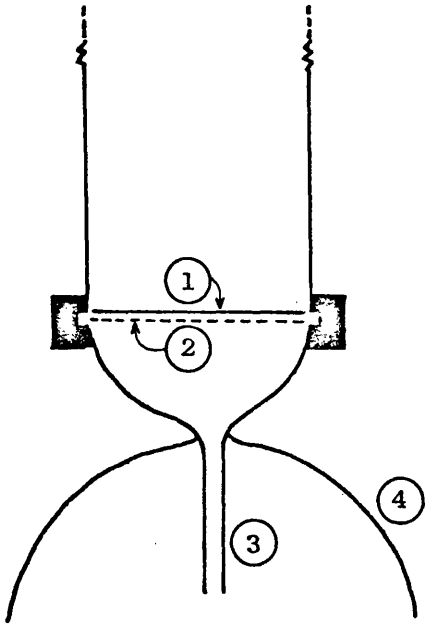

FIG. (2.18). SCHEMATIC REPRESENTATION OF THE LOWER PARTS OF THE FILTERING APPARATUS.

1. Sartorius membrane.
2. Perforated metal support.
3. Delivery tube.
4. Glass dome cover to protect cell from dust during filtration.

including the perforated metal support for the filter discs, the delivery tube and the glass dome cover. The light scattering photometer and filtration equipment were housed in a polyethylene tent and measurements and manoeuvres were conducted under this tent to minimise dust contamination.

Preparation and Clarification of Solutions. Double distilled water from an all glass apparatus, collected in a vessel under a dust cover, was used throughout for the preparation of solutions. A double filtration procedure, under positive pressure, was adopted using 0.2 μM sartorius membranes which had been boiled in several changes of double distilled water with the final filtration directly into a circular D101 cell, (supplied by Phoenix Precision Instrument Co.) in which measurements were made.

Calibration of the Light Scattering Photometer. Numerous publications have been concerned with the problems involved in calibrating light scattering photometer to give absolute values of turbidity. A critical survey is given by Kratohvil et al (139). The calibration usually necessitates the utilization of a reproducible standard, such as a polished perspex block, which gives a constant intensity of light scattered at 90^{o} to the incident beam. Such a block has the advantage of being stable and of a similar turbidity to normal surfactant solutions, and once it is calibrated and kept clean, dust free and scratch free, it is easy to use and to handle. The block is calibrated against a suspension of known turbidity. This was achieved according to the method given by Jennings and Jerrard (140).

A colloidal suspension of Syton X30 silica particles (supplied by Monsanto Ltd.) was filtered through a number 3 sintered glass filter and then centrifuged for one hour at 15000g. in an MSE ultra-centrifuge. Four dilutions containing nominally 0.6, 0.9, 1.5 and 3.0% w/v silica, as determined from the original concentration of the sample, were prepared from the supernatant. These suspensions were then filtered through a 0.22μ millipore membrane directly into a 4 cm. spectrophotometer cell. The optical density of each suspension was then read, over the range 420 - 600 nm in an SP1800 spectrophotometer against a reference cell containing double distilled water, filtered in the same way. The solutions were then placed in a circular cell (D101) treated as indicated before. Using the perspex block as a standard, readings were taken at the same wavelength as that for light scattering (546 nm) at 90^{o}, 135^{o} and 45^{o} and a measurement was taken of the vertical and horizontal components at 90^{o} for the Syton X30 suspensions, for unpolarized incident light. Date are given in Table (2.25).

The optical density of each Syton X30 suspension was then plotted against $1/\lambda^{4}$ and a straight line passing through the origin was obtained in each case (Figure 2.19) as predicted by equation (2.2) which is indicative of the absence of absorption and that the optical density was due only to scattering by the particles in suspension.

Values for the turbidity of the suspensions at 546 nm were then obtained from the following relationship:

$$\tau_s = \frac{O.D}{L} \times 2.303 \quad \ldots\ldots\ldots\ldots\ldots (2.40)$$

where τ_s is the turbidity of the suspension,

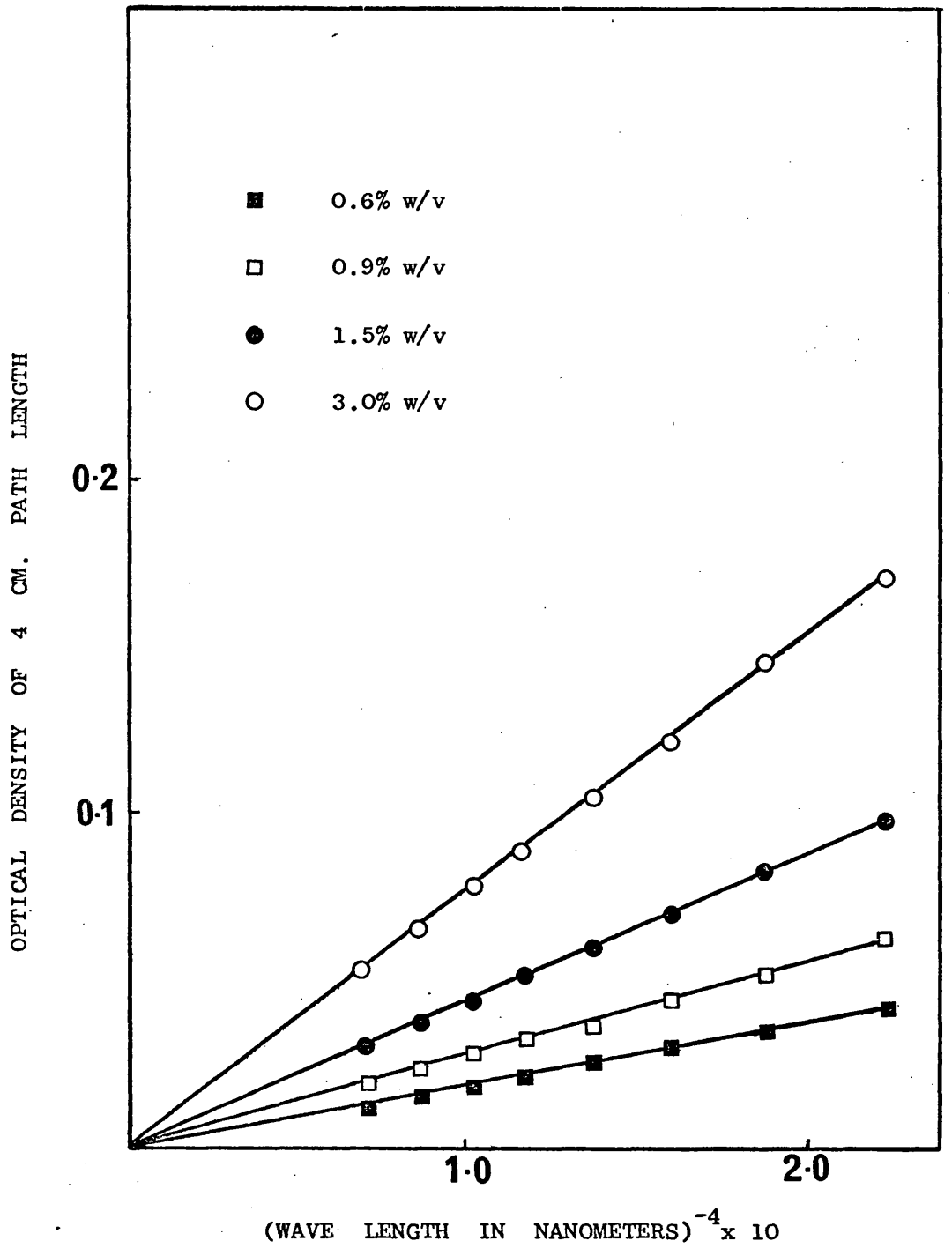

FIG. (2.19). OPTICAL DENSITY AGAINST $1/\lambda^4$ FOR DILUTIONS OF SYTON X30.

O.D. is the optical density of the suspension at 546 nm.

L is the length of the cell (4 cm).

From equation (2.20), modified to allow for depolarization

$$\tau_s = \frac{16\pi}{3} R_{90(s)} C_F \qquad \ldots\ldots\ldots\ldots\ldots\ldots (2.41)$$

and $$\tau_b = \frac{16\pi}{3} R_{90(b)} \qquad \ldots\ldots\ldots\ldots\ldots\ldots (2.42)$$

where τ_b is the turbidity of the block.

$$\therefore \quad \frac{\tau_s}{\tau_b} = \frac{R_{90(s)}}{R_{90(b)}} C_F = S_{90} C_F \qquad \ldots\ldots\ldots (2.43)$$

where S_{90} is the ratio of the light scattering galvanometer reading of the Syton suspension to that of the block.

Hence $$\tau_b = \frac{\tau_s}{S_{90} C_F}$$

The turbidity values, S_{90}s and all other parameters are given in Table (2.25).

Nominal Concentration of Syton X30 % w/v	Optical Density	S_{90}	$\frac{i_{135}}{i_{45}}$	ρ_u	C_F	τ_s	τ_b x 10^4
0.6	0.021	40.180	0.94	0.0117	0.97494	0.01209	3.0863
0.9	0.031	58.170	0.99	0.0134	0.97135	0.01785	3.1591
1.5	0.050	89.458	0.97	0.0183	0.96106	0.02879	3.3487
3.0	0.086	141.920	1.00	0.0261	0.94489	0.04951	3.6921

TABLE (2.25). Optical Density and Light Scattering Results for Suspensions of Syton X30 used to calibrate the Perspex Standard.

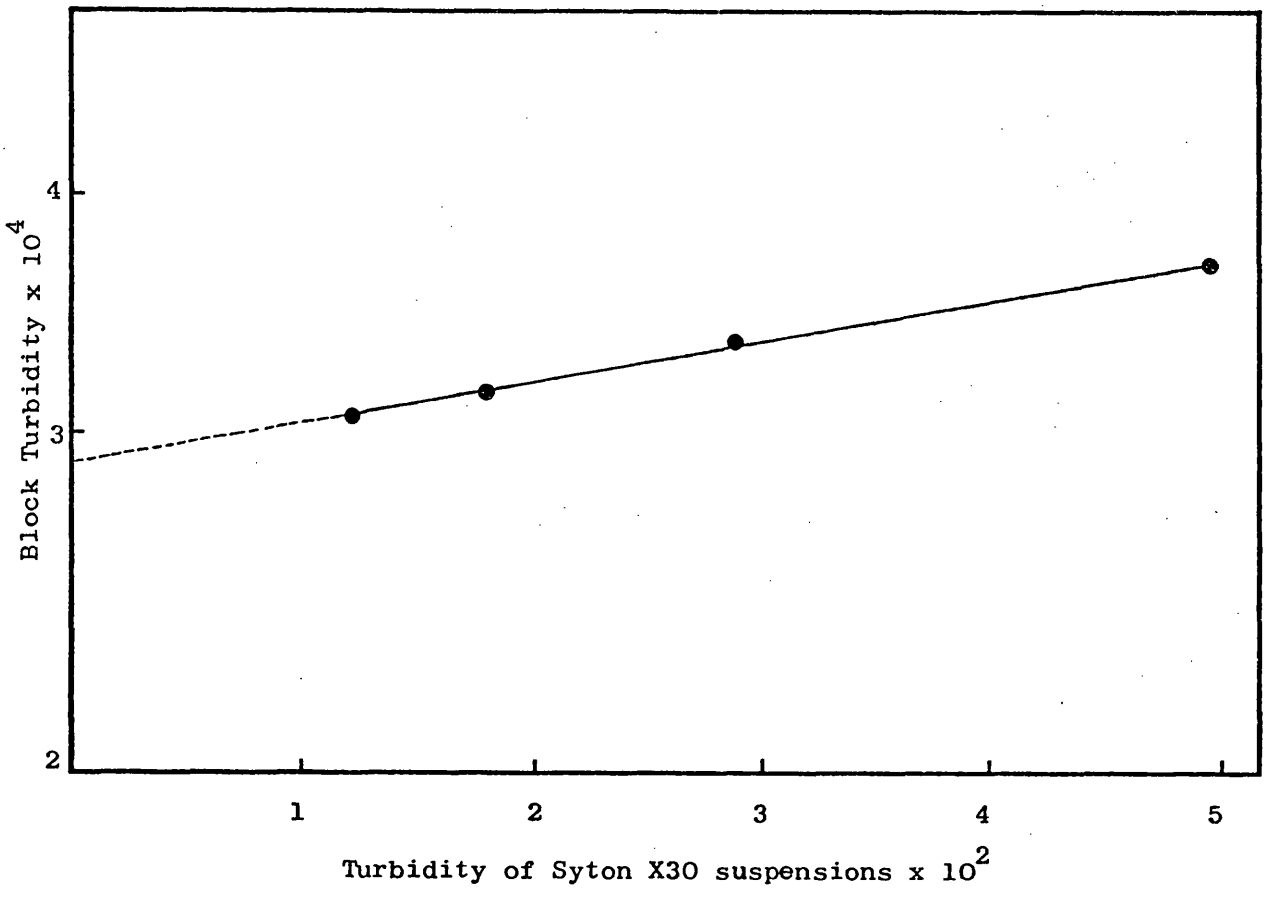

FIGURE (2.20). TURBIDITY OF PERSPEX BLOCK ON LOG SCALE AGAINST TURBIDITY OF SYTON X30 DILUTIONS TO DETERMINE LIGHT SCATTERING PHOTOMETER CALIBRATION CONSTANT.

As the concentration of the Syton X30 increases, its turbidity becomes less than the true value due to internal interference, which reduces S_{90}, and this causes the calculated turbidity of the standard to increase. The accepted procedure (140), is to extrapolate to zero concentration of Syton X30 to obtain the true turbidity, and hence the true calibration constant, of the standard block. This is achieved by plotting the calculated turbidity of the block, on a log scale, against the turbidity of the various dilutions of Syton X30 and extrapolating to zero concentration of Syton X30 as shown in Figure (2.20). The intercept on the y-axis, obtained by submitting the data to least squares regression analysis gives the block turbidity which is used as the calibration constant and which was found to be 2.9067×10^{-4}.

In order to validate the calibration constant, the turbidity of benzene was determined at 25° using equation (2.44) (141) where a refractive index correction has to be applied as the block

$$\tau_{benzene} = S_{90} \cdot \tau_b \left(\frac{n_{benzene}}{n_{water}} \right) \quad \ldots\ldots\ldots \quad (2.44)$$

calibration was effected against an aqueous suspension. The data are given in Table (2.26).

S_{90}	$\frac{i_{135}}{i_{45}}$	ρ_u	$n_{Benzene}$	n_{Water}	$\tau_{Benzene} \times 10^5$
0.865	0.940	0.41	1.502	1.334	28.3
0.874	0.935	0.41	1.502	1.334	28.6

TABLE (2.26). Turbidity of Benzene at 25° and 546 nm as determined using the Calibration Constant.

Using the data available in a comprehensive literature survey of "accepted" Rayleigh ratios for benzene (Kratohvil et al, 139), turbidity values ranging from 25.8×10^{-5} to 29.2×10^{-5} with a mean of 28.18×10^{-5} and a standard error of $\pm$ 1.7 (10 values) at 25° are obtained; depolarization figures lie between 0.4 and 0.42.

The values in Table (2.26) thus compare adequately with literature values and it was therefore concluded the block calibration was satisfactory.

Turbidity Determinations. The perspex block was dusted with a damp chamois leather and placed inside the light scattering photometer on the special platform. Readings were then taken, on a

galvanometer, at 90^{o} adjusting the sensitivity controls and the filters on the photometer to obtain readings within the galvanometer scale. The sensitivity scales were then kept constant.

The surfactant solutions were prepared in the usual way and filtered directly into the measurement cell, after discarding the first 10 mls. The cell was then covered and put into the light scattering photometer and housed in a circular cell heating jacket as described by Trementozzi (116). After equilibration to a temperature of 30^{o}, as determined by a thermocouple lowered into the upper part of the solution, readings were taken on the galvanometer at 90^{o}, 135^{o} and 45^{o} to the incident beam and also of the vertical and horizontal components of the light scattered at 90^{o} by means of the removable polarizing lens. This procedure was followed with all the solutions including those at the CMC under the conditions of the investigation which were taken to be 9×10^{-4}M in water and 7×10^{-5}M under all other conditions.

The turbidity (τ) of the solutions was then calculated from the following relationship:

$$\tau = S_{90} \times C_F \times \text{Calibration Constant} \quad \ldots (2.45)$$

where C_F is Cabannes factor.

The data for the turbidity values are given in Tables (2.29 - 2.32).

Refractive Index Determinations. To evaluate the constant H in equation (2.23) page 121, a knowledge of the absolute refractive index (n_o) for the solvent and the value of the refractive index

CTAB Concentration $g.ml^{-1}$ $\times 10^3$	Δ c (c-CMC) $g.ml^{-1}$ $\times 10^3$	I_{90} solution	I_{90} block	S_{90}	$\frac{i_{135}}{i_{45}}$	ρ_u	C_F	τ_s $\times 10^4$	$\frac{H \Delta c}{\Delta \tau}$ $\times 10^5$
0.0255122(CMC)	-	6.80	76.735	0.0886	0.9050	0.12730	0.75534	0.19453	-
1.45784	1.4324	46.12	75.918	0.6075	0.9530	0.03125	0.93432	1.64984	2.0171
2.18676	2.1612	62.04	73.469	0.8445	1.0000	0.02690	0.94324	2.31538	2.0884
2.91568	2.8902	82.29	76.735	1.0724	0.9074	0.02297	0.95138	2.96559	2.1375
3.64460	3.6191	99.18	76.735	1.2926	0.9660	0.01997	0.95758	3.59782	2.1794
5.46690	5.4414	135.51	76.735	1.7660	0.9556	0.00934	0.97995	5.03031	2.3061
7.28920	7.2637	169.35	76.735	2.2070	0.9640	0.00958	0.97944	6.28319	2.4449
10.93380	10.9083	231.25	77.551	2.9819	0.9530	0.00960	0.97940	8.48894	2.6952

TABLE (2.29). Light Scattering Data for CTAB in Water Adjusted to an Ionic Strength of 0.5 with Potassium Chloride at 30^{o}.

CTAB Concentration $g.ml^{-1}$ $\times 10^3$	Δ c (c-CMC) $g.ml^{-1}$ $\times 10^3$	I_{90} solution	I_{90} block	S_{90}	$\frac{i_{135}}{i_{45}}$	ρ_u	C_F	τ_s $\times 10^4$	$\frac{H \Delta c}{\Delta \tau}$ $\times 10^5$
0.0255122(CMC)	-	13.20	73.469	0.1797	0.816	0.11900	0.78266	0.40881	-
1.45784	1.4324	79.591	73.469	1.0833	0.826	0.00700	0.79050	2.48922	1.4315
2.18676	2.1613	93.550	73.469	1.2733	0.850	0.08050	0.83960	3.10744	1.6652
2.91570	2.8911	95.161	73.469	1.2953	0.886	0.04200	0.91158	3.43214	1.9882
3.64460	3.6191	98.742	73.469	1.3440	0.906	0.02130	0.95511	3.73124	2.2648
5.46690	5.4414	138.856	73.469	1.8900	0.955	0.01925	0.95969	5.27221	2.3263
7.28920	7.2637	181.028	73.469	2.4640	0.965	0.01890	0.95969	6.87340	2.3362
9.11150	9.0860	220.995	73.469	3.0080	0.970	0.01900	0.95969	8.39091	2.3667
10.93380	10.9083	261.270	73.469	3.5562	0.952	0.01600	0.96618	9.98722	2.3678
14.57840	14.5530	332.455	73.469	4.5251	1.009	0.0170	0.96339	12.67157	2.4675
21.86760	21.8400	467.410	73.469	6.3620	0.967	0.0106	0.97752	18.07672	2.5701

TABLE (2.30). Light Scattering Data for CTAB in Carbonate-Bicarbonate Buffer at pH 9.2 and 30^o ($\mu = 0.5$)

CTAB Concentration $g.ml^{-1}$ $\times 10^3$	Δc (c-CMC) $g.ml^{-1}$ $\times 10^3$	I_{90} solution	I_{90} block	S_{90}	$\frac{i_{135}}{i_{45}}$	ρ_u	C_F	τ_s $\times 10^4$	$\frac{H \Delta c}{\Delta \tau}$ $\times 10^5$
0.02551(CMC)	-	7.85	73.469	0.1069	0.750	0.13600	0.74074	0.23017	-
1.45784	1.4324	72.60	73.469	0.9778	0.770	0.03488	0.92696	2.63458	1.2609
2.18676	2.1613	82.70	73.469	1.1251	0.795	0.02275	0.95148	3.11165	1.5881
2.91568	2.8902	93.90	73.469	1.2778	0.821	0.01680	0.96432	3.58166	1.8257
3.64460	3.6191	101.00	73.469	1.3747	0.875	0.01300	0.97182	3.85327	2.0973
5.46690	5.4414	134.70	73.469	1.8333	0.930	0.00600	0.96993	5.16861	2.3326
6.56030	6.5348	156.45	73.469	2.1295	0.967	0.00501	0.98922	6.12309	2.3475
7.28920	7.2637	174.20	73.469	2.3709	0.952	0.00547	0.98824	6.81045	2.3367
9.11150	9.0860	210.00	74.286	2.8268	0.956	0.00450	0.99030	8.13696	2.4325
10.93400	10.9080	244.01	72.653	3.3586	0.959	0.00400	0.99138	9.67829	2.4439
14.57800	14.553	314.33	74.286	4.2314	0.945	0.00400	0.99138	12.19339	2.5750

TABLE (2.31). Light Scattering Data for CTAB in Carbonate-Bicarbonate Buffer at pH 9.2 and $\mu = 0.5$ at 30° in the Presence of 8×10^{-4}M Phenyl Acetate.

CTAB Concentration $g.ml^{-1} \times 10^3$	Δc (c-CMC) $g.ml^{-1} \times 10^3$	I_{90} solution	I_{90} block	S_{90}	$\frac{i_{135}}{i_{45}}$	ρ_u	C_F	$\tau_s \times 10^4$	$\frac{H \Delta c}{\Delta \tau} \times 10^5$
0.32810(CMC)	-	10.70	73.469	0.14564	0.912	0.1920	0.65104	2.75606	-
1.45784	1.1298	17.40	73.469	0.23683	0.914	0.1048	0.79428	5.46777	8.3583
2.18676	1.8590	17.60	73.469	0.23956	1.097	0.0877	0.82508	5.74527	12.4760
2.91568	2.5880	17.95	73.469	0.24444	0.977	0.0786	0.84175	5.98075	16.1010
3.64460	3.3170	18.20	73.469	0.24772	0.763	0.0730	0.85251	6.13848	19.6740
5.46690	5.1390	20.70	73.469	0.28174	0.694	0.0632	0.87108	7.13357	23.5520
7.28920	6.9610	24.10	73.469	0.32803	0.705	0.0570	0.88316	8.42080	24.6520
9.11150	8.7830	27.70	73.469	0.37703	0.692	0.0530	0.89095	9.76404	25.1430
10.93380	10.6060	30.24	73.469	0.41162	0.600	0.0501	0.89686	10.73053	26.6820

TABLE (2.32). Light Scattering Data for CTAB in Water at 30^{o}.

increments $\left(\frac{dn}{dc}\right)$ is necessary at the wavelength of light used for scattering, namely 546 nm.

(i) Absolute Refractive Index. The absolute refractive index (n_o) for the two values of the CMC were determined using an Abbé refractometer, fitted with a water heated prism block, and the mercury lamp from the light scattering photometer as the light source. The refractive index values were found to be 1.332 for CTAB in water at 30^o (CMC = 9×10^{-4}M) and 1.3365 under other conditions, in the presence of potassium chloride for the ionic strength adjustment (CMC = 7×10^{-5}M).

(ii) Differential Refractive Index Measurements. These were made by means of a Rayleigh-Haber-Löwe interferometer for liquids whose principle has been described in detail by Bauer et al (146). The technique is based on producing a set of interference bands by dividing two beams of light, from the same source, into two separate parts, upper and lower. The lower halves pass through air and the optical parts of the instrument while one upper beam passes through the solution to be examined and the other through a reference liquid, usually the solvent. The solution and the refrence liquid are contained in a two-compartment cell, thermostated to the correct temperature. When there is a difference in the refractive indices of the solution and the reference liquid, there is a displacement of the interference bands, the extent of which provides a method for obtaining the difference between the two refractive indices. White light is used initially to ascertain the position of the two black "zero order" bands whose alignment is

used for the measurement because when mono-chromatic light is used for the determinations at a specific wavelength these bands become difficult to distinguish.

Using white light, therefore, the zero order bands were aligned with the reference solution in both cells; final adjustment of the zero order bands was then made against green light and the micrometer reading was noted (zero reading). The sample solution was then introduced and the bands realigned by means of the micrometer using white light initially. Green light was then substituted to make the final adjustment by returning the micrometer to its original position. The displacement of the interference bands was then determined from the micrometer readings which had been previously calibrated by counting the number of bands which passed whilst returning the micrometer to the zero position. The refractive index increment $\left(\frac{dn}{dc}\right)$ was obtained from the following relationship (2.46):

$$\left(\frac{dn}{dc}\right) = \frac{\lambda}{L} \times \text{Slope} \quad \ldots\ldots\ldots\ldots\ldots \quad (2.46)$$

where the slope was obtained from plotting the number of bands shifted, N, against the concentration of micelles (c-CMC) in g ml^{-1} and L was the path length of the cell (1 cm).

Three determinations were carried out on each solution and the average of the three readings was taken as N for that solution. Determinations were carried out on the following systems:

CTAB in water

CTAB in water adjusted to an ionic strength of 0.5M with potassium chloride.

CTAB in carbonate-bicarbonate buffer at pH 9.2 adjusted to ionic strength, 0.5M.

CTAB in carbonate-bicarbonate buffer at pH 9.2 adjusted to ionic strength 0.5M, in the presence of 8×10^{-4}M phenyl acetate.

CTAB MOLAR CONCEN-TRATION x 10^3	BAND SHIFT (N)							
	CTAB IN H_2O		CTAB IN H_2O + KCl.		CTAB IN BUFFER		CTAB IN BUFFER + ESTER	
	c x 10^3 $g.ml^{-1}$	N	c x 10^3 $g.ml^{-1}$	N	c x 10^3 $g.ml^{-1}$	N	c x 10^3 $g.ml^{-1}$	N
4.0	1.13	7.5	1.43	6.6	1.43	7.2	1.43	7.4
6.0	1.86	9.3	2.16	8.6	2.16	9.0	2.16	9.3
8.0	2.59	11.2	2.89	10.2	2.89	11.0	2.89	11.2
10.0	3.32	13.0	3.62	12.2	3.62	12.7	3.62	13.0
15.0	5.14	17.5	5.44	16.6	5.44	17.0	5.44	17.7
20.0	6.96	22.0	7.26	21.0	7.26	21.8	7.26	22.3
30.0	10.61	30.9	10.91	30.4	10.91	31.0	10.91	31.6

TABLE (2.27). Band Shift in Refractometry Determination for the Various Systems Studied.

The data as presented in Table (2.27) and Figure (2.21) shows a representative plot of these determinations. Refractive index increments obtained this way were then used to evaluate H in equation (2.23) for each system. The refractive index increments and the calculated values of H are given in Table (2.28).

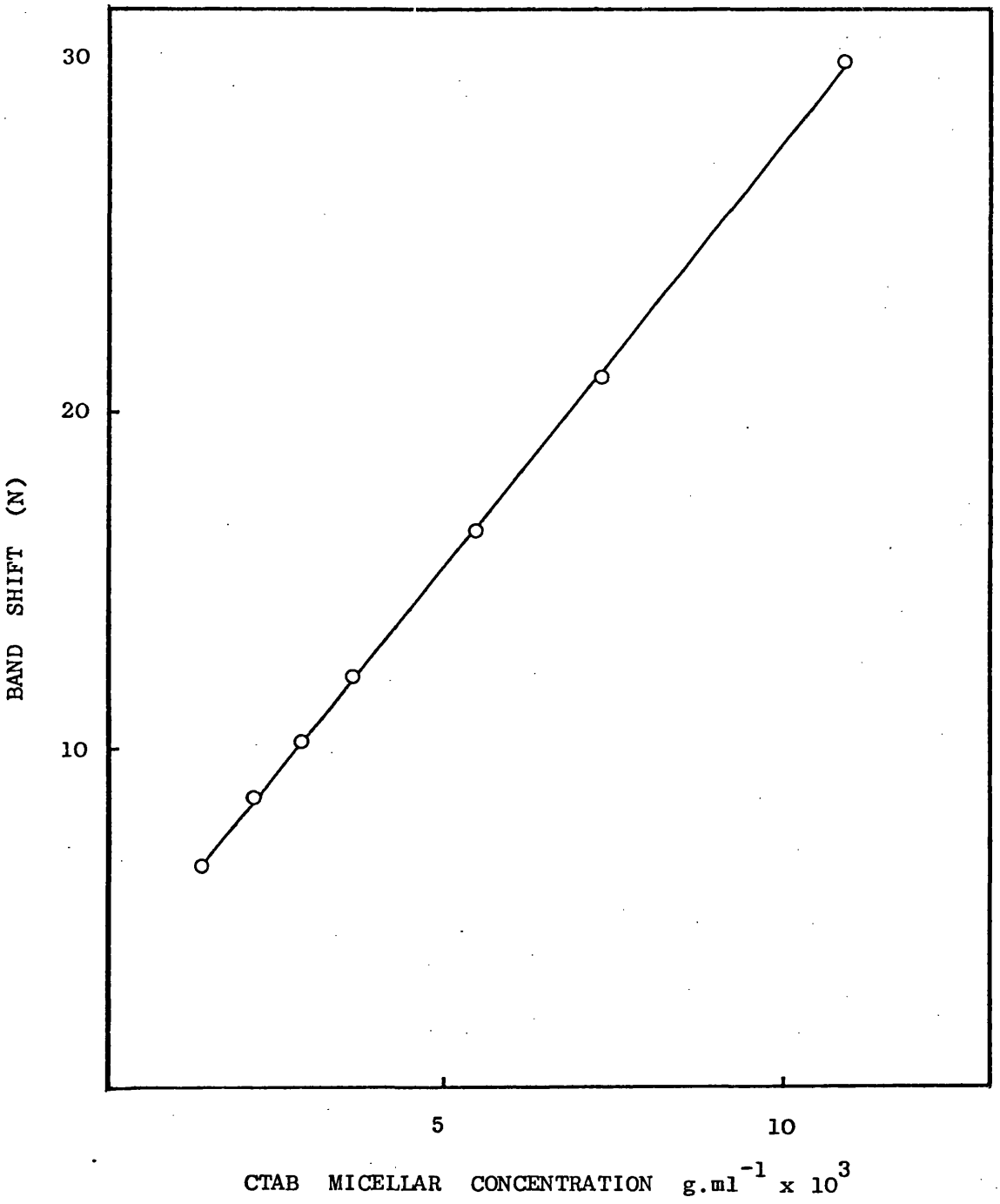

FIG. (2.21). BAND SHIFT (N) AGAINST CONCENTRATION (c-CMC) IN g.ml^{-1} FOR THE DETERMINATION OF REFRACTIVE INDEX INCREMENT OF CTAB IN WATER ADJUSTED TO AN IONIC STRENGTH OF 0.5M WITH POTASSIUM CHLORIDE.

SYSTEM	Refractive Index Increment(dn/dc) c = $g.ml^{-1}$	Refractive Index Increment(dn/dc) c = moles ml^{-1}	H x 10^6
Potassium Chloride in Water	0.12606	9.3978×10^{-3}	-
CTAB in Water	0.13525	4.9293×10^{-2}	2.00617
CTAB in Water + KCl (μ = 0.5)	0.13624	4.9654×10^{-2}	2.04940
CTAB in Buffer + KCl (μ = 0.5)	0.13722	5.0011×10^{-2}	2.07917
CTAB in Buffer + KCl + Phenyl Acetate (μ = 0.5)	0.13845	5.0450×10^{-2}	2.11658

TABLE (2.28). Refractive Index Increments and "H" Values of the Various Systems Studied at 30^{o} and 546 nm.

After obtaining H values, the various parameters of equation (2.29) page 123 were obtained for each system. These are given in Tables (2.29 - 2.32). From these data plots of $\frac{H \Delta c}{\Delta \tau}$ against Δc were constructed. (Figures (2.22 - 2.25)). The linear parts of each plot were then submitted to a least squares regression analysis programme and the slope and intercept of each were obtained. These values were then used according to equations (2.29, 2.38 and 2.39)

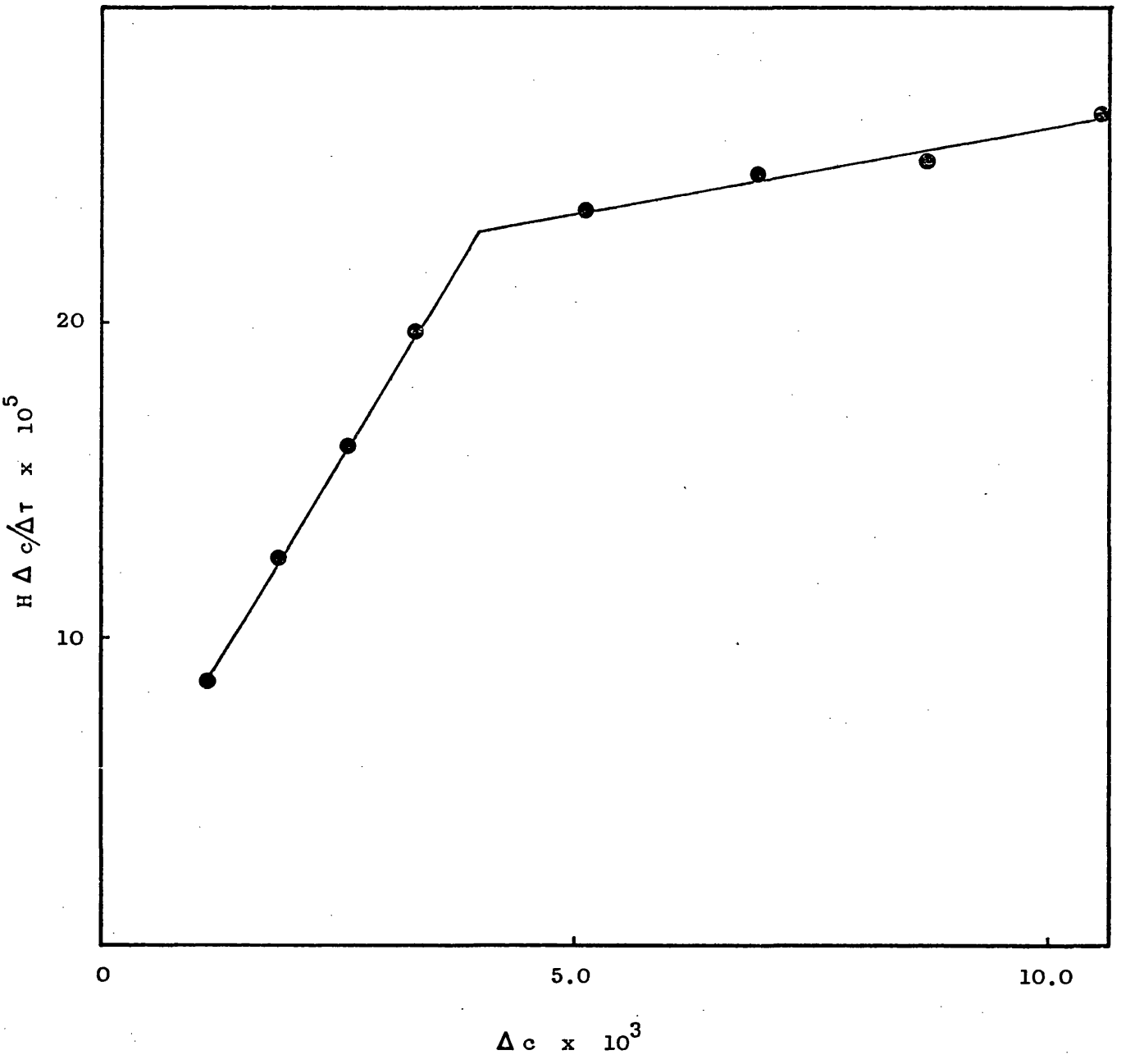

FIG. (2.22). H $\Delta c/\Delta\tau$ AGAINST Δc FOR CTAB IN WATER AT 30°

λ = 546 nm.

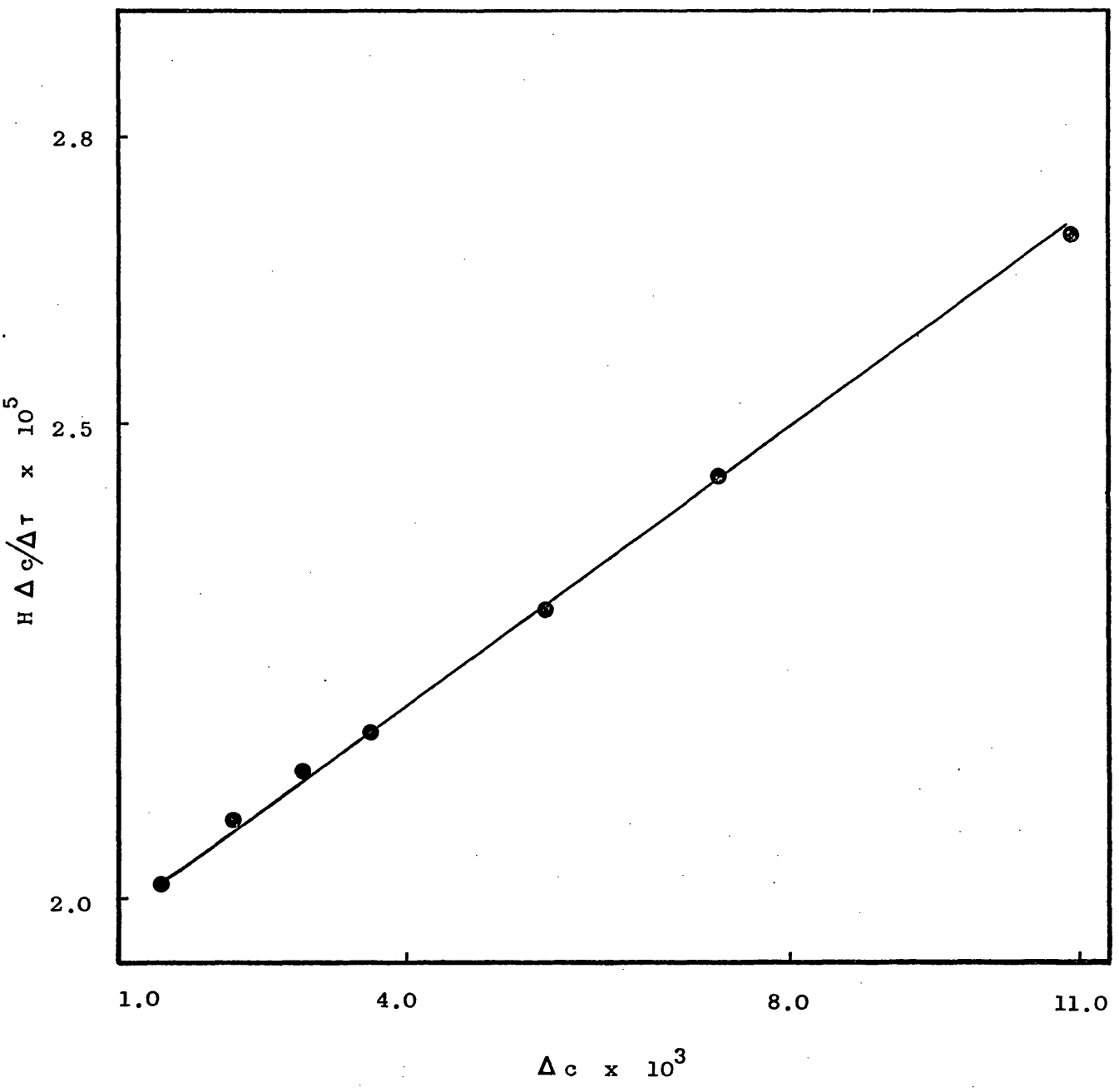

FIG. (2.23). H Δ c/Δ T AGAINST Δ c FOR CTAB IN WATER ADJUSTED TO IONIC STRENGTH 0.5M WITH POTASSIUM CHLORIDE AT 30°.

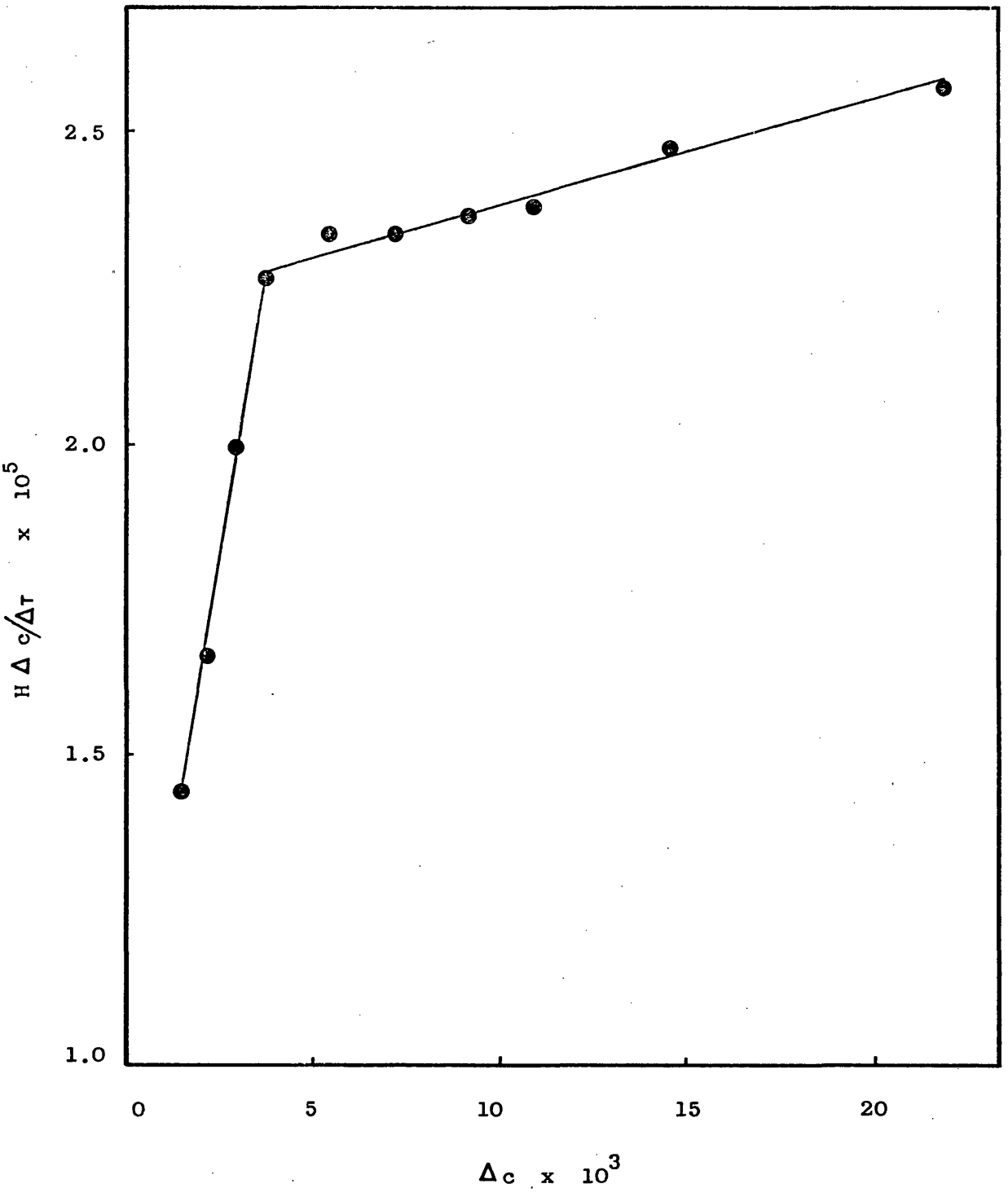

FIG. (2.24). H $\Delta c/\Delta T$ AGAINST Δ c FOR CTAB IN CARBONATE-BICARBONATE BUFFER AT pH 9.2 AND 30°.

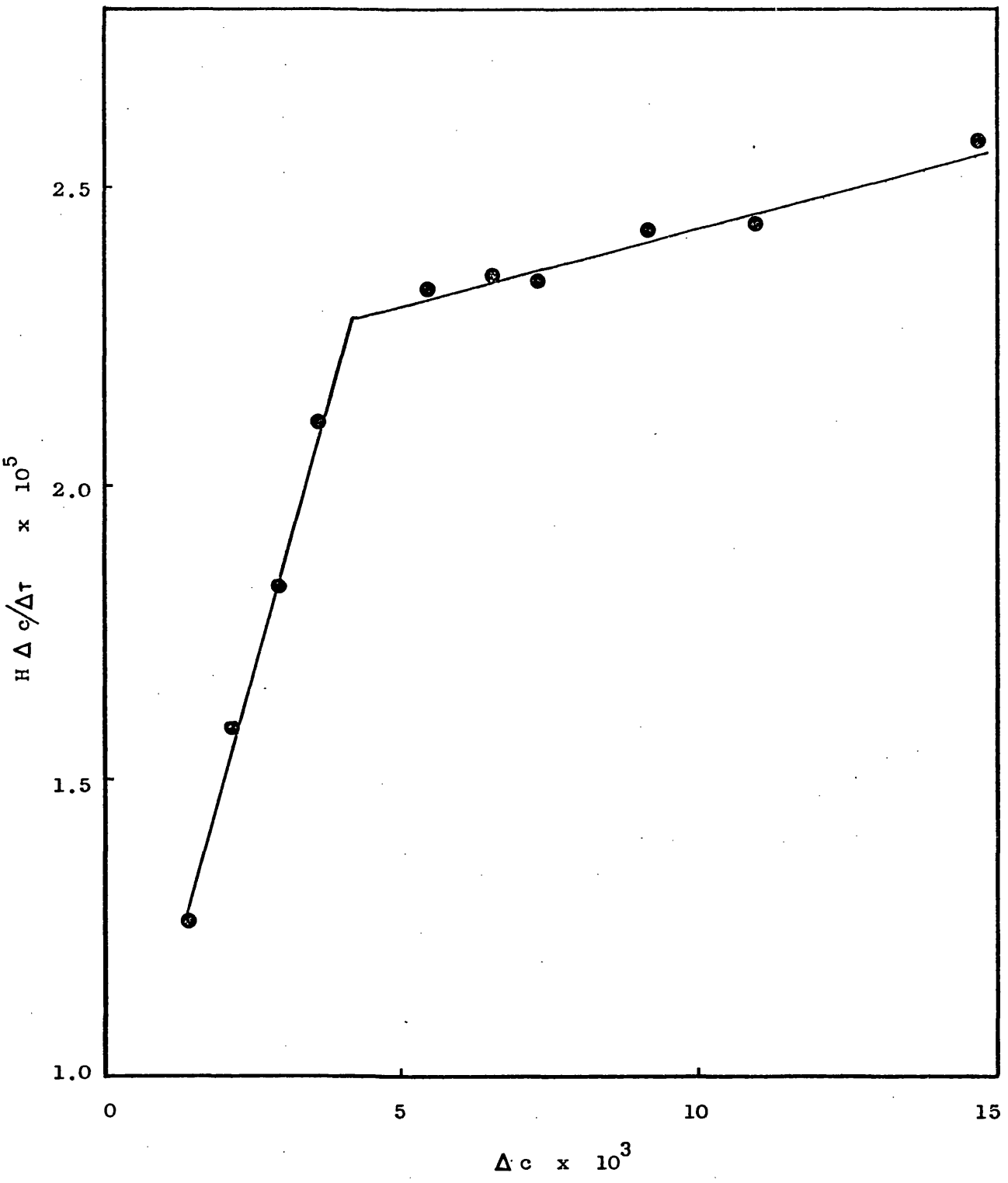

FIG. (2.25). H $\Delta c/\Delta_T$ AGAINST Δc FOR CTAB IN CARBONATE-BICARBONATE BUFFER AT pH 9.2 AND 30° IN THE PRESENCE OF 8 x 10^{-4}M PHENYL ACETATE.

SYSTEM	Low concentration of CTAB			High concentration of CTAB		
	M_w	p	n	M_w	p	n
CTAB in Water	3.71×10^4	12.00	113.60	4.82×10^3	0.36	13.59
CTAB in Water + KCl (μ=0.5M)	5.19×10^4	44.90	150.80	5.19×10^4	44.90	150.80
CTAB in Buffer + KCl (μ=0.5)	11.64×10^4	244.60	363.90	4.49×10^4	18.07	126.70
CTAB in Buffer + Phenyl Acetate(μ=0.5)	13.49×10^4	279.26	420.62	4.62×10^4	24.61	131.23

TABLE (2.33). Micellar Molecular Weight, Charge and Aggregation Number of the Various Systems Studied at 30^o as Determined by Light Scattering.

The low and high concentrations in Table (2.32) refer to the regions before and after the break in the $\frac{H \Delta c}{\Delta \tau}$ versus Δc profiles, respectively. It can be seen that the system in water adjusted to an ionic strength of 0.5 with potassium chloride (Figure (2.23)) did not exhibit such a break and the values in Table (2.32) for this system are the same under the low and the high CTAB concentration headings. The breaks in these systems around the concentration range of 0.01M CTAB can also be seen in plots of S_{90} against molar concentration as shown in Figure (2.26) for all the systems and Figure (2.27) on an enlarged scale for the system in water only.

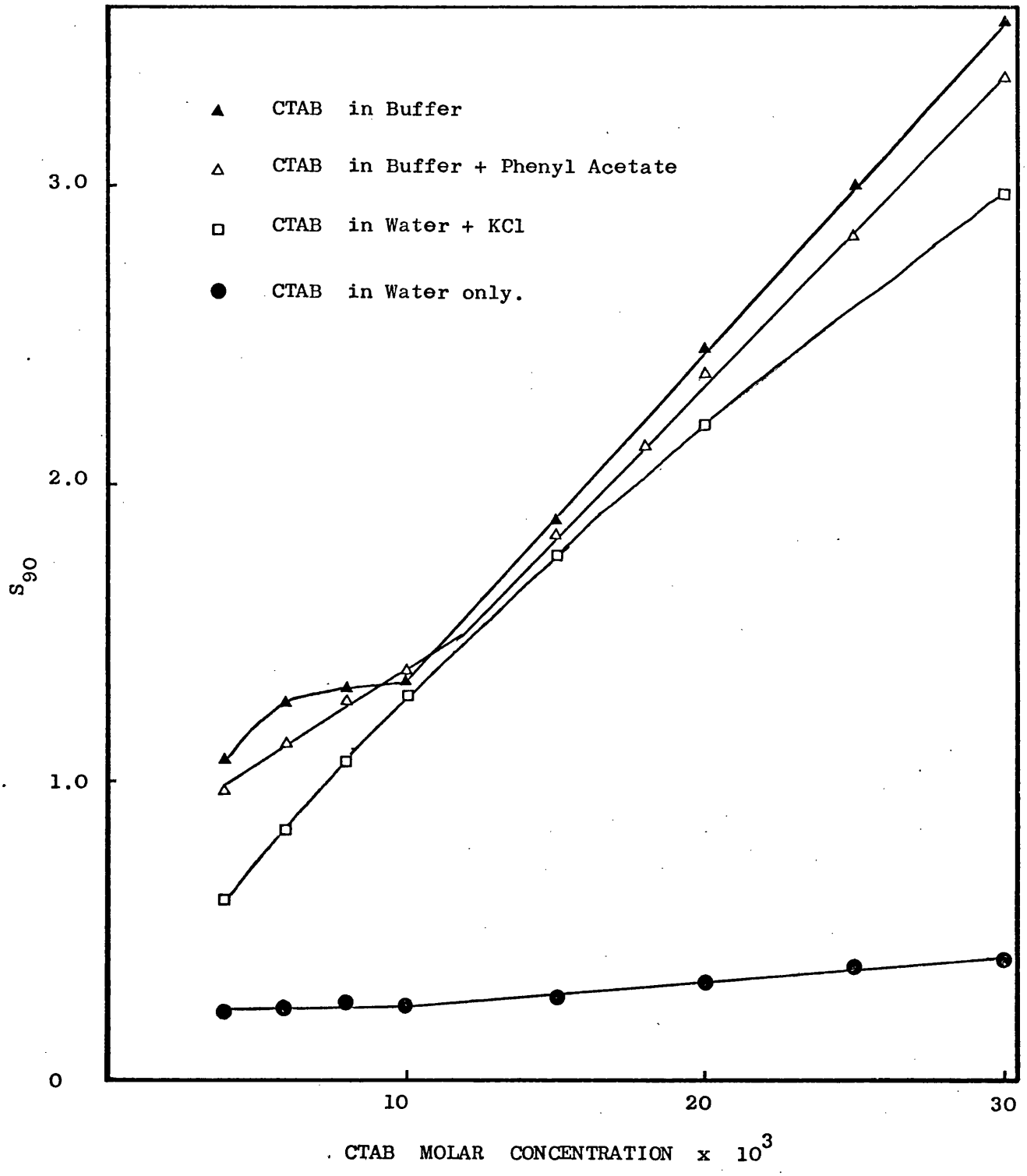

FIG. (2.26). S_{90} AGAINST MOLAR CONCENTRATION OF CTAB FOR ALL SYSTEMS INVESTIGATED AT 30^{o}.

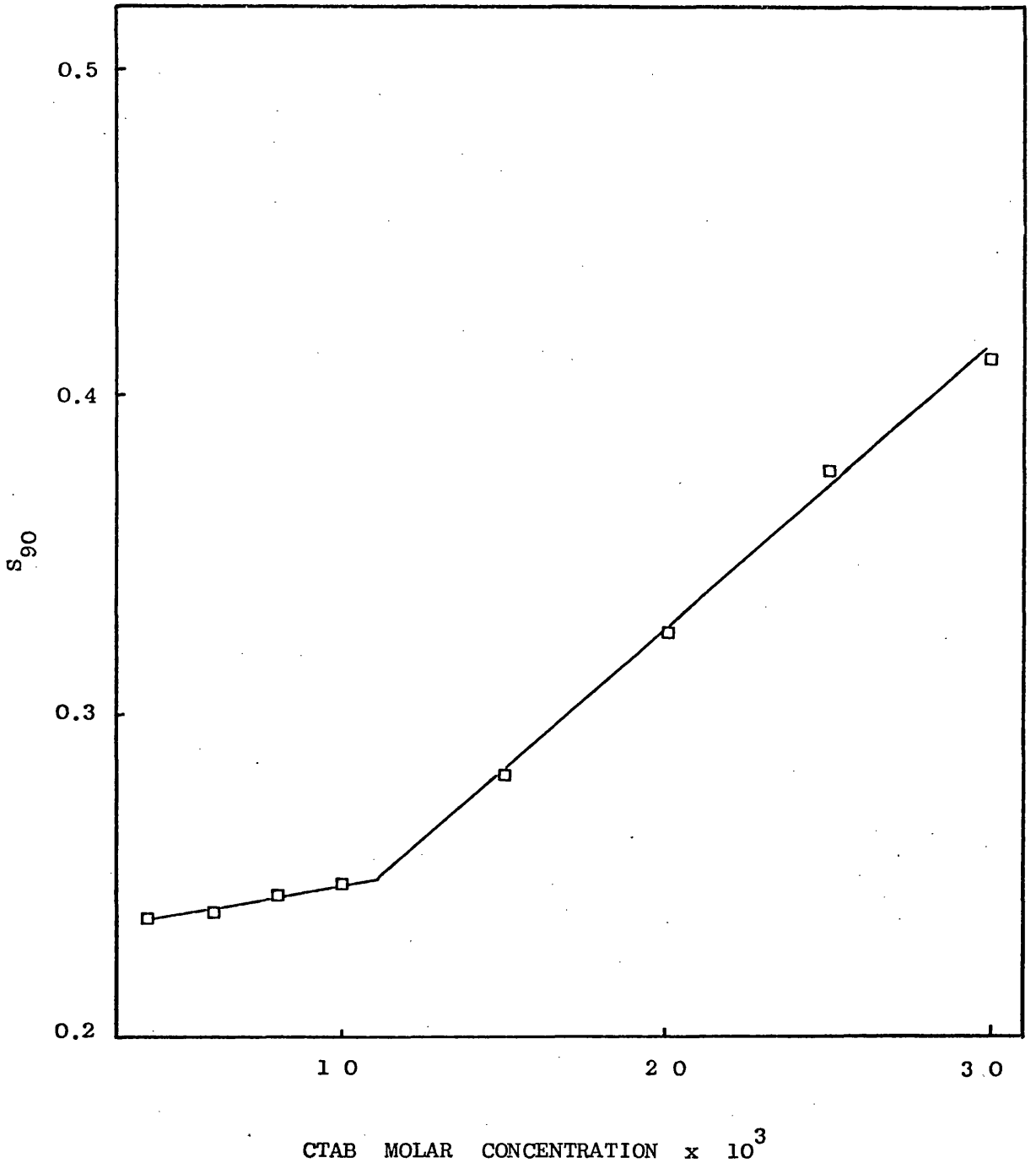

FIG. (2.27). S_{90} AGAINST MOLAR CONCENTRATION OF CTAB IN WATER AT 30°.

D I S C U S S I O N

DISCUSSION

This study has been concerned with the hydrolysis of phenyl acetate and with the influence of the cationic surfactant cetyltrimethylammonium bromide (CTAB) on this process. The study was conducted at a temperature of 30^{o} in order to avoid the Krafft point (around 23^{o}) which would result in the crystallization of the surfactant, and because it was easier to maintain this temperature in the face of external fluctuations. The plots of the percentage residual concentration of the ester, on a log scale, versus time, in the absence and presence of the surfactant, gave straight lines with, in all cases, high correlation coefficients (> 0.999) and values for the ratio of the slope to its standard deviation of > 50, indicating that the hydrolysis followed first order rate kinetics. The slopes obtained from these first order kinetic plots give a quantitative measure of the susceptibility of the hydrolytic process to effects from the surfactant.

Ester hydrolysis is a bimolecular reaction and as such it should be overall second order. As the ester is completely unionized over the pH range studied, if the hydrolysis conditions are chosen such that the concentration of the attacking species does not change effectively during the course of the reaction, then

$$\frac{dc}{dt} = -k_{obs} = -k_o\left[H_2O\right] - k_1\left[H_3O^+\right] - k_2\left[OH^-\right] \qquad \ldots\ldots\ldots\ldots\ldots\ldots (3.1)$$

As shown on page 5, in general, it has been found that k_o is very small, water not being a strong nucleophile, and does not significantly contribute to k_{obs}. In buffer systems at high pH, therefore, equation (3.1) approximates to equation (3.2) which reduces to equation (3.3)

$$k_{obs} = k_2 \left[OH^-\right] \quad \ldots\ldots\ldots\ldots\ldots\ldots \quad (3.2)$$

$$\log k_{obs} = \log k_2 - pK_w + pH \quad \ldots\ldots\ldots\ldots \quad (3.3)$$

and a plot of log k_{obs} against pH should be linear with a positive slope of unity when the hydroxyl ion catalysis is predominant and buffer and salt effects are absent.

General acid-base effects were investigated at pH 9.2, 9.8 and 10.2 using the Delory and King carbonate-bicarbonate buffer (117) at single and double strength in the absence and in the presence of the highest concentration of CTAB used (8×10^{-2}M) at a constant ionic strength of 0.5M adjusted with the addition of the neutral salt potassium chloride. The observed first order rate constants obtained are given in Table (3.1), together with their standard deviations and the calculated and tabulated t-test values at a probability level of 0.05. It is evident from the data that buffer effects are absent in the presence of carbonate-bicarbonate buffer at these pHs. This buffer system could not be used at pH 8. Both borate and phosphate buffers, at this pH, were shown, in preliminary experiments, to catalyse the hydrolysis. For this reason control at pH 8 was maintained during the experimental period by means of a pH-stat, although the carbonate-bicarbonate buffer salts were also present in order to retain

pH	WITHOUT CTAB						With 8×10^{-2}M CTAB					
	SINGLE STRENGTH		DOUBLE STRENGTH		t-test		SINGLE STRENGTH		DOUBLE STRENGTH		t-test	
	Rate Constant min^{-1}	Standard Deviation	Rate Constant min^{-1}	Standard Deviation	Calculated	Tabulated	Rate Constant min^{-1}	Standard Deviation	Rate Constant min^{-1}	Standard Deviation	Calculated	Tabulated
9.2	3.7294×10^{-3}	1.5594×10^{-5}	3.7132×10^{-3}	1.2371×10^{-5}	0.815	2.3	1.2605×10^{-3}	1.7651×10^{-6}	1.2539×10^{-3}	2.580×10^{-6}	2.10	2.3
9.8	1.4318×10^{-2}	7.1012×10^{-5}	1.4204×10^{-2}	7.0952×10^{-5}	1.13	2.3	5.4261×10^{-3}	3.8702×10^{-5}	5.3502×10^{-2}	1.0768×10^{-5}	1.90	2.15
10.2	3.4603×10^{-2}	7.5884×10^{-5}	3.4679×10^{-2}	9.0162×10^{-5}	0.62	2.15	1.0876×10^{-2}	4.4365×10^{-5}	1.0843×10^{-2}	1.9859×10^{-5}	0.675	2.15

Table (3.1). Rate Constants and Standard Deviations for the Hydrolysis of 8×10^{-4}M Phenyl Acetate in the Absence and Presence of 8×10^{-2}M CTAB in Single and Double Strength Carbonate-Bicarbonate Buffer.

the same ionic environment. In this way it was ensured that the results at all pH values could be directly compared.

When the hydrolysis of phenyl acetate was investigated at pH 8, 9.2, 9.8 and 10.2, in the absence of the surfactant, and a plot of the observed rate constant at each pH was plotted, on a log scale, against pH, on a linear scale, a straight line was obtained, as shown in Figure (3.1), with a positive slope of 0.97. This shows, therefore, that the reaction is specifically hydroxyl ion catalysed and that it belongs to group II of Figure (1.2) page 6. The specific OH^- catalysed rate constant, k_2, has a value of 4.5×10^2 minutes^{-1}.

The surfactant chosen for this study is the cationic quaternary ammonium compound cetyltrimethyl ammonium bromide (CTAB). The sample was purified by extraction and repeated crystallization and assessed by melting point (232^o lit. $226\text{-}235^o$(86)), surface tension, molecular weight and mass spectrometry. The surface tension versus log concentration plot showed no minimum indicating freedom from alkyl bromides. The purity was found to be more than 99% by mass spectrometry. All the concentrations utilized for the kinetic studies were above the CMC, determined under the conditions of the study. The CMC values of the different systems were obtained from surface tension and conductivity measurements and were taken from the point of the intercept of the two linear parts when the physical property measurements were plotted against the appropriate function of the concentration of the surfactant. This practice is generally accepted and has been adopted by many workers (12). The values of the CMC have been taken as 9×10^{-4}M for the system in water only and as 7×10^{-5}M

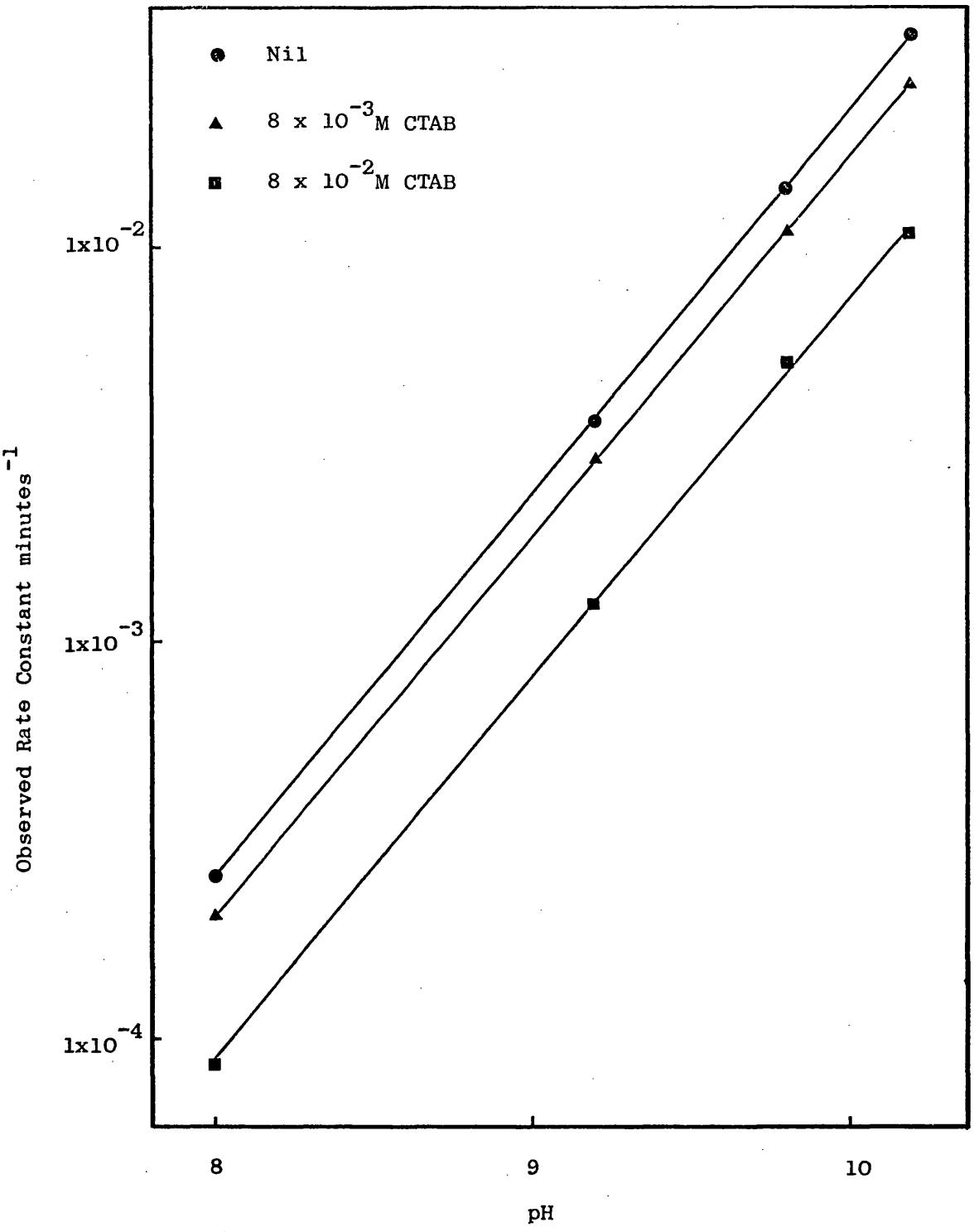

FIG. (3.1). OBSERVED RATE CONSTANT AGAINST pH IN THE ABSENCE AND PRESENCE OF CTAB AT 30°.

for the system in buffer and salt solutions at an ionic strength of 0.5M. The value for the system in water agrees closely with published values of 8.4×10^{-4} - 9.1×10^{-4} at 30^{o} (12,142). No values are available for comparison in the buffer systems.

Investigations below the CMC were not attempted because although surfactant monomer effects have been reported for homologues of CTAB (90) they have not been substantiated subsequently nor was the CMC quoted in that report determined under the conditions of the reaction system.

In all cases investigated it was found that the addition of CTAB caused a decrease in the rate of hydrolysis. The extent of this protection at the different pH's can be compared when the results are calculated as the surfactant effect ratio (ratio of the observed first order rate constant in the presence and absence of CTAB, respectively). Figure (3.2) shows a plot of these values against molar concentration of CTAB for pH's 8, 9.2, 9.8 and 10.2. It can be seen that the effect of CTAB is the same at all pH's. Further evidence of this is provided in Figure (3.1), where the slopes of log k_{obs} versus pH profiles are 0.96 and 0.97 in the presence of the two concentrations of CTAB compared to 0.97 in the absence of CTAB. Thus degradation, in all cases, is due to specific OH^{-} ion catalysed reactions. At each pH studied, therefore, the surfactant reduces k_{obs} by a constant proportion. This could be explained if ester molecules partition into micelles, so that the greater the number of micelles the greater the proportion of the ester in the micelles and thus the greater the degree of protection.

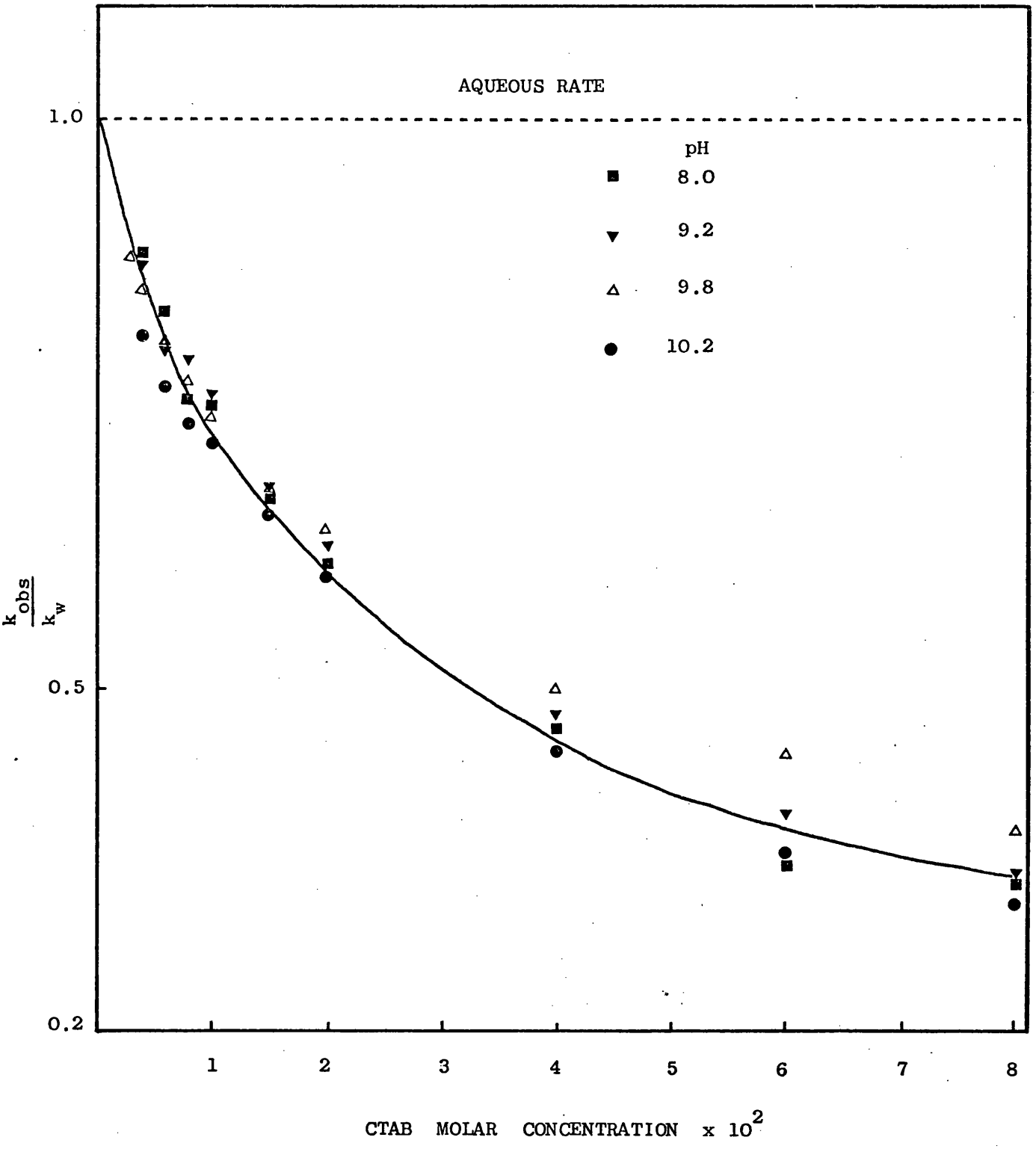

FIG. (3.2). SURFACTANT EFFECT RATIO $\frac{k_{obs}}{k_w}$ AGAINST CTAB MOLAR CONCENTRATION FOR THE HYDROLYSIS OF PHENYL ACETATE AT pHs 8, 9.2, 9.8 AND 10.2 AT 30^{o} IN CARBONATE-BICARBONATE BUFFER (μ = 0.5)

From simple electrostatic considerations advocated by Hartley (85) it would be predicted that the base catalysed hydrolysis of phenyl acetate, being an uncharged ester, would be enhanced in the presence of the cationic micelles of CTAB, provided that the ester was associated at or close to the micellar surface. Protective properties of CTAB have been reported before by Winterborn et al (95) who have shown that CTAB, above its CMC, increased the rate of base catalysed hydrolysis of ethyl p-nitro-benzoate and p-nitro-phenyl acetate and decreased the rate of p-amino-phenyl acetate and ethyl-amino benzoate. In a further report (96), these authors showed that the tendency of CTAB to promote or retard hydrolysis could be predicted from the Hammett substituent constant for a series of four substituted ethyl benzoates. They concluded that the results were a combined function of a reduced dielectric constant at the micellar surface, which retarded hydrolysis, and an increase in OH^- ion concentration at the micellar surface, which increased the hydrolysis. The observed effect depends on the relative magnitude of these two factors. In the case of phenyl acetate it has to be assumed that the dielectric constant effect predominates.

In order to explain the effect of CTAB micelles on the hydrolysis, a simple TWO-COMPARTMENT model was adopted. This visualizes the system, as illustrated in Figure (3.3) as being divided into the bulk aqueous compartment and the micellar compartment, consisting of the micelles themselves and their associated double layers. If the rates in these two compartments are different they will contribute to the overall rate according to the given relationship

$$k_{obs} = k_w C_w + k_m C_m \quad \ldots\ldots\ldots\ldots\ldots\ldots \quad (3.4)$$

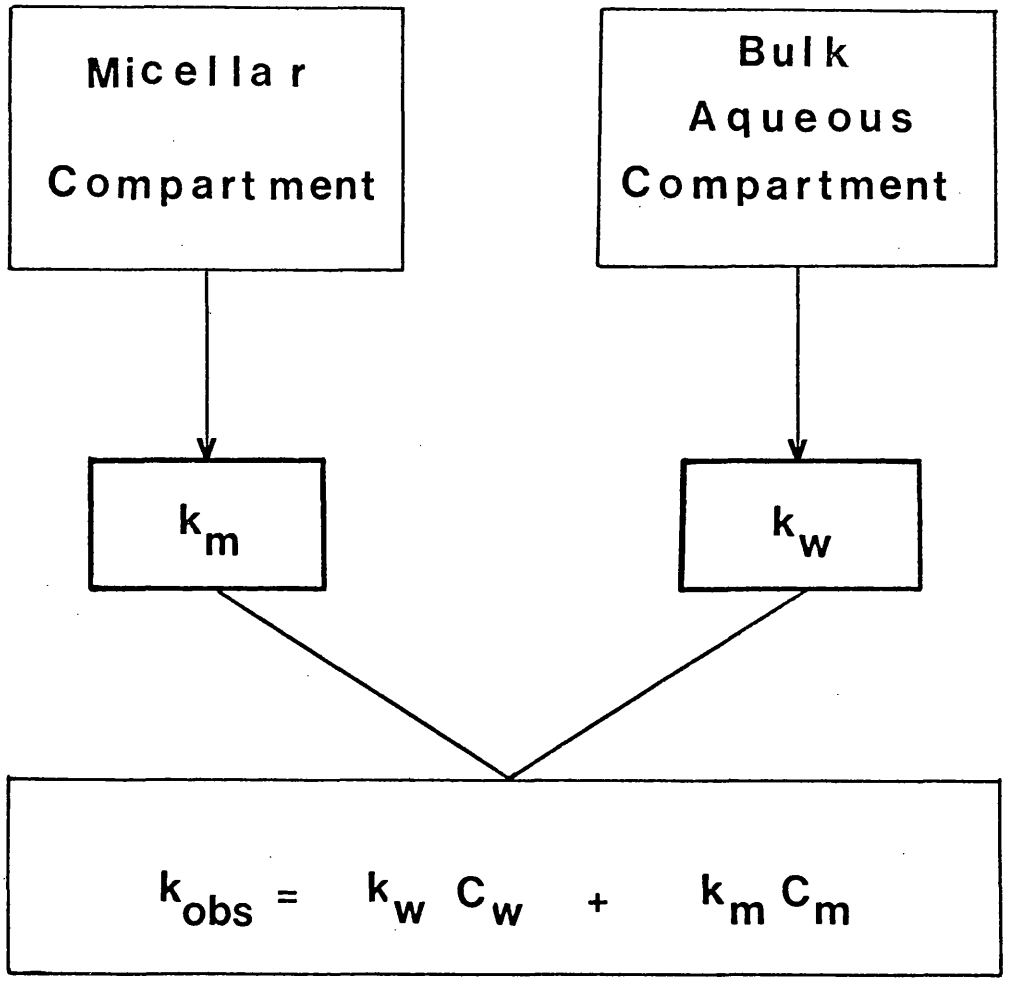

FIG. (3.3). THE TWO COMPARTMENTS OF A MICELLAR SYSTEM AND THEIR CONTRIBUTIONS TO THE OVERALL OBSERVED RATE OF REACTION.

where k_w is the aqueous rate and k_m is the micellar rate and C_w and C_m represent the fractions of the drug in the aqueous and the micellar phases respectively. The assumption is made that the fraction of the ester associated with the micelles in any given system, remains constant throughout the degradation process and is, therefore, unaffected by the presence of degradation products. This is a reasonable assumption to make since the first order kinetic plots are linear over the entire period observed which in some cases was down to 20% residual concentration indicating that the observed rate is unaffected by degradation products. This association between the ester and the micelles can be quantified through the partition coefficient of the ester between the micellar and the bulk phases.

Since $C_w + C_m = 1$ ..... (3.5)

$\therefore \quad C_m = (1 - C_w)$ ..... (3.6)

and equation (3.4) becomes

$$k_{obs} = k_w C_w + k_m (1 - C_w) \quad \text{..... (3.7)}$$

From equation (2.5) we can obtain equation (3.8)

$$K_p = \frac{[C_m]}{[C_w]} = \frac{n_m}{n_w} \left(\frac{1 - V}{V}\right) \quad \text{..... (2.5)}$$

$$\therefore \quad \frac{n_m}{n_w} = K_p V/(1 - V) \quad \text{..... (3.8)}$$

and $$C_w = \frac{1}{\left(1 + \frac{n_m}{n_w}\right)} \quad \text{..... (3.9)}$$

and $\therefore$ $$C_w = \frac{1}{\left(1 + \frac{K_p V}{(1 - V)}\right)} = \frac{1 - V}{(1 - V) + K_p V} \quad \text{..(3.10)}$$

Substituting for C_w (from equation 3.10) in equation (3.7) we obtain equation (3.11)

$$k_{obs} = \frac{k_w}{1 + \frac{K_p V}{(1 - V)}} + k_m \left[1 - \frac{1}{1 + \frac{K_p V}{(1 - V)}} \right] \quad .. (3.11)$$

$$= \frac{k_w}{1 + \frac{K_p V}{(1 - V)}} + k_m - \frac{k_m}{1 + \frac{K_p V}{(1 - V)}}$$

$$= \frac{k_w + k_m \left(1 + \frac{K_p V}{(1 - V)}\right) - k_m}{1 + \frac{K_p V}{(1 - V)}}$$

$$\therefore \; k_{obs} \left(1 + \frac{K_p V}{(1 - V)}\right) = k_w + k_m \left(1 + \frac{K_p V}{(1 - V)}\right) - k_m$$

$$k_{obs} + \frac{k_{obs} K_p V}{(1 - V)} = k_w + k_m + \left(\frac{k_m K_p V}{(1 - V)}\right) - k_m$$

$$k_{obs} + \frac{k_{obs} K_p V}{(1 - V)} = k_w + \frac{k_m K_p V}{(1 - V)}$$

and $\therefore$ $$\frac{k_{obs} K_p V}{(1 - V)} = k_w - k_{obs} + \frac{k_m K_p V}{(1 - V)}$$

and $$k_{obs} = \frac{(1 - V)}{K_p} \left[\frac{(k_w - k_{obs})}{V} \right] + k_m \quad ..... (3.12)$$

As V, the volume fraction of the micellar phase is very small at the level of CTAB concentrations used during this study $(1 - V) \simeq 1$, and if $\bar{v}$ is the partial specific volume then

$V = \bar{v} \cdot C_m$ where C_m is the micellar concentration in $g.ml^{-1}$

and if C is the molar concentration and M is the molecular weight of the surfactant, then

$$C_m = \frac{(C-CMC)M}{1000}$$

$$\text{and } \therefore \quad V = \bar{v}\,\frac{MC}{1000} \qquad \ldots\ldots\ldots\ldots\ldots\ldots (3.13)$$

substituting for V in equation (3.12)

$$k_{obs} = \frac{1}{K_p}\left[\frac{k_w - k_{obs}}{\frac{\bar{v}\,MC}{1000}}\right] + k_m \qquad \ldots\ldots\ldots (3.14)$$

$$= \frac{1000}{K_p \bar{v}\, M}\left[\frac{k_w - k_{obs}}{C}\right] + k_m \qquad \ldots\ldots\ldots (3.15)$$

According to equation (3.15) a plot of k_{obs} against $(k_w - k_{obs})/C$ will be linear with

$$\text{Slope} = \frac{1000}{K_p \bar{v}\, M} \qquad \ldots\ldots\ldots\ldots\ldots (3.16)$$

$$\text{and} \quad \text{Intercept} = k_m$$

and from the slope, therefore, the partition coefficient, K_p, can be evaluated

$$K_p = \frac{1000}{(\text{Slope})\, M\, \bar{v}} \qquad \ldots\ldots\ldots\ldots\ldots\ldots (3.17)$$

From the kinetic data of pH 9.2, 9.8 and 10.2 given in Tables (2.11), (2.12) and (2.13) respectively the necessary parameters for plotting the data in accordance with equation (3.15) were calculated and these are given in Table (3.2).

CTAB Molar Concentration (C) x 10^3	pH 9.2		pH 9.8		pH 10.2	
	k_{obs} x 10^3	$\frac{(k_w - k_{obs})}{C}$	k_{obs} x 10^2	$\frac{(k_w - k_{obs})}{C}$	k_{obs} x 10^2	$\frac{(k_w - k_{obs})}{C}$
NIL	3.7132	-	1.4204	-	3.4677	-
3.0	-	-	1.2498	0.5687	-	-
4.0	3.2446	0.11715	1.2114	0.5226	2.8170	1.6268
6.0	3.0854	0.10463	1.1443	0.4602	2.6598	1.3465
8.0	2.9411	0.09652	1.0961	0.4054	2.5570	1.1384
10.0	2.8273	0.08859	1.0702	0.3502	2.4891	0.9786
15.0	2.5324	0.07872	-	-	2.2723	0.7970
20.0	2.3511	0.06810	0.9077	0.2564	2.0982	0.6848
40.0	1.7800	0.04833	0.7073	0.1783	1.5394	0.4821
60.0	1.4620	0.03752	0.6300	0.1317	1.2360	0.3720
80.0	1.2539	0.03074	0.5329	0.1110	1.0843	0.2979

Table (3.2). Kinetic Date for pH 9.2, 9.8 and 10.2 According to Equation (3.15) for the Hydrolysis of 8 x 10^{-4}M Phenyl Acetate at Different Concentrations of CTAB.

The data are presented, graphically, in Figures (3.4), (3.5) and (3.6) respectively.

It can be seen that, in every case, the profiles show two linear parts with a distinctive break which occurs in each case at approximately 1×10^{-2}M CTAB. These two linear parts are designated A and B where A represents the region below this concentration and will be referred to as the low CTAB concentration region and B represents the high CTAB concentration, being the region above 1×10^{-2}M CTAB. It is interesting to note, at this point, that in a previous study (121) involving the hydrolysis of ethyl-p-amino benzoate in the presence of CTAB, in which retardation of the hydrolysis was observed, the data were plotted in a similar manner and described as linear whereas two regions can be distinguished with an obvious break in the linearity of the plot.

The implication of this break is that it gives two values for the partition coefficient; one is characteristic of all values of CTAB above the CMC and below 1×10^{-2}M and the other for values above this concentration up to at least 8×10^{-2}M. These partition coefficient values were obtained from the slopes of the two linear parts upon submitting the data to a least squares regression analysis programme. The intercepts of these lines give a measure of the micellar rate constants, k_m. These values are given in Table (3.3).

The derived partition data are presented graphically in Figure (3.7) from which it can be seen that the K_p values at the high concentration of CTAB are fairly uniform. The K_p values at the low concentration of CTAB, however, decrease with a decrease in pH.

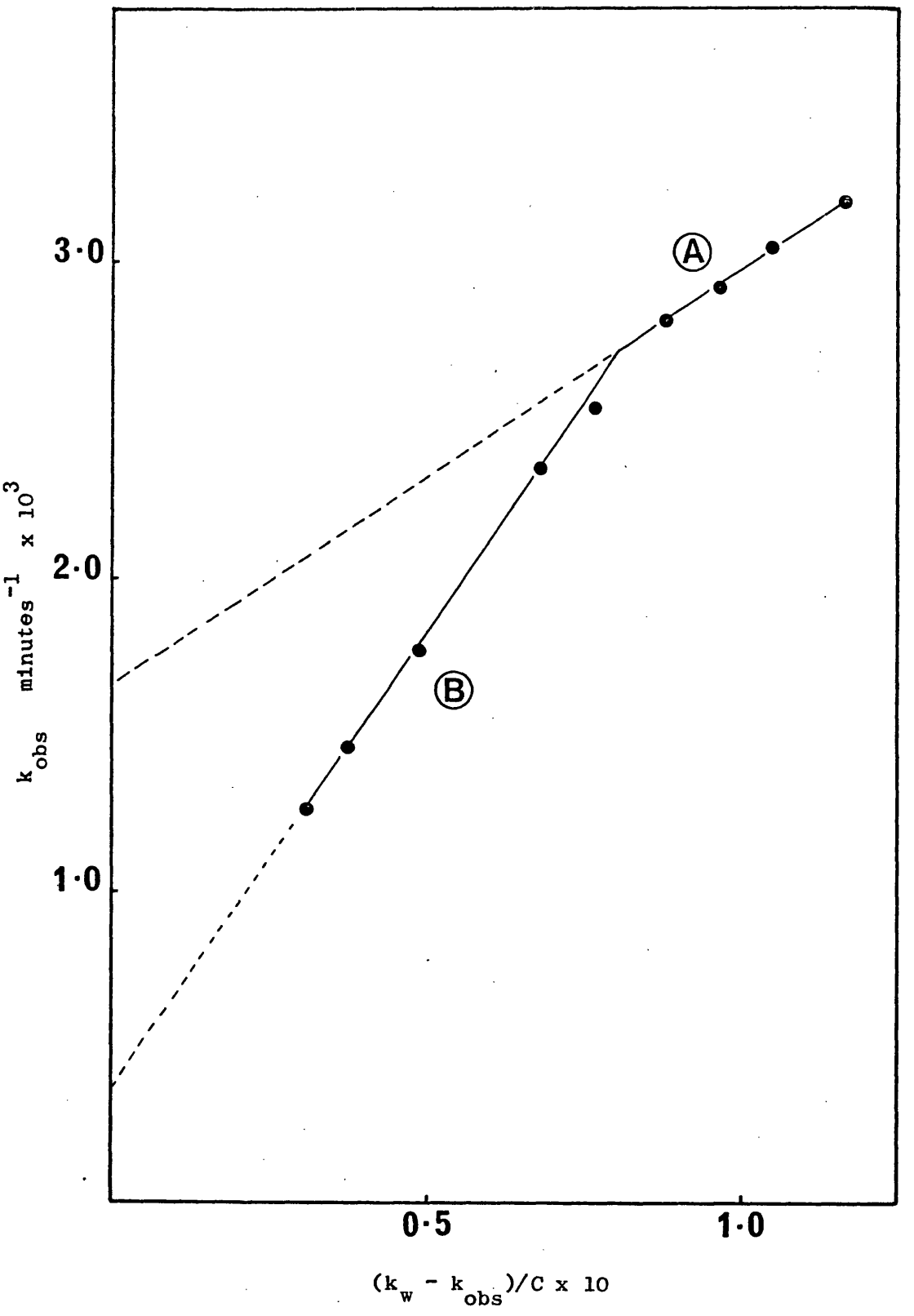

FIG.(3.4). A PLOT OF k_{obs} AGAINST $(k_w - k_{obs})/C$ FOR THE HYDROLYSIS OF PHENYL ACETATE IN CARBONATE-BICARBONATE BUFFER AT pH 9.2 AND 30°C.
IONIC STRENGTH 0.5.

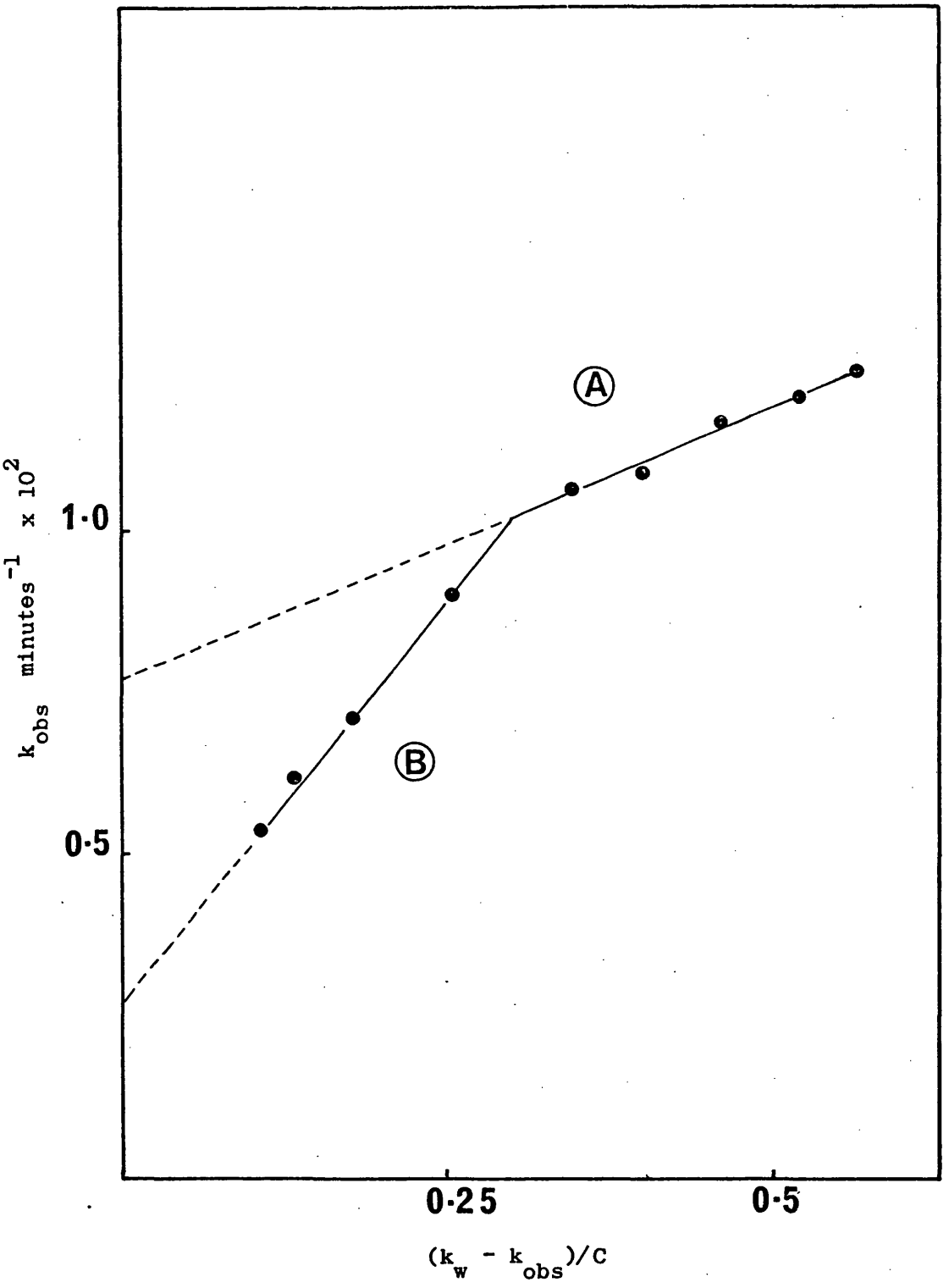

FIG. (3.5). A PLOT OF THE OBSERVED RATE CONSTANT AGAINST $(k_w - k_{obs})/C$ FOR THE HYDROLYSIS OF PHENYL ACETATE IN CARBONATE-BICARBONATE BUFFER AT pH 9.8 AND 30° $\mu = 0.5$.

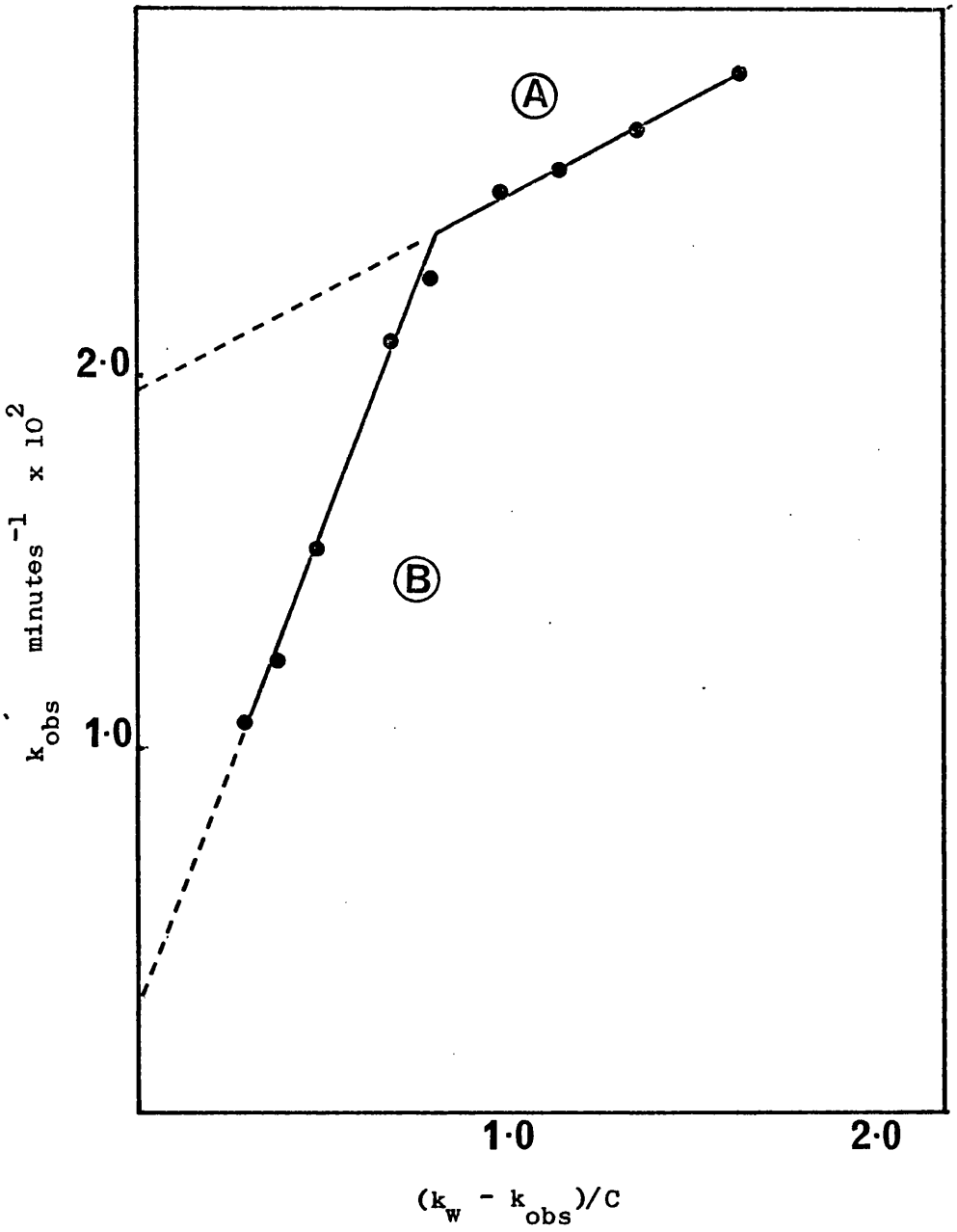

FIG.(3.6). A PLOT OF THE OBSERVED RATE CONSTANT AGAINST $(k_w - k_{obs})/C$ FOR THE HYDROLYSIS OF PHENYL ACETATE IN CARBONATE-BICARBONATE BUFFER AT pH 10.2 AND 30°C. IONIC STRENGTH 0.5.

pH	LOW CTAB CONCENTRATION A			HIGH CTAB CONCENTRATION B		
	INTERCEPT (k_m) min^{-1}	Slope	K_p	INTERCEPT (k_m) min^{-1}	Slope	K_p
9.2	1.5201×10^{-3}	1.4790×10^{-2}	189.30	3.5905×10^{-4}	29.2970×10^{-2}	95.57
9.8	7.5884×10^{-3}	8.5718×10^{-3}	326.63	2.8008×10^{-3}	24.470×10^{-2}	114.41
10.2	1.9838×10^{-2}	5.0838×10^{-3}	550.73	2.6945×10^{-3}	2.6570×10^{-2}	105.37

Table (3.3). Micellar Rates (k_m) and Partition Coefficient (K_p) for the Hydrolysis of Phenyl Acetate at pH 9.2, 9.8 and 10.2 in Carbonate-Bicarbonate Buffer ($\mu = 0.5$) at 30^o as Determined Kinetically.

If this trend continues, according to the curve in Figure (3.7), then it might be expected that at a pH of about 8.0 the value of K_p would have decreased to that characteristic of the high CTAB concentrations. If this is true then at pH 8.0 a plot according to equation (3.15) shculd be linear over the whole CTAB concentration range and not exhibit a break as occurs at higher pH's.

In order to obtain from these data another estimate of where the difference between high and low CTAB concentrations might disappear, the angle θ between the two linear parts of Figures (3.4 - 3.6) were measured. This is shown diagrammatically in Figure (3.8) and is clearly seen that θ increases as the pH decreases. The angles θ_1, θ_2, θ_3 and θ_4 in Figure (3.8) were plotted, on a log scale, against the pH, on a linear scale as shown in Figure (3.9). By extrapolating

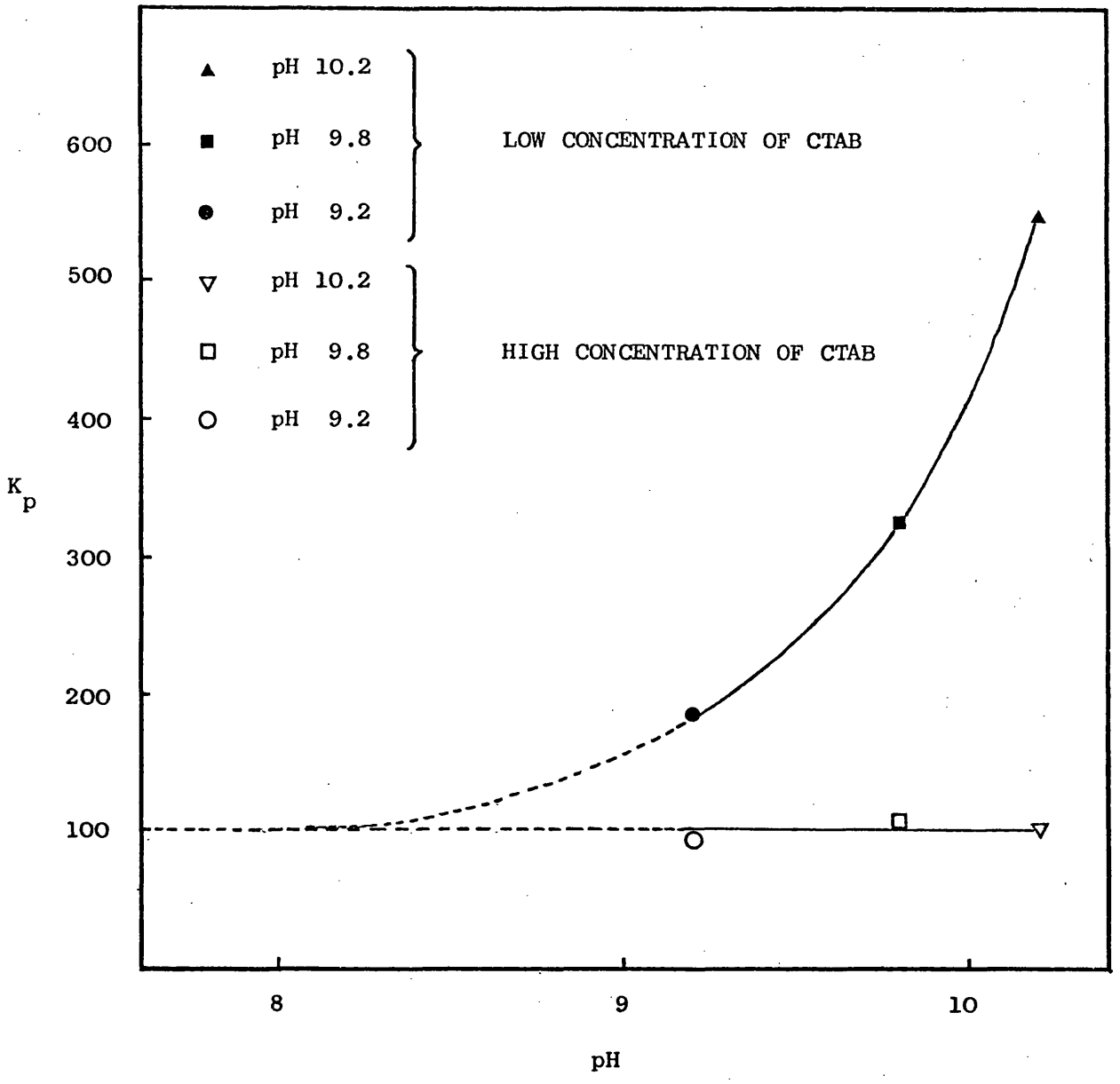

FIG. (3.7). PARTITION COEFFICIENT K_p AGAINST pH FOR PHENYL ACETATE AT 30° IN CARBONATE-BICARBONATE BUFFER ($\mu = 0.5$)

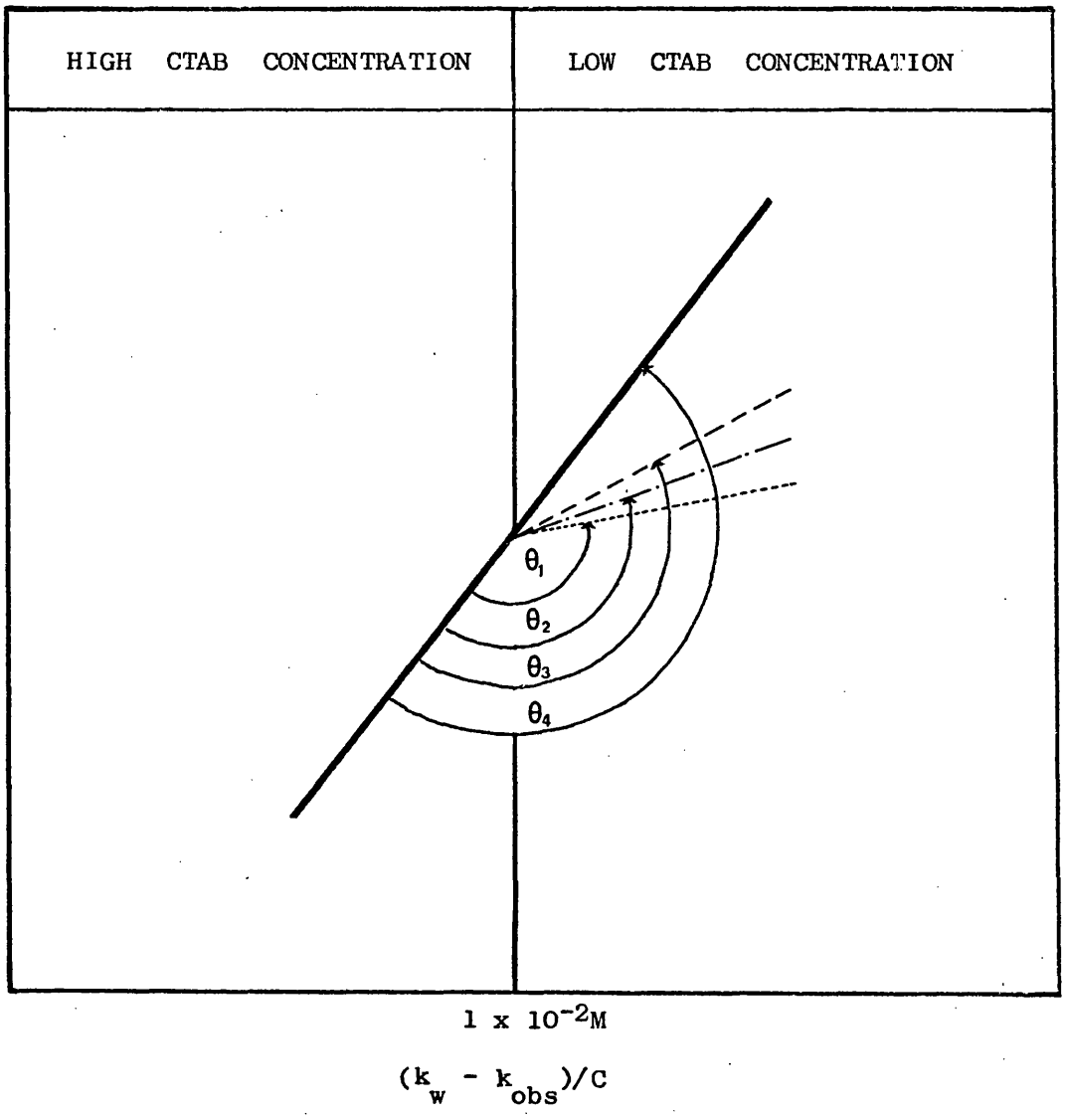

FIG. (3.8). DIAGRAMMATIC REPRESENTATION OF THE PLOT OF k_{obs} vs $(k_w - k_{obs})/C$ TO SHOW INCREASE OF θ WITH DECREASE OF pH.

	pH	θ
———	8.0	4
– – – – –	9.2	3
–·–·–·–	9.8	2
·····	10.2	1

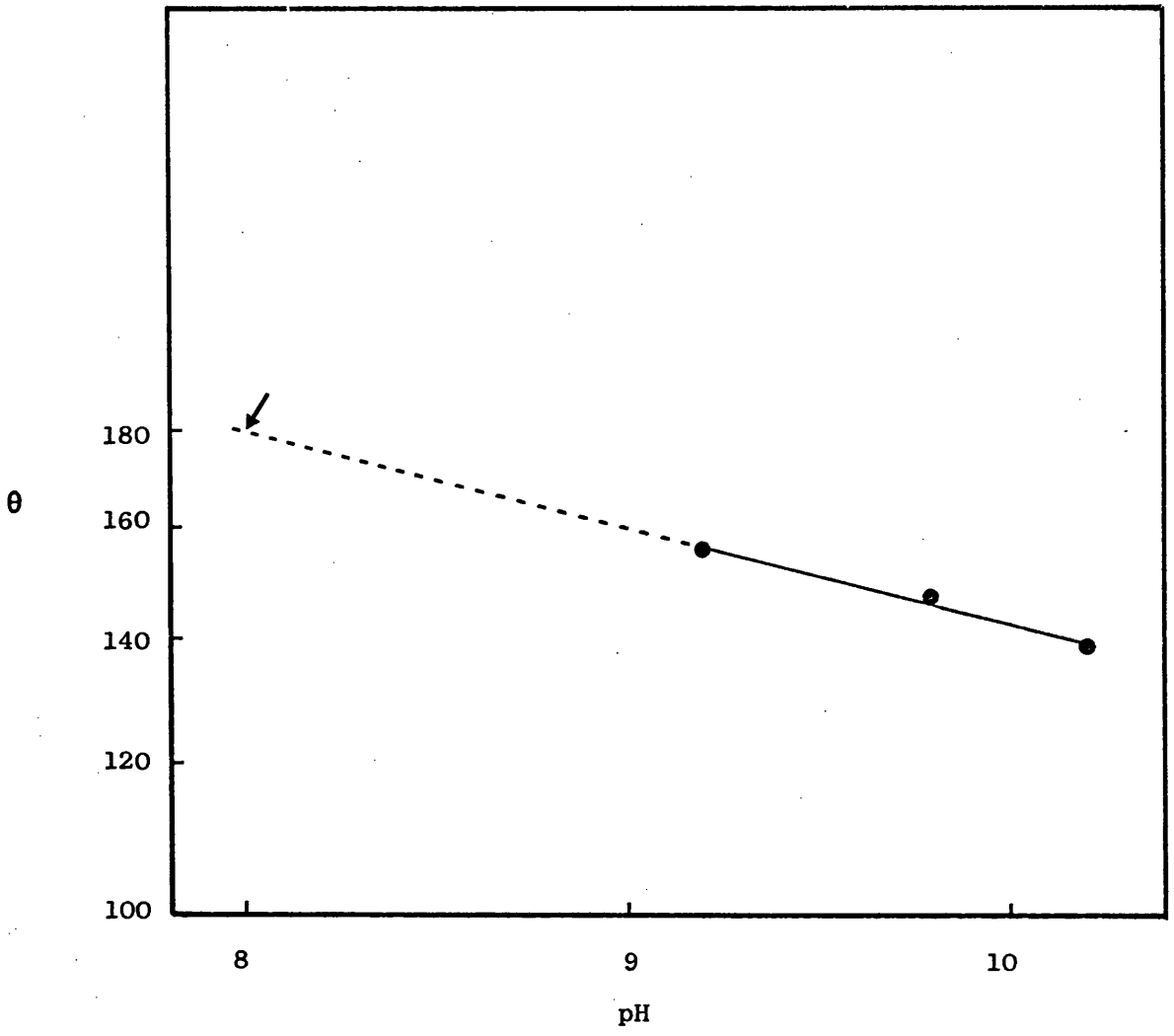

FIG. (3.9). THE ANGLE θ BETWEEN THE STRAIGHT LINE AND THE LINES SHOWING A BREAK (FIGURE 3.8)

the resulting line to an angle of 180° it can be seen that this angle, representing a straight line, occurs at a pH of about 8.

Kinetic studies were, therefore, performed at pH 8.0 in carbonate-bicarbonate buffer and ionic strength of 0.5M, adjusted with potassium chloride with pH maintenance being provided with a pH-stat. The results are given in Table (2.15). When these results were treated according to equation (3.15) the data in Table (3.4) were obtained.

CTAB MOLAR Concentration (C) x 10^3	k_{obs} x 10^4	$\left(\frac{k_w - k_{obs}}{C}\right)$ x 10^3
NIL	2.55616	-
3.84	2.24601	8.0768
5.76	2.12525	7.4811
7.68	2.01291	7.0736
9.6	1.91733	6.6545
14.4	1.72159	5.7956
19.2	1.56409	5.1670
38.4	1.19170	3.5533
57.6	0.98397	2.7295
76.8	0.83985	2.2348

Table (3.4). Kinetic Data for pH 8.0 According to Equation (3.15) for the Hydrolysis of Phenyl Acetate at Different Concentrationsof CTAB.

These results are shown graphically in Figure (3.10) and it can be seen that at pH 8 there is no break in the region of 1×10^{-2}M CTAB.

The partition coefficient values obtained through kinetic data are only notional values; that is to say the way that the rate constant varies with the CTAB concentration at the different pH values can be explained, with certain assumptions, if the partition coefficient changes at a specific CTAB concentration. If the two-compartment model is valid, then physical measurements of the partition coefficient might be expected to show different values above and below 1×10^{-2}M CTAB.

Two different physical techniques were employed in the course of this work to obtain these values, namely gel filtration and solubility studies. Meaningful measurements, however, could only be carried out at low pH, as at the pH's of the kinetic studies degradation was too fast. The system used, therefore, was double distilled water adjusted to an ionic strength of 0.5M with potassium chloride and which has a pH of 5.6. Using this system, partition coefficient values of 119.18 and 94.16 were obtained by gel filtration and solubility techniques respectively. These values fall within the range of those obtained at high CTAB concentration at pH 9.2, 9.8 and 10.2 and agree with the single value obtained at pH 8.0, Figure (3.11). They serve, therefore, to corroborate the validity of the treatment of the kinetic data to give values of K_p and k_m. These results suggest that, perhaps, the micellar structure is different at high and low concentrations above a pH of 8.0, causing a change in size and/or shape of the micelles.

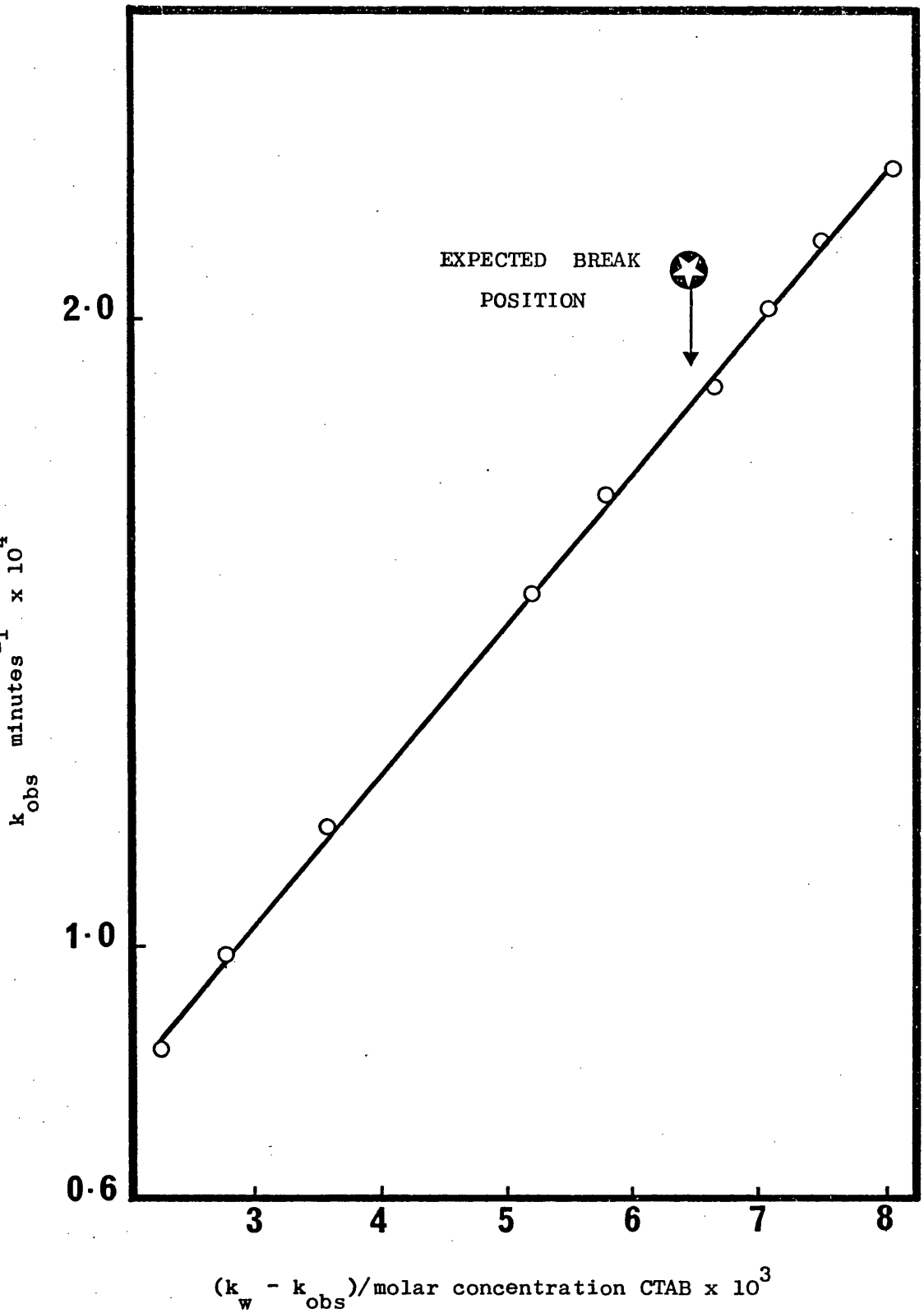

FIG. (3.10). OBSERVED RATE CONSTANT AGAINST $(k_w - k_{obs})/C$ FOR THE HYDROLYSIS OF PHENYL ACETATE IN CARBONATE-BICARBONATE BUFFER AT pH 8.0 μ = 0.5 AT 30°.

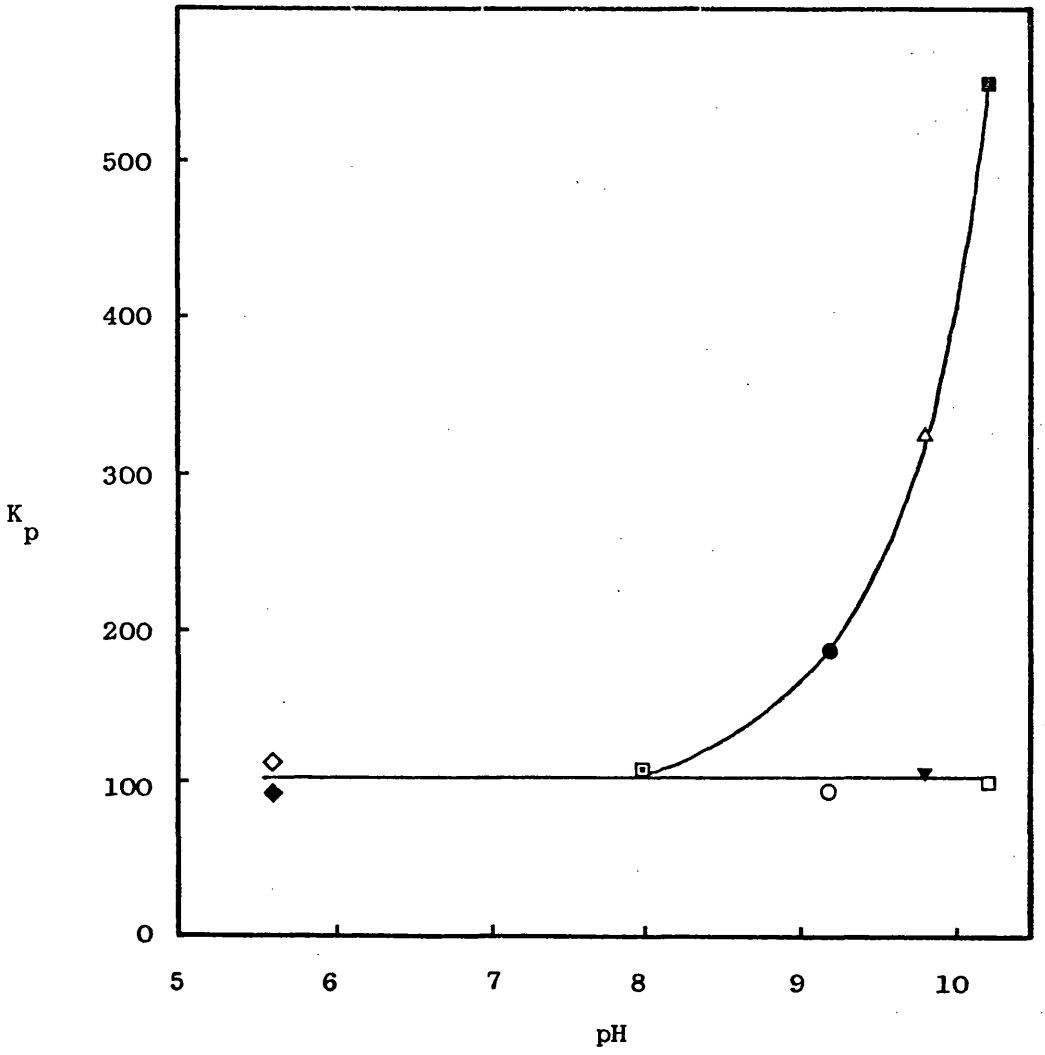

FIG. (3.11). PARTITION COEFFICIENT K_p AGAINST pH FOR PHENYL ACETATE IN CTAB AT 30°.

■	pH 10.2	LOW CTAB CONCENTRATION (CARBONATE-BICARBONATE BUFFER)
△	pH 9.8	
●	pH 9.2	
□	pH 10.2	HIGH CTAB CONCENTRATION (CARBONATE-BICARBONATE BUFFER)
▼	pH 9.8	
○	pH 9.2	
⊡	pH 8.0	CARBONATE-BICARBONATE BUFFER
◇	GEL FILTRATION	WATER ADJUSTED TO $\mu = 0.5$ pH = 5.6
◆	SOLUBILITY	

This change that serves to increase the ability of the micelles to partition the ester molecules increases with pH, since the partition coefficient value is 110 at pH 8.0 increasing to 550 at pH 10.2. This micellar change which occurs at approximately 1 x 10^{-2}M if it does lead to a change in micellar shape or structure should be detectable through light scattering and viscosity studies. Such changes have been reported before, through these techniques by Ekwall et al (44) around the same region. The only interpretation they put to the findings was that a change occurs and its true nature has to be elucidated through further work.

In order to attempt to elucidate the nature of these changes light scattering experiments were carried out with the CTAB in different ionic environments, namely: aqueous solution, aqueous solution adjusted to an ionic strength of 0.5M with potassium chloride, both at pH 5.6, in carbonate-bicarbonate buffer at a pH 9.2 adjusted to an ionic strength of 0.5 with potassium chloride and in carbonate-bicarbonate buffer at pH 9.2 adjusted to an ionic strength of 0.5M with potassium chloride but in the presence of 8 x 10^{-4}M phenyl acetate. In simple aqueous solution, as can be seen in Figure (2.22) a break is obtained at a concentration of approximately 1 x 10^{-2}M. The micellar molecular weight obtained from the linear part of the graph below the break is 37000 which compares with Ekwall's value of 34000 - 35000 (44), and with the value of 33000 obtained by Barry and Russell (143). The value obtained from the linear part above the break is 4800 and although Ekwall has carried out measurements extending to this range of concentrations he does not use them to calculate micellar molecular weight. His data however yield a value

of 4600, in this region, when extrapolated to the intercept of his plot according to equation (2.29).

Upon the addition of potassium chloride to the aqueous solutions to adjust them to an ionic strength of 0.5M, there is a marked increase in the micellar molecular weights. This is consistent with the fact that the micellar weight increases with the addition of a neutral salt since the reduction of the repulsive forces between head groups facilitates the formation of bigger micelles. It is interesting to note that in this system the break has disappeared and, therefore, only one value for the micellar molecular weight is obtained. Since physical determinations, using gel filtration and solubility were carried out under the same conditions (water adjusted to an ionic strength of 0.5M with potassium chloride - pH 5.6) it is possible that the answer obtained, namely of only one K_p value, is a function of the measuring conditions. It is possible that in the presence of high amounts of potassium chloride micelles behave differently than in the presence of buffer or in simple aqueous solutions. It is interesting to note that Winterborn (121) observed non linearity in the gel filtration plots (Figure 22 of reference 121) involving CTAB and ethyl-p-aminobenzoate which he attributed to Donnan effects arising from the small number of carboxyl groups on the gel, since they could be eliminated by increasing salt concentration. It is of particular interest that although not many points were obtained the break occurs at between 1 and 2 x 10^{-2}M CTAB.

In the carbonate-bicarbonate buffer at pH 9.2 in the absence and presence of phenyl acetate the system shows the two regions below and above the 1 x 10^{-2}M CTAB. This is evidenced by the change of the slopes in Figures (2.24, 2.25), when the data were plotted according

to equation (2.29), below and above the 1×10^{-2}M CTAB concentration. This change in the slope probably reflects a change in micelle size and/or shape. Some support for this interpretation is provided by the observation of measurable dissymmetry in the light scattering measurements. In the buffer system, dissymmetry is evident at the low concentrations where aggregation numbers are high, consistent with large assymmetric micelles. Dissymmetry tends to disappear at the high concentration region where the aggregation numbers are smaller, about 130 monomers per micelle. The system in potassium chloride only does not show dissymmetry at both concentration regions. In water, the low concentration region does not show dissymmetry and although the number of monomers per micelle, as calculated from the data in Table (2.29), decrease sharply at the high CTAB concentration region a marked dissymmetry is obtained. This suggests that the results obtained do not reflect the true picture of the system in this region. One possible explanation would be that the micelles enlarge to such an extent that "shielding" can occur and the amount of light scattered by the system is no longer quantitatively related to the number or size of the micelles present. Another interpretation could be that the micelles take on a complicated form to which equation (2.29) does not apply. It is obvious that further thorough and detailed investigation of the system is necessary under controlled conditions of either a fixed CTAB concentration or a fixed salt concentration. In this study the main concern has been the kinetic conditions where a constant ionic strength had to be maintained which meant that the ratio of the added electrolyte to the concentration of the CTAB was continually changing. This was due to the fact that the contribution from the surfactant itself to the overall ionic strength had to be taken into

account and this, in turn, meant the reduction of the amount of salt added, for ionic strength adjustment, as the CTAB concentration was increased. These fluctuations ranged between 0.497M (in the presence of 0.003M CTAB) and 0.42M (in the presence of 0.08M CTAB). When the highest factor of 0.42M was applied to equations (2.38) and (2.39) for the calculation of charge and aggregation number, respectively, in the aqueous system containing potassium chloride it reduced the charge from 44.9 to 41.1 and the aggregation number from 150.8 to 150.1. The system of aqueous solution with potassium chloride was chosen so as to be able to isolate the true nature of the salt contribution. In buffer systems, the buffer salts are contributing largely to the overall ionic strength and from the data in Table (2.33) it appears that the system behaves differently in buffer as compared to in potassium chloride alone. This is not unexpected since different salts have different effects on surfactant systems. This fact has to be borne in mind when viewing the light scattering results in this study since the overall ionic strength of 0.5M was not considered in its true nature with the respective contributions from potassium chloride and buffer salts. The application of the PHPM equation (2.35) to the buffer systems is, therefore, not strictly valid since severe approximations have been made regarding the refractive index increments and the ionic strength.

The presence of phenyl acetate in the system alters both the charge and the aggregation number significantly. This is a reflection of the effect of solubilization on micellar systems which leads to a reduction in surfactant head group repulsions and hence the growth of large micelles. From the geometrical considerations advocated by Schott (53) and Tanford (54) it seems unlikely that the micelles in

this system are spherical particularly in the presence of potassium chloride and buffer salts. However, although it is not intended to interpret the results quantitatively they do confirm that a change in micellar size does occur and that it takes place at approximately 1×10^{-2}M, in these systems, thereby confirming the findings of the kinetic and the physical measurements by gel filtration and solubilization.

Interpretation of viscosity data is also difficult but the results are qualitatively consistent with physical changes in micelle structure in aqueous and buffer systems. The plot of reduced specific viscosity against micellar concentrations of CTAB in water Figure (2.17) is almost identical to results obtained by Ekwall (44) using the same system. Measurements using higher CTAB concentrations than those utilized for the kinetic studies were made in order to enable a direct comparison with published data and to establish the degree of confidence in the experimental technique.

Figure (2.15) shows the relative viscosity of CTAB, in all systems investigated, plotted against the % concentration of CTAB. It is clear that the viscosity increases with an increase in surfactant concentration. In water, the high viscosity obtained, as compared to the other systems, could be due to an electroviscous effect which is absent in the presence of high electrolyte concentrations. The electroviscous effect is the term used to describe the electrostatic contributions made by charged colloidal particles to the viscosity of a solution (144). The thicker the particles double layer (the lower the ionic strength) the more evident the effect. Another possible factor contributing to the high viscosity of the system in water could be the

assymmetry of particles. This is a reasonable conclusion since assymmetry is shown to exist in this system by light scattering. Extrapolation of the linear part of the plot for this system in Figure (2.15) would give a volume fraction of about 14 indicating a high deviation from spherical shape.

Examining the profiles of Figure (2.16) for other systems shows that the viscosity decreases as compared to the system in water signifying, perhaps, the reduction in electroviscous effect in these systems due to the high electrolyte content. It is evident however, from Figure (2.15) that some sort of change takes place in the region of 1×10^{-2}M CTAB since the profiles show marked difference in the region below and above this concentration. It is interesting to note that if the uplift of the profiles, Figure (2.15), of the buffer systems were to continue a high intrinsic viscosity would be obtained for the low CTAB concentrations. This is in direct agreement with light scattering results which show high aggregation numbers in the low surfactant concentration in these two systems. Mukerjee (145) has pointed out, however, that the numerical values of intrinsic viscosities are very sensitive to the measured value of the viscosity at the CMC and because, at the low CTAB concentrations the observed viscosity will be very close to the viscosity at the CMC, a small error in the value of the observed viscosity can produce a large error in the reduced specific viscosity. This could explain the anomolous results obtained at the low concentrations of CTAB in water.

Viscosity results, in line with other results obtained in this study, point to the possibility of a difference in the behaviour of the system when in potassium chloride alone as compared to its behaviour in the buffer solutions. This is shown by the different profile of the

system in potassium chloride as compared to the other three profiles in Figure (2.15). If the linear parts of the plots for buffer and for potassium chloride systems, at the high CTAB concentration, were extrapolated, however, they show an intrinsic viscosity not far removed from that associated with spherical particles. Once again, this interpretation agrees with that of the light scattering determinations since the micelles in this region are relatively small, having an aggregation number of about 130.

The physical and kinetic results, therefore, seem to augment each other. The persistent break in the region of 1×10^{-2}M CTAB obtained from the kinetic studies above pH 8, being consistent with light scattering and viscosity data. The data from unbuffered CTAB–potassium chloride systems however, are qualitatively different and do not support structural micellar changes for this situation. This seems to lead to two conclusions: that the system behaves differently in potassium chloride than it does in carbonate-bicarbonate buffer and that the presence of OH^- ions seems to increase the binding efficiency of the micelles at low concentrations of CTAB up to a concentration of 1×10^{-2}M. The increase in binding ability, reflected through higher partition coefficient values, is linked, in turn, to the presence of bigger micelles since the highest K_p value obtained is that of 550 at a pH of 10.2 in the low CTAB concentration where light scattering studies have shown the aggregation to be at its highest. In the buffer system studied at pH 9.2 the K_p associated with an aggregation number of 420 is 189.3 while that associated with an aggregation number of 131 is only 95.6. From the data in Table (2.33) it appears that the binding efficiency is linked also to the charge density per monomer in the micelle. In the case just cited, the

fractional charge associated with monomers in the micelles at the low CTAB concentration (i.e. high aggregation number and high K_p) is 0.66 while that associated with the low K_p at the high CTAB concentration is only 0.19. It seems therefore that the binding efficiency is governed by three factors -

(1) pH,

(2) the size of the micelle,

and (3) the fractional charge on the micelle.

The simple two-compartment model used assumes that the micellar compartment remains unchanged in all experimental conditions, but in the light of the results shown this is difficult to accept. When considering the micellar compartment the whole environment of the micelle has to be taken into account, that is to say, the micelle and its associated diffuse layer. The latter is influenced by the ionic strength of the medium and, in turn, it influences the micellar reactions through dielectric constant changes, solubility in the vicinity of the micelle and the surface pH of the micelle. These are not easy parameters to quantify. The most likely site of association of phenyl acetate with CTAB micelles is at or near the surface and changes that could occur in this area will, therefore, markedly affect the ester with regard to its orientation and its susceptibility to nucleophilic attack.

In order to validate, or otherwise, the two-compartment model it would be desirable to carry out the kinetic investigations in an environment ideal for physical measurements. In this study, the reverse has been the case, as the project was conceived and designed on a kinetic approach. The observation of kinetic anomolies led to

physical measurements being carried out in the kinetic situation in the hope of explaining these anomolies but the system set up in this way has proved to be too complex for ready interpretation.

BIBLIOGRAPHY

REFERENCES

1. LAIDLER, K.J. (1965). "Chemical Kinetics." McGraw-Hill, Inc., New York.

2. BENSON, S.W. (1960). "The Foundations of Chemical Kinetics." McGraw-Hill Book Company, New York.

3. ROBINSON, R.A. and STOKES, R.H. (1968). "Electrolyte Solutions." Butterworths, London.

4. INGOLD, C.K. (1969). "Structure and Mechanism in Organic Chemistry." 2nd Edition, Cornell University Press, N.Y.

5. GOULD, E.S. (1959). "Mechanism and Structure in Organic Chemistry." Holt, Rinehart and Winston, New York.

6. MARTIN, A.N., SWARBRICK, J. and CAMMARATA, A. (1969). "Physical Pharmacy." Lea and Febiger, Philadelphia.

7. HARTLEY, G.S. (1937). "Aqueous Solutions of Paraffin Chain Salts." Hermann, Paris.

8. SCHWARTZ, A.M., PERRY, J.W. and BERCH, J. (1958). "Surface Active Agents and Detergents." Vol.II. Interscience, New York.

9. MOILLIET, J.L., COLLIE, B. and BLACK, W. (1961). "Surface Activity." 2nd Edition. Spon Ltd., London.

10. McBAIN, M.E.L. (1913). Trans. Faraday Soc., 9, 99.

11. SHINODA, K., NAKAGAWA, T., TAMAMUSKI, B. and ISEMURA, T. (1963). "Colloidal Surfactants." Academic Press Inc., London.

12. MUKERJEE, P. and MYSELS, K.J. (1971). "Critical Micelle Concentrations of Aqueous Surfactant Systems." NSRDS - NBS 36, U.S. Government Printing Office, Washington D.C.

13. MUKERJEE, P., MYSELS, K.J. and DULIN, C.I. (1958). J. Phys. Chem., 62, 1390.

14. SCHICK, M.J. (1963). J. Phys. Chem. 67, 1796.

15. FLOCKHART, B.D. (1961). J. Colloid Sci., 16, 484.

16. EMERSON, M.F. and HOLTZER, A. (1967). J. Phys. Chem., 71, 3320.

17. SCOTT, A.B. and TARTAR, H.V. (1943).
J. Am. Chem. Soc., 65, 692.

18. KLEVENS, H.B. (1948).
J. Phys. & Colloid Chem., 52, 130.

19. CORRIN, M.L. and HARKINS, W.D. (1947).
J. Am. Chem. Soc., 69, 683.

20. CORRIN, M.L. (1948).
J. Colloid Sci., 3, 333.

21. TARTAR, H.V. (1962).
J. Colloid Sci., 17, 243.

22. SCHICK, M.J. (1964).
J. Phys. Chem. 68, 3585.

23. HARKINS, W.D., MITTELEMANN, R. and CORRIN, M.L. (1949).
J. Phys. & Colloid Chem., 53, 1350.

24. BECHER, P. (1965).
J. Colloid Sci., 20, 728.

25. ERIKSSON, J.C. and GILLBERG, G. (1966).
Acta. Chem. Scand., 20, 2019.

26. FOURNET, G. (1951).
Discuss. Faraday Soc., 11, 121.

27. STRYER, L. (1968).
Science, 162, 526.

28. TANFORD, C. (1973).
"The Hydrophobic Effect: Formation of Micelles and Biological Membranes." John Wiley & Sons, Inc., N.Y.

29. CLIFFORD, J. and PETHICA, B.A. (1964).
Trans. Faraday Soc., 60, 1483.

30. POVICH, M.J., MANN, J.A. and KAWAMUTO, A. (1972).
J. Colloid Interf. Sci. 41, 145.

31. CLIFFORD, J. (1965).
Trans. Faraday Soc., 61, 1276.

32. MULLER, N. and BIRKHAM, R.H. (1967).
J. Phys. Chem., 71, 957.

33. MULLER, N. and SIMSOHN, H. (1971).
J. Phys. Chem., 75, 942.

34. STIGTER, D. (1974).
J. Phys. Chem., 78, 2480.

35. STIGTER, D. and MYSELS, K.J. (1955).
J. Phys. Chem., 59, 45.

36. CORKHILL, J.M., GOODMAN, G.F. and WALKER, T. (1967).
Trans. Faraday Soc., 63, 768.

37. STIGTER, D. (1967).
J. Colloid Interf. Sci., 23, 379.

38. KRESHNECK, G.C., HAMORI, E., DAVENPORT, G. and SCHEGARA, H.A.(1966).
J. Am. Chem. Soc., 88, 246.

39. LANG, J. and EYRING, E.M. (1972).
J. Poly. Sci. A-2, 10, 89.

40. FLORENCE, A.T. and PARFITT, R.T. (1971).
J. Phys. Chem., 75, 3554.

41. GRABER, E. and ZANE, R. (1970).
Kolloid-Z., 238, 479.

42. Van BUREAU and GOTZ, K.G. (1958).
Discuss. Faraday Soc., 25, 71.

43. JAYCOCK, M.J. and OTTEWILL, R.H. (1967).
Chemistry, Physics and Application of Surface Active Substances. Proceedings of the 4th Int. Cong. on Surf. Active Subs., Brussels, 1964.

44. EKWALL, P., MANDELL, L. and SOLYOM, P. (1971).
J. Colloid Interf. Sci., 35, 519.

45. DEBYE, P. and ANACKER, E.W. (1951).
J. Phys. & Colloid Chem., 55, 644.

46. KUSHNER, L.M., DUNCAN, B.C. and HOFFMAN, J.I. (1952).
J. Res. Nat. Bur. Stand., 49, 85.

47. KUSHNER, L.M., HUBBARD, W.D. and PARKER, R.A. (1957).
J. Res. Nat. Bur. Stand., 59, 113.

48. HYDE, A.J. and ROBB, D.J.M. (1963).
J. Phys. Chem., 67, 2093.

49. SASAKI, T. and SHIGEHARA, K. (1967).
Proc. Int. Cong. Surf. Sctive Substances, 4th, 2, 1964.

50. GRANATH, K. (1953).
Acta. Chem. Scand., 7, 297.

51. REISS, HUSSON, F. and LUZZATI, V. (1964).
J. Phys. Chem., 68, 3504.

52. TOKIWA, F. and OHKI, K. (1968).
Kolloid-Z., 223, 38.

53. SCHOTT, H. (1971).
J. Pharm. Sci. 60, 1594.

54. TANFORD, C. (1972).
J. Phys. Chem. 76, 3020.

55. TARTAR, H.V. (1959).
J. Colloid Sci., 14, 115.

56. DEBYE, P. (1949).
Ann. N.Y. Acad. Sci., 51, 575.

57. ATTWOOD, D., ELWORTHY, P.H. and KAYNE, S.B. (1970).
J. Phys. Chem., 74, 3529.

58. SCHERAGA, H.A. and BACKUS, J.K. (1951).
J. Am. Chem. Soc., 73, 5108.

59. MUKERJEE, P. (1972).
J. Phys. Chem., 76, 565.

60. BIRDI, K.S. (1972).
Kolloid-Z. Z.Polym., 250, 731.

61. FRANK, H.S. (1970).
Science, 169, 635.

62. MUKERJEE, P. (1967).
Adv. Phys. Org. Chem., 8, 271.

63. CORKILL, J.M., GOODMAN, J.F. (1969).
Adv. Colloid Sci., 2, 297.

64. ELWORTHY, P.H., MYSELS, K.J. (1966).
J. Colloid Sci., 21, 331.

65. BAIR, E.J. and KRAUS, C.A. (1951).
J. Am. Chem. Soc., 73, 1129.

66. PHILLIPS, J.N. (1955).
Trans. Faraday Soc., 51, 561.

67. LOEB, A.L., OVERBEEK, J.G. and WIERSEMA, P.H. (1961).
"The Electrical Double Layer Around a Spherical Colloid Particle." M.I.T. Press, Cambridge, Mass.

68. RASSING, J., SAMS, P.J. and WYN-JONES, E. (1974).
J. Chem. Soc. Faraday Trans. (2), 7, 1247.

69. RIGG, M.W. and LIU, F.W.J. (1953).
J. Am. Oil Chem. Soc., 30, 14.

70. VENABLE, R.L. and NAUMAN, R.V. (1964).
J. Phys. Chem. 68, 3498.

71. HERRIES, D.G., BISHOP, W. and RICHARDS, F.M. (1964).
J. Phys. Chem., 68, 1842.

72. PATEL, N.K. and KOSTENBAUDER, H.B. (1958).
J. Am. Pharm. Ass. (Sci. Edn.), 47, 289.

73. MOLYNEUX, P. and RHODES, C.T. (1967).
J. Chem. Soc. A, 561.

74. NAKAGAWA, T. and TORI, K. (1964).
Kolloid-Z., 194, 143.

75. RIEGELMAN, S., ALLAWALA, N.A., HRENOFF, M.K. and STRAIT, L.A.
J. Colloid Sci., 13, 208. (1958).

76. McBAIN, M.E.L. and HUTCHINSON, E. (1955).
"Solubilization." Academic Press, New York.

77. ELWORTHY, P.H., FLORENCE, A.T. and MACFARLANE, C.B. (1968).
"Solubilization by Surface Active Agents and its application in Chemistry and the Biological Sciences." Chapman and Hall, London.

78. HYDE, A.J. and STEVENSON, D.M. (1969).
Kolloid-Z.Z.Polym., 232, 797.

79. PATTERSON, L.K. and VIEIL, J. (1973).
J. Phys. Chem., 77, 1191.

80. THAKKAR, A.L. and HALL, N.A. (1968).
J. Pharm. Sci., 57, 1394.

81. DORRANCE, R.C. and HUNTER, T.F. (1972).
J. Chem. Soc. Faraday Trans., 1, 1312.

82. FENDLER, J.H. and FENDLER, E. (1970).
Adv. Phys. Org. Chem., 8, 271.

83. MORAWETZ, H. (1969).
Advances in Catalysis, 20, 341.

84. BAUMRUCKER, J., CALZADILLA, M. and CORDES, E.H. (1973).
"Reaction Kinetics in Micelles." Pleonum Press, New York.

85. HARTLEY, G.S. (1934).
Trans. Faraday Soc., 30, 444.

86. DUYNSTEE, E.F.J. and GRUNWALD, E. (1959).
J. Am. Chem. Soc., 81, 4540, 4542.

87. TWITCHELL, J. (1906).
J. Am. Chem. Soc., 28, 196.

88. BEHME, M.T.A. and CORDES, E.H. (1965).
J. Am. Chem. Soc., 87, 260.

89. ROMSTED, L.R. and CORDES, E.H. (1968).
J. Am. Chem. Soc., 90, 4404.

90. MENGER, F.M. and PORTNOY, C.E. (1967).
J. Am. Chem. Soc., 89, 4698.

91. Van SENDEN, K.G. and KONINGSBERGER, C. (1960).
Tetrahedron Letts., 1, 7.

92. CREMATY, E. and ALEXANDER, A.E. (1967).
Tetrahedron Letts., 59, 5271.

93. MUKERJEE, P. and BANERJEE, K. (1964).
J. Phys. Chem., 68, 3567.

94. HARTLEY, G.S. and ROE, J.W. (1940).
Trans. Faraday Soc., 36, 101.

95. MEAKIN, B.J., WINTERBORN, I.K. and DAVIES, D.J.G. (1971).
J. Pharm. Pharmacol., 23, 255.

96. WINTERBORN, I.K., MEAKIN, B.J. and DAVIES, D.J.G. (1974).
J. Pharm. Sci., 63, 64.

97. BUNTON, C.A., ROBINSON, L. and SEPULVEDA, L. (1970).
J. Org. Chem., 35, 108.

98. BUNTON, C.A., ROBINSON, L., SCHAAK, J. and STAM, M.F. (1971).
J. Org. Chem., 36, 2346.

99. BUNTON, C.A. and ROBINSON, L. (1969).
J. Org. Chem., 34, 773.

100. BUNTON, C.A., ROBINSON, L. and SEPULVEDA, L. (1969).
J. Am. Chem. Soc., 91, 4813.

101. BULST, G.J., BUNTON, C.A. ROBINSON, L. SEPULVEDA, L.
and STAM, M.F. (1970).
J. Am. Chem. Soc., 92, 4072.

102. BUNTON, C.A. and IONESCU, L.G. (1973).
J. Am. Chem. Soc., 95, 2912.

103. BUNTON, C.A., ROBINSON, L. and STAM, M.F. (1970).
J. Am. Chem. Soc., 92, 7393.

104. Van SENDEN, K.G. and KONINGSBERGER, C. (1966).
Tetrahedron, 22, 1301.

105. ROMSTED, L.R., DUNLAP, R.B. and CORDES, E.H. (1967).
J. Phys. Chem., 71, 4581.

106. DUNLAP, R.B. and CORDES, E.H. (1968).
J. Am. Chem. Soc., 90, 4395.

107. ABRIZZIO, J., ARCHILA, J., RODULFO, T. and CORDES, E.H. (1972).
J. Org. Chem., 37, 871.

108. BAUMRUCKER, J. et al (1970).
J. Phys. Chem., 74, 1152.

109. BAUMRUCKER, J. et al (1972).
J. Am. Chem. Soc., 94, 8164.

110. ROBINSON, L. (1969).
Ph.D. Thesis, University of California, U.S.A.

111. BUNTON, C.A., FENDLER, E.J., SEPULVEDA, L. and YANG, K.U. (1968).
J. Am. Chem. Soc., 90, 5512.

112. BUNTON, C.A., MINCH, M. and SEPULVEDA, L. (1971).
J. Phys. Chem. 75, 2707.

113. BUNTON, C.A., MINCH, M.J., HIDALGO, J. and SEPULVEDA, L. (1973).
J. Am. Chem. Soc., 95, 3262.

114. MUKERJEE, P., and MYSELS, K.J. (1955).
J. Phys. Chem. 77, 2938.

115. MANN, F.G. and SAUNDERS, B.C. (1952).
"Practical Organic Chemistry", Logmans, Green & Co. London.

116. TREMENTOZZI, Q.A. (1957).
J. Polym. Sci. 23, 887.

117. Documenta Geigy (1970).
Scientific Tables, 7th Edition, Geigy Pharmaceutical Company Ltd., Manchester.

118. BATES, R.G. (1954).
"Electrometric pH Determinations", Chapman & Hall Ltd., London.

119. HARKINS, W.D. and ALEXANDER, A.E. (1960).
"Physical Methods of Organic Chemistry" Vol.I. Part I page 757.
Edited by Weissberger. Interscience Publishers Inc., New York.

120. "Handbook of Chemistry and Physics" (1969-70). 50th Edition.
The Chemical Rubber Company, Cleveland, Ohio, U.S.A.

121. WINTERBORN, I.K. (1972).
Ph.D Thesis, University of Bath, U.K.

122. MUKERJEE, P. (1962).
J. Phys. Chem., 66. 1733.

123. American Society for Testing and Materials Standards, (1969).
pt. 17, pp. 289-294. A.S.T.M., Philadelphia.

124. ASHWORTH, R.W. and HEARD, D.D. (1966).
J. Pharm. Pharmaco, 18, 98S.

125. DONBROW, N., AZAZ, E. and HAMBURGER, R. (1970).
J. Pharm. Sci., 59, 1427.

126. COOPER, P.F. and WOOD, G.C. (1968).
J. Pharm. Pharmac., 20, 150S.

127. MARTIN, A.J.P. and SYNGE, R.L.M. (1941).
J. Biochem., 35, 135.

128. VOEKS, J.F. (1959).
J. Polym. Sci., 36, 333.

129. KAWAI, T. and NAITO, R. (1960).
J. Applied Polym. Sci., 3, 232.

130. B.S. 188, (1957). British Standards Institution.

131. RAYLEIGH, Lord (1900).
Phil. Mag. 49, 324.

132. ANACKER, E.W. (1970).
Chapter 7, "Cationic Surfactants"
Edited by E. Jungerman, Mercel Dekker, Inc., N.Y.

133. SMOLUCHOWSKI, M. (1908).
Ann. Physik, 25, 205.

134. DEBYE, P. (1947).
J. Phys. and Colloid Chem., 51, 18.

135. MYSELS, K.J. (1955).
J. Colloid Sci., 10, 507.

136. CABANNES, J. and ROCARD, Y. (1929).
In "La diffusion moleculaire de la lumiere".
Les Presses Universitaires de France, Paris.

137. PRINS, W. and HERMANS, J.J. (1956).
Koninkl. Ned. Akad. Wetenschap., 59, 298.

138. PRINCEN, L.H. and MYSELS, J. (1957).
J. Colloid Sci., 12, 594.

139. KRATOHVIL, J.P. (1962).
J. Polym. Sci., 57, 59.

140. JENNINGS, B.R. and JERRARD, H.G. (1964).
J. Polym. Sci., (A) 2, 2025.

141. HERMANS, J.J. and LEVISON, S. (1951).
J. Opt. Soc. Am., 41, 460.

142. LARSEN, J.W. and MAGID, L.J. (1974).
J. Phys. Chem. 78, 834.

143. BARRY, B.W. and RUSSELL, G.F.J. (1972).
J. Colloid. Interf. Sci., 40, 174.

144. BULL, H.B. (1964).
"An Introduction to Physical Biochemistry",
F.A. Davis Company, Philadelphia, Pa.

145. MUKERJEE, P. (1964).
J. Colloid Sci., 19, 722.

146. BAUER, N., FAJANS, K. and LEWIN, S.Z. (1960). "Physical Methods of Organic Chemistry" Vol. I Part II Page 1139 Edited by Weissberger, Interscience Inc. N.Y.